UNIVERSITY OF LONDON

"LOCAL PHONON EFFECTS IN SUPERCONDUCTING ALLOYS"

A THESIS SUBMITTED FOR THE

DEGREE OF DOCTOR OF PHILOSOPHY

By

GOZA TAY

Physics Department,
Imperial College of Science and Technology,
London, S.W. 7.

August, 1971

ABSTRACT

The effect of virtual recoil on non-magnetic transitional impurities on the normal state and superconducting state of a non-transitional metal is studied. The Anderson model is employed for the study. The systems investigated are dilute alloys of iron-group metal impurities (especially Mn and Cr) in aluminium.

The virtual recoil of the impurity is represented by the emission and absorption of phonons at the impurity site. These are the local phonons and their presence modify the admixture term of the Anderson Hamiltonian. A consequence of this modification is an additional contribution to the electronic properties of the system in the normal state.

A temperature-dependent width and a T^2-dependence in the residual resistivity are obtained. It is also found that the recoil leads to the enhancement of the masses of the s- and d-electrons. In addition, a contribution to the specific heat is obtained.

In the superconducting state, an attractive interaction between s- and d-electrons is proposed.

This interaction is investigated in the weak coupling limit. The new mechanism leads to a BCS type expression for the critical temperature and the superconducting density of states, both depending on the impurity concentration. The connection with BCS results is made through the transformation $\lambda_s \rightarrow f\lambda_s$. This leads to an enhancement of the energy gap as well as the transition temperature T_c of the alloy as obtained by Kiwi and Zuckermann, also Ratto and d'Agliano and Kaiser. The density of states curve shows the familiar BCS peak with a shift towards the low frequencies at higher impurity concentrations.

The thermodynamic properties are investigated in the temperature ranges $0 \lesssim T << T_c$ and $0 << T \lesssim T_c$. It is found that they assume the same form as in the case of BCS superconductors. Finally the results are compared with previous calculations, in which the impurity is assumed to be recoil-less.

ACKNOWLEDGEMENTS

The author wishes to thank Dr. M.J. Zuckermann for suggesting the problem investigated in the thesis, for his general supervision and direction of the work. His appreciation also goes to Professor Stanley Englesberg for his interest and encouragement during the initial stages of the work, as well as the many useful discussions which author had with him.

Several discussions held with members of the Solid State Theory Group, Imperial College, London, especially Dr. G. Morandi, are also kindly acknowledged.

The author is indebted to Professor Amiram Ron of the Israel Institute of Technology, Haifa, for introducing him to the Many-Body Theory during a year's stay at the Technion.

He is also grateful to the University of Science and Technology (UST), Kumasi for granting him study leave overseas and for supporting him throughout the course of the work.

The encouragement, patience, and interest shown by his wife has sustained the author throughout this study and he is most grateful to her. Not the least, the

author's greatest appreciation goes to his children and parents for the long period of absence they had to endure.

The author wishes to thank Mr. N.F. Zewu for his patience in typing the thesis.

Finally, the thesis is dedicated to the author's late father.

GOZA TAY

Kumasi

August 1971

TABLE OF CONTENTS

	PAGE
TITLE PAGE	1
ABSTRACT	2
ACKNOWLEDGEMENTS	4
TABLE OF CONTENTS	6
LIST OF FIGURES AND TABLES	10
INTRODUCTION	13
CHAPTER 1 : A REVIEW OF THEORIES ON THE EFFECTS OF IRON-GROUP IMPURITIES ON SUPERCONDUCTING AND NORMAL STATE ALLOYS ...	16
1.1 Non-magnetic Superoonducting Alloys ...	16
1.2 Localized Spin Fluctuations in a Superconductor	21
1.3 Non-magnetic Alloys in the Normal State	23
1.4 Virtual Recoil of the Impurity ...	24
1.4.1. Normal State	25
1.4.2. Superconducting State ...	27
1.5. Magnetic Alloys	28
1.5.1. Kondo Effect in the Normal State	28
1.5.2. Kondo Effect in the Superconducting State	32

PAGE

PART ONE : NORMAL STATE ALLOYS 37

CHAPTER 2 : INTRODUCTION : RESONANCE SCATTERING 38

2.1. Friedel Virtual Bound State ... 38
2.2 The Extra-orbital Model of Anderson 39
2.3 Anderson Hamiltonian for the One Impurity Problem 41
2.4 Anderson Hamiltonian Extended to the Case of Many Impurities ... 46
2.5 Virtual Recoil Contribution to the Normal State Hamiltonian ... 47

CHAPTER 3 : GREEN'S FUNCTION FORMALISM ... 50
3.1. The Diagram Technique ... 51
3.2 The Interaction representation ... 51
3.3 The Green's function 60
3.4 Wick's Theorem 62
3.5 Rules for Construction Feynman Diagrams 65
3.5.1 Diagrams in Coordinate-time Space ... 65
3.6 Diagrams in Momentum-frequency Space for the Perturbation Expansion of $G(k, \omega)$ 68
3.6.1 Rules for Evaluating Diagrams in Momentum-frequency Space ... 69
3.7 Dyson Equation and the Self-Energy Operator 72
3.8 The Green's function of Imaginary Time 75

PAGE

CHAPTER 4 : SELF-ENERGIES OF THE S- AND D-ELECTRON 82

4.1 Recoil Contribution to the d-electron Self-energy, $\Sigma_d^{rec}(i\omega_n)$ ... 88

4.2 Recoil Contribution to the s-electron energy, $\Sigma_s^{rec}(i\omega_n)$ ... 102

CHAPTER 5 : ELECTRONIC PROPERTIES OF THE NORMAL STATE ALLOY 106

5.1 The Electronic Specific Heat ... 106

5.2 Residual Resistivity 112

5.3 Concluding Remarks ... 118

PART TWO : THE SUPERCONDUCTING STATE ... 119

CHAPTER 6 : INTRODUCTION 120

6.1 The Nambu-Schrieffer Method ... 123

6.2 The s- and d-electron self-energies ... 127

6.3 The Effect of Recoil on the Superconducting Transition Temperature of Al-Mn and Al-Cr 133

6.4 The Energy Gap Equation ... 140

6.5 The Superconducting Density of States 144

6.6 Calculation of the Energy Gap Δ_G at Zero Temperature 145

		PAGE
CHAPTER 7 :	THERMODYNAMIC FUNCTIONS ...	162
7.1.	Thermodynamic Properties of the Superconducting Alloy for $T \approx T_c$	162
7.1.1	The Energy Gap	162
7.1.2	The Electronic Specific Heat ...	165
7.1.3	The Critical Magnetic Field H_c	169
7.2	Thermodynamic Properties for $T << T_c$	170
7.2.1	The Energy Gap	170
7.2.2	The Electronic Specific Heat ...	176
CHAPTER 8.1	DISCUSSION OF RESULTS ...	180
8.2	CONCLUSION	185
APPENDIX A :	k-summation of the s-electron Green's function $G_k(\omega)$ ...	187
APPENDIX B :	Frequency Summations used in text	190
REFERENCES	... ...	193

LIST OF FIGURES AND TABLES

FIGURES PAGE

CHAPTER 1

1. Experimental ΔT_c vs Concentration for Aluminium Systems (After Boato et al[1]) ... 17

2. ΔT_c vs n_i for Zn-Co, Zn-Fe and Zn-Ni (ibid.) 18

3. $\rho(T)$ vs T 29

4. ΔT_c vs n_i for Zn-Cr and Zn-Mn (op. cit) 34

CHAPTER 2

5. d-electron spectral weight function $A_d(\omega)$ vs ω 44

6. Magnetic/non-magnetic behaviour of the alloy 45

CHAPTER 3

7. Pictorial representation of some functions 64

8. Zero-temperature diagrams in coordinate space 67

9. Zero-temperature diagrams in momentum-frequency space 71

10. Dyson equation in diagram form ... 73

11. Examples of self-energy diagrams at finite temperature 80

PAGE

CHAPTER 4

12. (a), (b) : S- and d-electron self-energy diagrams - repeated Scattering at the same impurity site 85

(c) Scattering at different impurity sites 86

13. Contour used in the self-energy calculations 91

14. Plot of $G_1(\Theta_D/T)$ vs T/Θ_D ... 98

15. Plot of $\Gamma_{eff}(T)$ vs T/Θ_D for Al-Mn and Al-Cr 99

CHAPTER 5

16. Hartree-Fock Approximation for $\Sigma^{\sigma}_{dd}(\omega)$ (First-order in U)... ... 108

17. Plot of $\rho(T)$ vs n_i :

(a) $E_d = 0.5$ eV; $T/\Theta_D = 0.2$ and 2.0 115

(b) $E_d = 1$ eV; $T/\Theta_D = 0.2$ and 2.0 116

(c) $T/\Theta_D = .2$; $G_1(\Theta_D/T) = 1.19$ and $\Gamma_{eff}(T) = .1732$ eV; $E_d = 0$ eV, .5 eV and 1 eV ... 117

...

CHAPTER 6

19. Nambu-Schrieffer representation of the self-energy $\hat{\Sigma}_s(i\omega_n)$ and $\hat{\Sigma}_d(i\omega_n)$ ... 128

20. Plot of normalized superconducting density of state $N(\omega)/N(0)$ vs ω/Δ_{00} ... 146

21. Plot of zero-temperature normalized gap Δ_{G0}/Δ_{00} vs n_i 149

PAGE

22. Plot of $\Delta T_c / T_{co}$ vs n_i for Al-Mn and Al-Cr ... 152

23. Plot of g_{eff} vs n_i : (a) Al-Mn ... 159
(b) Al-Cr ... 160

CHAPTER 7

24. Plot of $\Delta_G(T) / \Delta_{00}$ vs T/T_{co} for Al-Mn and Al-Cr ... 175

25. Specific Heat vs temperature ... 179

TABLES

CHAPTER 5

I. Data used in the analysis - pure Aluminium 100

II. Summary of experimental results on Al-Mn and Al-Cr (Aoki and Ohtsuka; Boato et al) 100

CHAPTER 6

III. ΔT_c vs n_i for Al-Mn and Al-Cr ... 159

IV. Summary of results of present analysis on Al-Mn and Al-Cr ... 157

CHAPTER 7

V. Data used by Martin [52] ; and Kiwi and Zuckermann [6] 168

INTRODUCTION

Alloys of iron-group (i.e. 3-d transion metal) impurities in simple metals (e.g. Cu, Zn, Al) have received much attention both experimentally and theoretically by several authors [1-3, 15-18]. In particular, the experimental work of Boato et al has revealed that the normal state resistivity $\rho(T)$ and the superconducting transition temperature T_c at low impurity concentration are strongly affected by the presence of these impurities. It is generally accepted that systems such as Zn - Fe, Al - Mn and Al - Cr do not sustain any magnetic moment, even though the impurities are by themselves magnetic. On the other hand, Zn-Mn, Zn-Cr and Cu-Fe have well-defined moments.

This thesis is concerned with the virtual recoil of the impurity atoms as a result of the scattering process, i.e. impurities are no longer considered as static scattering centres. The mechanism of "virtual recoil" is extended to the study of transition metal impurities in normal and superconducting hosts in the "non-magnetic" limit.

In Chapter 1, a review of previous work on dilute alloys of iron-group impurities in simple metallic hosts is given. The effects of magnetic and non-magnetic

impurities as well as localized spin fluctuations in both the normal and superconducting states are discussed. Chapter 2 deals with the Hamiltonian proposed by Anderson for handling problems on resonance scattering. There is also a section on the modification produced by the inclusion of the virtual recoil of the impurity. The Green's function formalism is introduced in Chapter 3 and the diagrammatic method is thoroughly reviewed. Chapter 4 deals with the self-energies of s- and d-electrons. In Chapter 5 the electronic properties of the normal state of the alloy are obtained and estimates of the various physical quantities are also given.

The superconducting state is taken up in Chapter 6, where the Nambu-Schrieffer formalism is employed. The superconducting transition temperature T_c is depressed by the presence of transition metal impurities. However, when an additional attractive interaction between electrons due to the recoil of the impurity is included, the rate of depression of T_c is reduced.

Chapter 7 discusses thermodynamic properties of the superconducting alloy at temperatures close to T_c and close to $0^{\circ}K$. The results are then compared with the case when the impurities are assumed to be recoil-

less.

Chapter 8 gives a discussion of the results obtained and also concludes the thesis.

CHAPTER ONE

A REVIEW OF THEORIES ON THE EFFECTS OF IRON-GROUP IMPURITIES ON SUPERCONDUCTING AND NORMAL STATE PROPERTIES

1.1 NON-MAGNETIC SUPERCONDUCTING ALLOYS

The main interest in the study of superconducting alloys is to find the effects of the minor constituent (impurity) on the superconducting transition temperature T_c. Experimentally it has been observed that non-magnetic superconducting alloys, such as Al-iron group alloys, show a gradual decrease in T_c with increasing impurity concentration n_i. The initial decrease of T_c with n_i, $(\partial T_c / \partial n_i)_{n_i = 0}$ for the Al-Mn system is $9.1^{\circ}K/at.\%$. A lower rate of decrease has been observed for aluminium and zinc doped with non-transition metal impurities. See Figs. (1) and (2).

Coles [13] and also Boato et al [1] suggested that the decrease in T_c is due to the existence of a virtual bound state at each impurity site. Boato et al analysed their experimental results by making use of two different theories. Firstly, they used the theory of Markowitz and Kadanoff which deals essentially with a non-transition metal impurity in a superconducting matrix

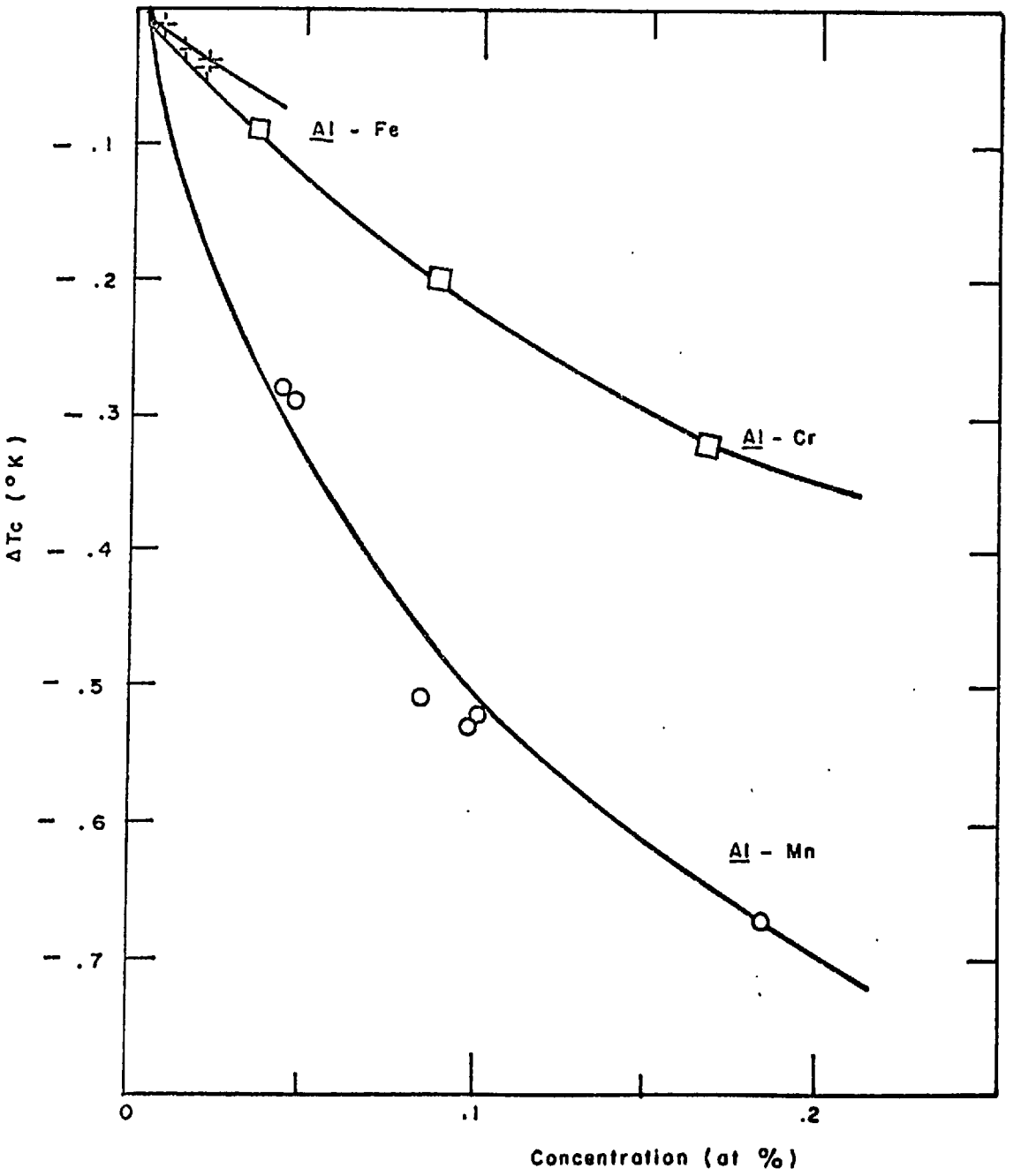


Fig. 1

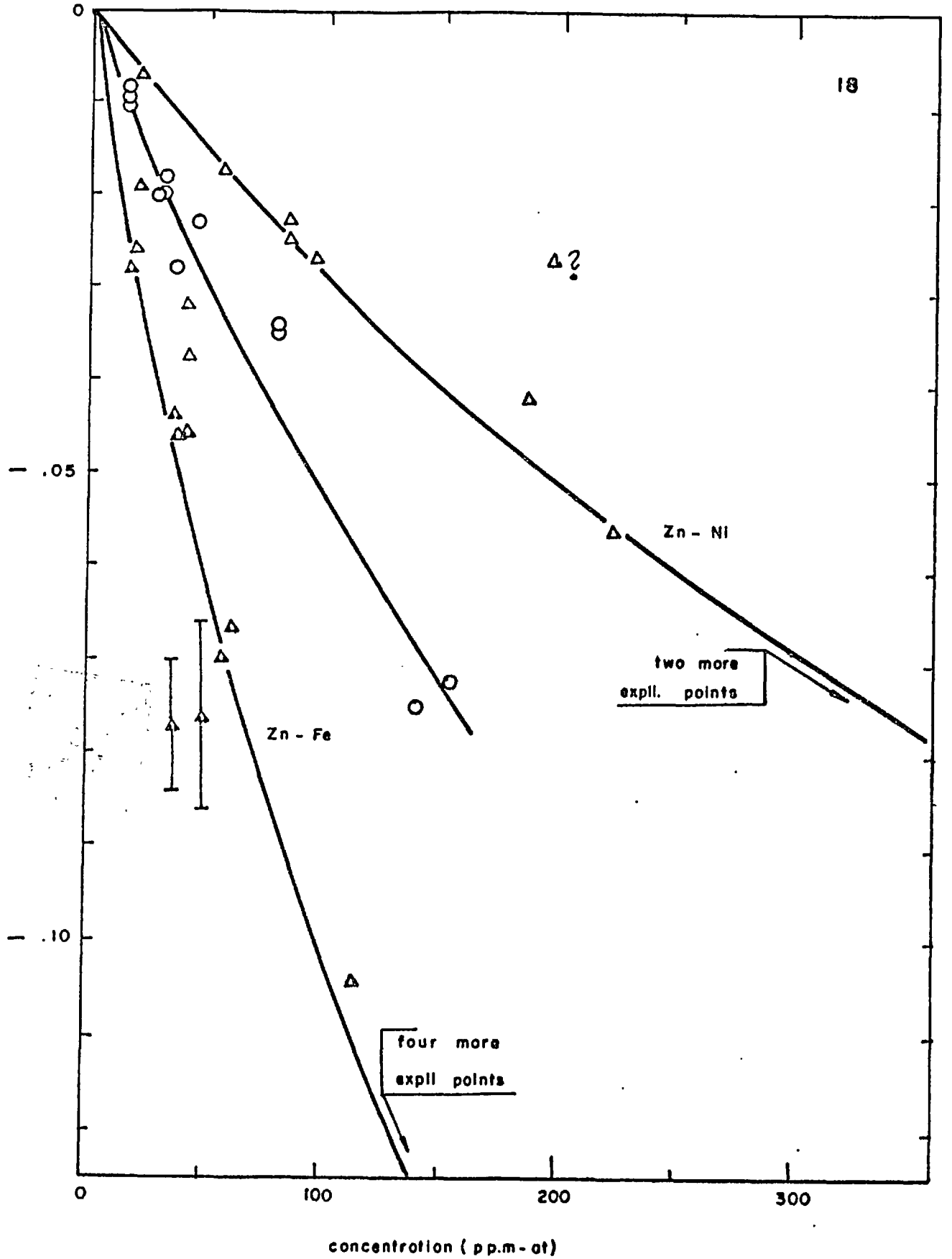

0
18
.05
.10
Zn - Ni
two more
expll. points
Zn - Fe
four more
expll points
0
100
200
300
concentration (p.p.m - at)

Fig. 2

and considers the smearing-out of the gap anisotropy which results from mean free path effects, in such cases the depression of T_c is usually small. Secondly, they used the theory of resonance scattering from the virtual d-level of an impurity [5]. This theory is based on the Anderson [15] model of the non-magnetic impurity in a simple metal host in the limit $\Gamma >> U$, where Γ is the half-width of the d-resonance and U is the intra-atomic Coulomb d-d repulsion. For an isotropic superconductor, the transition temperature T_c depends on n_i, Γ, and the energy of the resonance state E_d with respect to the Fermi energy ϵ_F of the host. The decrease of T_c with impurity concentration is greatest when the resonance level is very close to the Fermi level and is negligible in the limit $|E_d - \epsilon_F| >> \Gamma$. * See below

Zuckermann and Singh [11] later extended the theory of resonance scattering in dilute superconducting alloys to include the anisotropy of the host matrix. They concluded that

$$\Delta T_c = (\Delta T_c)_{res} + (\Delta T_c)_{anis} + (\Delta T_c)_{cross} \quad \ldots \quad 1.1$$

where ΔT_c is the total change in T_c, $(\Delta T_c)_{res}$ refers to the contribution from resonance scattering

* The resonance has the greatest effect on T_c when it is very close to the Fermi level because the density of electron states is largest in this case.

anisotropy of the host and $(\Delta T_c)_{across}$ is a cross-term between the first two contributions. It turns out that $(\Delta T_c)_{cross}$ is very small compared with the other two and so can be neglected. Eq. (1.1) is of the same form as the result obtained by Markowitz and Kadanoff for non-transition metal impurities and so justifies the analysis of Boato et al.* The relationship applies only to those alloys in which the resonance level is close to the Fermi level of the host, such as in Al-Mn and Al-Cr alloys. For the other aluminium-iron group alloys, Zuckermann and Singh suggested that the difference in valence between the impurity and host ions must be taken into account.

In order to clarify the nature of superconductivity in the dilute non-magnetic superconducting alloys, Kaiser[16] made a detailed self-consistent calculation of the excitation spectrum and order parameter of the alloys. He showed that these dilute non-magnetic superconducting alloys are essentially BCS superconductors, in which the pairing interaction is weakened as a result of the intra-atomic Coulomb d-d repulsion. By contrast, in the

---

* However, in the case of non-transition metal impurities there is no effect due to resonance scattering, since the phase shifts are all small. By contrast, for transition metal impurities, one of the phase shifts becomes large. In consequence the decrease in T_c becomes much greater.

strongly. This is discussed further in Section 1.5.2.

1.2 Localized Spin Fluctuation in a Superconductor

In recent years, localized spin fluctuations (LSF) at the impurity site have been suggested to explain the gradual decrease of T_c with n_i for aluminium-iron group alloys and, in particular, Al-Mn [17-21]. Using the renormalized random phase approximation (RRPA), Zuckermann obtained the following expression for the initial decrease in T_c with n_i :

$$\left.\frac{\partial T_c}{\partial n_i}\right|_{n_i=0} = -\frac{N_d(0)}{N(0)}\alpha\left\{Z_1 + \frac{\Gamma_\alpha/\Gamma_s Z_1}{1+\Gamma/(\Gamma_s Z_1}\right\}\ldots \quad 1.2$$

where

$$\alpha = \ln\left(\frac{1.14\omega_D}{kT_c}\right) \quad \ldots \quad 1.3$$

and $N_d(0) = 5/\pi\Gamma$ is the d-electron density of states in absence of the localized spin fluctuations. Γ is the half-width of the resonance, Γ_s is the inverse life-time of the LSF, $Z_1 = \left(\frac{\partial \Sigma^{sf}}{\partial \omega}\right)_{\omega=0}$ is the renormalization constant due to the LSF and Σ^{sf} is the LSF contribution to the d-electron self-energy. Ratto and d'Agliano [18] obtained the following expression by including correlations, but not LSF, in the limit $U << \pi\Gamma$:-

$$\left.\frac{\partial T_c}{\partial n_i}\right|_{n_i=0} = -\frac{N_d(0)}{N(0)}\,\alpha\left\{1+\frac{1}{5}N_d(0)\,U_{eff}\,\alpha\right\} \qquad 1.4$$

where $U_{eff} = U/(1+\pi\Gamma)$ ... 1.5

In order to compare Zuckermann's result with that of Ratto and d'Agliano, eq. (1.2) is rewritten as

$$\left.\frac{\partial T_c}{\partial n_i}\right|_{n_i=0} = -\frac{N_d^{eff}(0)}{N(0)}\,\alpha\left\{1+\frac{1}{5}N_d^{eff}(0)\,U_{eff}^{s}\,\alpha\right\} \qquad 1.6$$

where

$$N_d^{eff}(0) = N_d(0)\;Z_1 \qquad \ldots \quad 1.7\,a$$

and

$$U_{eff}^{s} = \frac{\pi\Gamma^2/\Gamma_s Z_1}{1+\Gamma/\Gamma_s Z_1} \qquad \ldots \quad 1.7\,b$$

Comparing eqs. (1.5) and (1.7 b), we see that U can be replaced by U^s which is given by

$$U^s = \pi\Gamma^2/\Gamma_s Z_1 \qquad \ldots \quad 1.8$$

Thus the localized spin fluctuations tend to enhance the d-electron density of states by the factor Z_1. Also the effective interaction U_{eff}^{s} depends on the parameter of the resonance level and the inverse lifetime of the LSF.

The RRPA is applicable to fast spin fluctuations, where a moment is not sustained at the impurity site as in the case of Al-Mn and Al-Cr.

1.3 Non-magnetic Alloys in the Normal State

For the class of alloys in which no magnetic moment is sustained at the impurity site, it has always been assumed that $\rho_{res}(T)$ is temperature-independent [5,11]. Recent measurements by Caplin [22] on Zn-Fe and by Caplin and Rizutto [23] on Al-Mn and Al-Cr have, however, revealed the presence of a weak low-temperature resistance minimum. These alloys are traditionally regarded as non-magnetic. Also a negative T^2-dependence that is practically independent of impurity concentration was found for the residual resistivity. The implication of the weak minimum is that a moment is trying to form at the impurity site. As a result, these alloys are not really "non-magnetic", but may rather be described as "weakly magnetic". The T^2-dependence has been explained by Caplin and Rizutto on the "localized spin fluctuation" (LSF) theory of Rivier et al [24]. They expressed their result in the form

$$\rho_{res}(T) = \rho_o \left\{ 1 - \left(\frac{T}{\theta} \right)^2 \right\} \qquad \ldots \quad 1.9$$

where Θ is some characteristic spin fluctuation temperature. $\Theta = 560^{o}K$ for Al-Mn and $\Theta = 1200^{o}K$ for Al-Cr and ρ_o is the residual resistivity at $0^{o}K$.

The theoretical expression for $\rho_{res}(T)$ obtained by Rivier et al shows the Kondo singularity in the high temperature limit $\Gamma_s < kT$, for $\Gamma >> E_d > 0$, where Γ_s is the inverse life-time of the spin fluctuations. Their expression for this limit is

$$\rho_{res}(T) = \frac{n_i \Gamma}{\pi N(0)} \left\{ \Gamma^2 + E_d^2 \left[1 + \frac{U}{\pi\Gamma} \ln\left(\frac{2kT + 1/\tau_o}{\Gamma}\right)\right]\right\}^{-1} \quad \ldots \quad 1.10$$

In the low temperature limit, $kT >> 1/\tau_s$, they obtained the following result for Al-Mn :

$$\rho_{res}(T) = \rho_o \left(1 - A \tau_s^2 T^2\right), \quad (E_d = 0) \quad \ldots \quad 1.11$$

where

$$A = \frac{1}{3} \pi^2 \left(\frac{U}{\pi\Gamma}\right) \left(1 + \frac{2U}{\pi\Gamma}\right) \sim 10 \quad \ldots \quad 1.12$$

For RRPA, $\rho_{res}(T)$ is given by [55]

$$\rho_{res}(T) = \rho_o\left(1 - (T/\Theta)^2\right) \quad \ldots \quad 1.13$$

where

$$\frac{1}{\Theta^2} = \frac{\pi^2 k^2}{3\Gamma^2} \left(\frac{3}{2} \frac{\Gamma^2}{\Gamma_s^2} + Z_1\right) \quad \ldots \quad 1.14$$

1.4. Virtual Recoil of the Impurity

All the earlier theories on resonance scattering have assumed that the d-electrons do not recoil when the conduction electrons are scattered off them. In order

to throw more light on the peculiar behaviour of Al-Mn for which the resonance scattering is strongest, a study is made of the effect of the d-electron recoil. This is characterized by the creation or annihilation of virtual phonons at the impurity site.* See below

1.4.1 Normal State

In the normal state, the inclusion of the d-electron recoil leads to the modification of the admixture term H_{sd} in the Anderson Hamiltonian and results in inelastic scattering of the conduction electrons. This situation is analogous to the inelastic, diffuse reflections in x-ray spectra as opposed to the recoil-less or elastic Bragg reflections. Again in Mossbauer effect, the sharp γ-ray line corresponds to the recoil-less emission of the γ-ray, while the broad background is due to the recoil of the atom.

Since the recoil of the impurity introduces an additional scattering channel for the d-electrons to hop onto the conduction band and vice versa, some modifications in the normal state properties of the alloy are to be expected. An enhancement in the

* The inclusion of the recoil processes into the analysis is an attempt to obtain a better agreement with the experimental results of Beato et al and Aoki and Ohtsuka on the aluminium iron group alloys.

of the resonance is also affected, resulting in the modified d-electron density of state as well as a change in the residual resistivity.

The effect of virtual recoil on the thermopower of dilute alloys of Na, Rb, Cs in K has been studied by Nielson and Taylor[25]. They found some contribution to the thermopower of these alloys as a result of the virtual recoil mechanism. Taylor[26] has also employed the same mechanism to explain the anomalous behaviour in the specific heat of the same alloys at low temperatures. Using the free electron model, which is applicable to these alloys, Taylor obtained the following result

$$C_e = C_e^o (1 - \rho / \rho_o) \qquad \ldots \qquad 1.15$$

where C_e is the electronic specific heat of the alloy and C_e^o is that of the pure specimen: ρ and ρ_o are the resistivities of the alloy and host, respectively. He predicted a 0.2% change over the rigid band calculation for K-Na with 2.4 at.% Na.

For Ag-Pd and Ag-Cd the Bloch model is applicable and it is found that the virtual recoil mechanism explains fairly adequately the observed discontinuity

in the slope of C_e with concentration n_i. However, the mechanism fails to predict the absolute value of the electronic specific heat in these alloys.

1.4.2 Superconducting State

In the superconducting state, it is proposed that the recoil phonons lead to an additional pairing interaction between conduction and localized electrons. The interaction strength $g^{rec}(\omega_n)$ is different from the BCS coupling strength g. In the weak coupling limit, where the phonon exchange between electrons is replaced by an equivalent instantaneous interaction, the interaction strength g^{rec} is taken to be constant for electron energies less than the Debye energy as in BCS theory. The analysis indicates that the superconducting transition temperature T_c is greater than the values predicted by Ratto and Blandin[7] and Ratto and d'Agliano[18] for increasing concentration of impurity. The superconducting density of states of the alloy shows a similar structure to the BCS density of states for the pure specimen, confirming Kaiser's observation[16]. The density of states of the alloy is, however, strongly dependent on the impurity concentration. An enhancement of the energy gap is obtained and a similar effect

appears in other thermodynamic properties of the alloy, such as the specific heat jump at T_c and the critical magnetic field H_c.

1.5 Magnetic Alloys

We review, briefly, the class of alloys with well-defined magnetic moments, in contrast with the non-magnetic (or weakly magnetic) alloys discussed earlier.

1.5.1 Kondo effect in the Normal State

The magnetic alloys exhibit the familiar Kondo anomaly [27], namely, the resistivity $\rho(T)$ shows a minimum at low temperatures. Fig. (3). The temperature at which the minimum appears, T_m, usually depends on the impurity concentration according to the empirical relation

$$T_m \sim n_i^{1/5} \qquad \ldots \qquad 1.16$$

The total resistivity is given by

$$\rho(T) = \rho_{res}(T) + \rho_{latt}(T) \qquad \ldots \qquad 1.17$$

where $\rho_{latt}(T)$ is the contribution from the ideal

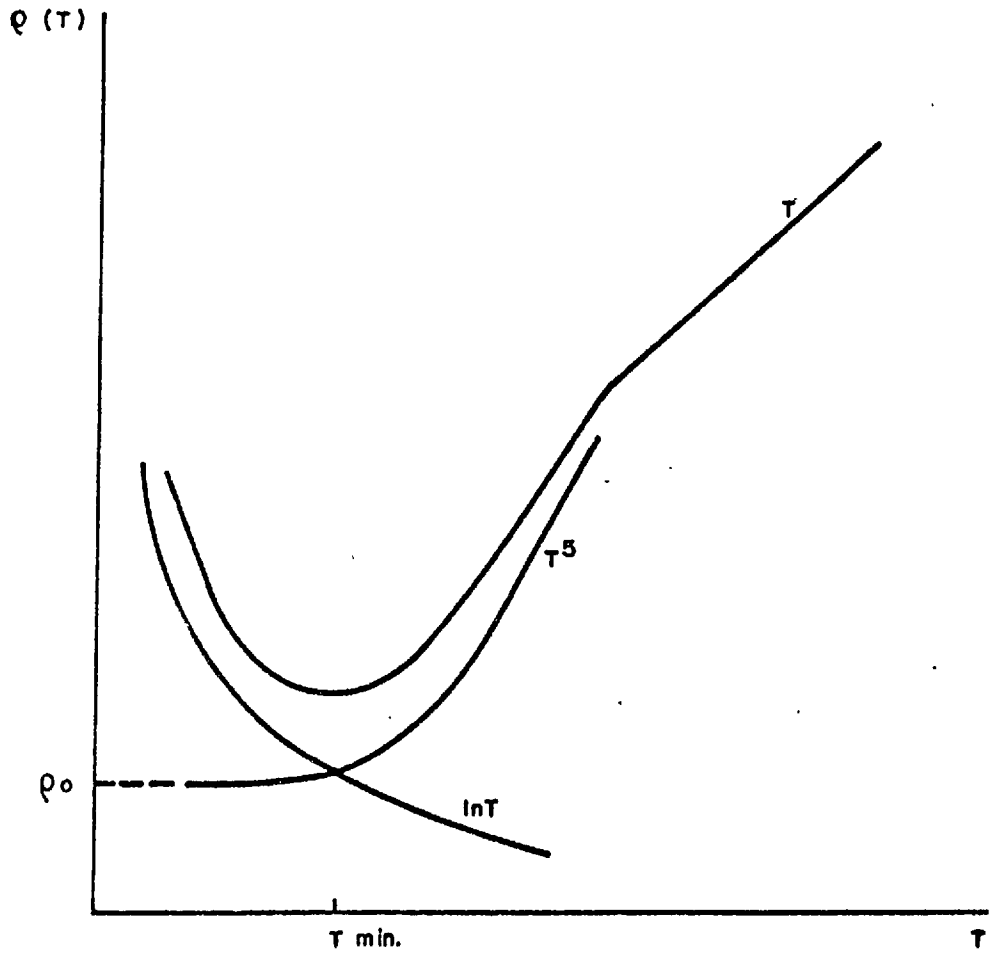


Fig. 3

lattice and $\rho_{res}(T)$ is the residual resistivity. At low temperatures ($T < \Theta_D/10$), $\rho_{latt}(T)$ has a T^5-dependence for a perfect lattice:

$$\rho_{latt}(T) = BT^5 \qquad \ldots \qquad 1.18$$

where B is a constant and Θ_D is the Debye temperature of the host.

The Kondo effect is due to the s-d exchange interaction H_{sd}^{ex}, which is given in the second quantization formalism by

$$H_{sd}^{ex} = -J \sum_{k,l} \sum_{ss'} (\underline{\sigma} \cdot \underline{S})_{ss'} a_{ks}^{+} a_{ls'} \qquad \ldots \qquad 1.19$$

where $\underline{\sigma}$ is the Pauli spin matrix and J is the coupling constant of the exchange interaction between the conduction electrons and the localized spin. For a resistance minimum to show up, J must be negative, that is, the coupling must be antiferromagnetic.

a_{ks}, a_{ks}^{+} are the annihilation and creation operators for the conduction electron of momentum $\underline{k}$ and spin s.

Kondo calculated the residual resistivity to third order in perturbation theory (i.e. the second Born approximation) and obtained the following expression :

$$\rho_{res}^{K}(T) = \rho_o \left\{ 1 - |J| \ln(kT/\epsilon_F) \right\} \quad \ldots \quad 1.20$$

provided that there exists a sharp Fermi surface. ρ_o is the residual resistivity at $T = 0^oK$ and depends on the spin S of the impurity as well as the coupling constant J for the s-d exchange interaction, viz

$$\rho_o \sim n_i J^2 S(S + 1) \quad \ldots \quad 1.21$$

Doniach [28] and Abrikosov [29] extended the perturbation theory to all orders and showed that the resistivity becomes infinite (i.e. an instability appears in the system) at a temperature T_K, called the Kondo temperature. T_K is given by

$$k T_K = \epsilon_F e^{-N/(2N(0)|J|)}, \quad (J < 0) \quad \ldots \quad 1.22$$

where N is the total number of atoms in the crystal.

In his study of the s-d interaction Hamiltonian of eq. (1.19), Nagaoka [30] employed the double-time Green's function method and a decoupling scheme on the lines used by Zubarev [31] for the study of superconductivity. Nagaoka showed that near the Fermi surface and at very low temperatures, a cloud of conduction electrons with spin antiparallel to that of the impurity

is formed around the impurity. A quasi-bound state between the conduction electron and the localized impurity spin appears and the impurity spin is compensated by singlet pairing. This effect is known as the Abrikosov-Suhl-Nagaoka condensation. The compensation is assumed to be complete at $T = 0^{\circ}K$, which is called the unitarity limit. The scattering is assumed to be maximum in this limit.

For $T << T_K$, Nagaoka solved a set of self-consistent equations for two unknown averages which appeared in his theory. He then obtained an anomalous resonance of width $\Gamma(T)$ which decreased continuously with increasing temperature, becoming negligible for $T >> T_K$. His calculation of the residual resistivity for $T < T_K$ disagreed with Abrikosov's result.

Bloomfield and Hamann [32] solved Nagaoka's equations exactly and showed that there was no instability at $T = T_K$. Rather they obtained a smooth transition from $T << T_K$ to $T > T_K$.

1.5.2 Kondo Effect in the Superconducting State

The experiments of Collings et al [2], Hedgcock and Muir [3] as well as Boato et al [1] confirm the existence of magnetic moments in some dilute superconducting alloys such as Zn-Mn, and Zn-Cr. These alloys exhibit

a steep initial drop in the superconducting transition temperature T_c with impurity concentration n_i, in the dilute limit. The linearity is most pronounced in Zn-Mn as shown in Fig. (4) where the initial decrease in T_c, $(\partial T_c / \partial n_i)_{n_i = 0} \sim 300^{\circ}K/at.\%$. Such alloys have been analysed by Abrikosov and Gorkov [33], by Zuckermann [34] and Zittartz and Mueller-Hartmann [50] who extended the Nagaoka's decoupling scheme to include the BSC pairing, by Liu [35], Maki [36], Skalski et al [37], Griffin [38] and Bannemann [39]. Exchange interactions between the conduction electrons and the impurity spin inhibits the formation of Cooper pairs. This pair-breaking which is due to spin-flip scattering is reflected in the decrease of T_c. Superconductivity is completely destroyed at a certain critical impurity concentration n_i^c, i.e. T_c vanishes at n_i^c. An interesting feature of the theories of Abrikosov and Gorkov (op. cit.) and Skalski et al (op. cit.) is that at any temperature below T_c, there is a range of impurity concentration for which the superconductor becomes gapless. The impurity concentration n_i then satisfies the relation $0.9\, n_i^c < n_i < n_i^c$.

In order to contrast the Kondo problem with the localized spin fluctuation (LSF) problem, the strong

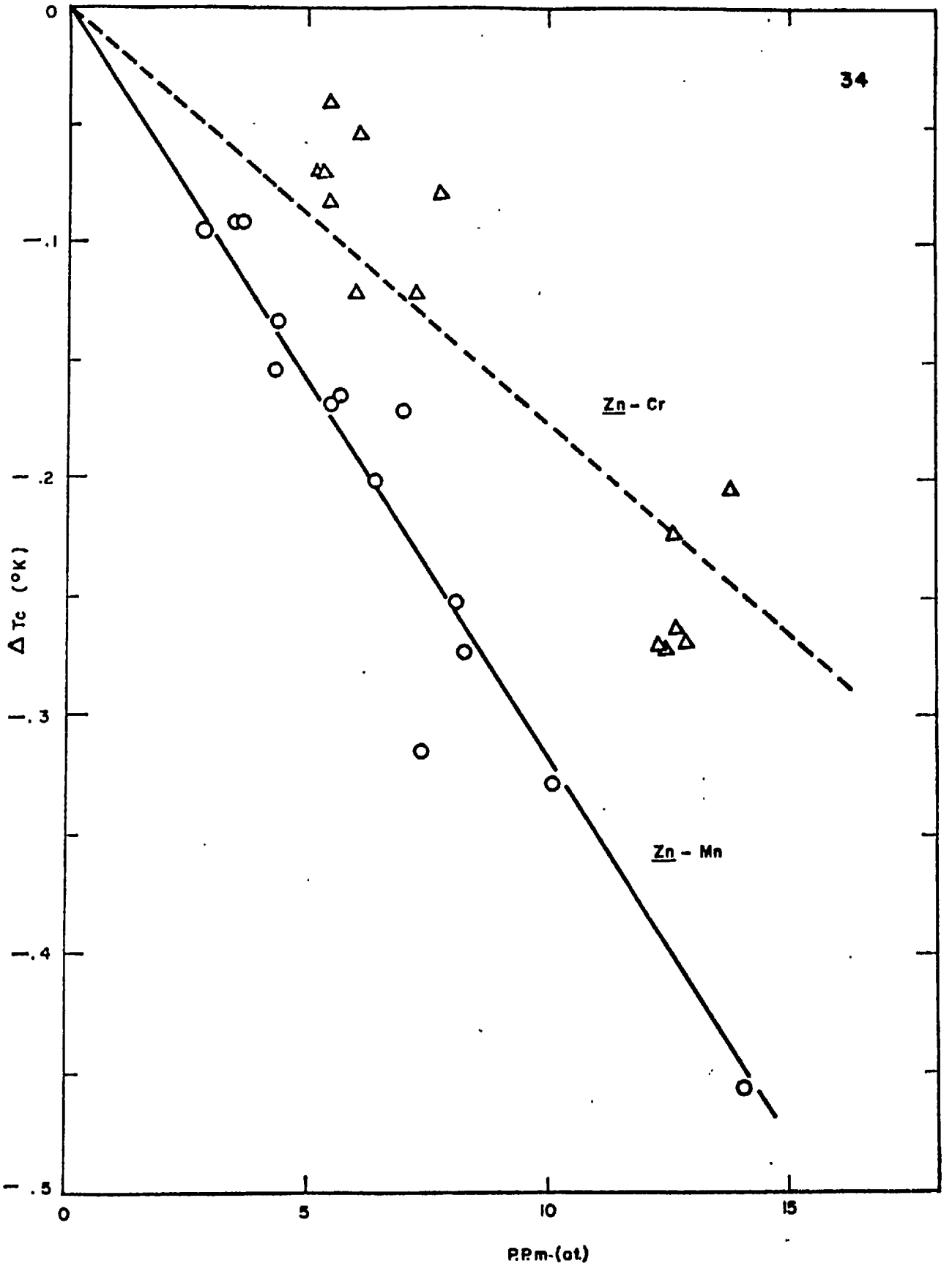


Fig. 4

magnetic limit of the LSF theory of dilute superconducting alloys[21] is considered. In this limit ($U >> \Gamma$), the lifetime of the fluctuations is large compared with the thermal energy kT_c, i.e. $\tau_s = \Gamma_s^{-1} >> kT_c$. The suppression of the superconducting transition temperature T_c with impurity concentration n_i is given by[21]

$$\left(\frac{\partial T_c}{\partial n_i}\right)_{n_i=0} = -\frac{5 n_i \Gamma}{2\pi N(0) k\, \Xi(T_{co})} \left\{ \alpha k T_{co} + \frac{\pi}{2} \Xi^{\frac{1}{2}}(T_{co}) \right\} \quad \ldots \quad 1.23$$

where $\Xi(T) = kT\, t^N(\omega_n = 0)$ and $\alpha = \ln(2\gamma\omega_D/\pi kT_{co})$. $t^N(\omega_n)$ is the t-matrix in the normal state. At $T = T_c$, $\Xi(T_c) \gg \Gamma^2 \gg (kT_c)^2$. Hence the second term on the right hand side of eqn (1.21) is much greater than the first term which can, therefore, be neglected. The second term is due to the pair-breaking effect of the spin-fluctuations and this effect gives the dominant decrease in T_c.

Zuckermann, accordingly, concluded that the transition temperature is :

$$\ln \frac{T_{co}}{T_c} \approx \psi\left(\tfrac{1}{2} + \frac{1}{\pi k T_c \tau_s}\right) - \psi\left(\tfrac{1}{2}\right) \quad \ldots \quad 1.24$$

where $\psi(x)$ is the digamma function and τ_s is given in the RRPA and for $\Xi(T_c) \approx U^2$ by

$$\tau_s^{-1} = \frac{5 n_i \Gamma}{2 \pi N(0) U} \qquad \ldots \qquad 1.25$$

The decrease in T_c given by eq. (1.24) is identical to that obtained by Abrikosov and Gorkov for impurities with well-defined localized spin in the Born approximation. However, the theory as it stands at present does not give satisfactory expression for $\tau_s(T)$. It is conjectured that a more detailed theory may include Kondo's logarithmic temperature term.

In the case of the well-defined moment the suppression of T_c with n_i due to pair-breaking effect of the localized spin is given by [33]

$$\ln \frac{T_{co}}{T_c} \Big|_{AG} = \psi\left(\frac{1}{2} + \frac{1}{\pi k T_c \tau_{AG}}\right) - \psi\left(\frac{1}{2}\right) \qquad 1.26$$

where τ_{AG} is the relaxation time of the conduction electrons due to the spin disorder scattering. τ_{AG} is given by

$$\tau_{AG} \approx \frac{3 n_i}{16} \pi N(0) |J|^2 \qquad \ldots \qquad 1.27$$

J is the coupling constant of the exchange interaction between the conduction electrons and the localized spin.

PART ONE

NORMAL STATE ALLOYS

CHAPTER TWO

2. INTRODUCTION : RESONANCE SCATTERING

Alloys of transition metal impurities in non-transition metal hosts (e.g. Cu, Al, Zn) have been successfully described using either of two models. One is due to Friedel and the other due to Anderson.

2.1 Friedel's Virtual Bound State

Friedel[40] considered the scattering of conduction electrons by a single impurity in a simple metal. The presence of the impurity causes an extra potential $\delta V_\sigma(r)$ at the impurity site, and a corresponding charge difference ΔZ. Here σ is the spin direction ($\uparrow$ or $\downarrow$) of the conduction electron.

In order to calculate properties of the system in terms of the phase shifts δ_l^σ between the incident and scattered components of the l-th spherical harmonics, the Schrödinger equation is solved self-consistently for the radial wave function. The only assumption made about the impurity is that the charge difference ΔZ between the host ion and the impurity is specified.

By considering the total displaced charge $\Delta\rho$ inside a sphere of large radius R, Friedel derived the condition for charge neutrality inside the sphere to be

$$\Delta Z = \frac{2}{\pi} \sum_{l=0} (2l + 1)\, \delta_l(k_F) \qquad 2.1$$

This is the Friedel sum rule, which gives the self-consistency condition on the potential.

Resonance scattering occurs for a given quantum number l when the phase shift $\delta_l = 0$ and when $l \neq l'$. Only an s-wave resonance will be considered here. In this case, $\delta_0(k_F) \sim \pi/2$. This so-called resonance constitutes the virtual bound state of Friedel and its effect is not felt outside the region of the perturbing potential. Only Rudermann-Kittel type oscillations remain in the regions outside the perturbing potential. This term is, however, small and is neglected.

$\delta_l(k_F) > 0$ corresponds to charge accumulation while $\delta_l(k_F) < 0$ corresponds to charge deficit.

2.2 The Extra-orbital Model of Anderson

Anderson [15] proposed that the introduction of iron-group impurities into a non-transitional metal matrix leads to the formation of virtual bound states at energy ϵ_d within the conduction band of the host.

These localized states are resonance scatterers for the conduction electrons. He assumed that the impurity orbital $\varphi_d(r)$ must be orthogonal to the conduction states $\psi_k(r)$, i.e. $(\psi_k, \varphi_d) = 0$. In addition, the spin-up and the spin-down electrons on a particular d-orbital repel each other by the intra-atomic Coulombic force. Mixing between the conduction and localized states leads to a broadening of the virtual level. Let the coupling constant of the Coulombic force be U and let the half-width of the virtual level (assumed for simplicity to be at the Fermi level) be Γ. Then in the limit $U \ll \pi\Gamma$, the impurity will be non-magnetic, whereas in the limit $U \gg \pi\Gamma$, the impurity should possess a well-defined magnetic moment. This was first pointed out by Anderson. However, Anderson's Hartree-Fock theory is incorrect, since it demands an unequal occupation of spin-up and spin-down d-states, thereby destroying spin-rotational invariance.

2.3 Anderson Hamiltonian for the one impurity problem

The model proposed by Anderson to describe a transition metal impurity in non-transition metal host is described formally by the following Hamiltonian :

$$H = H_{os} + H_{od} + H_{sd} + H_{dd} \quad \ldots \qquad 2.2$$

H_{os} gives the kinetic energy of the free electrons of the conduction (i.e. s) band of the host and is expressed as

$$H_{os} = \sum_{k\sigma} \epsilon_k \, a^{+}_{k\sigma} \, a_{k\sigma} \qquad \ldots \qquad 2.3$$

The summation is performed over all electron momentum and spin states. $a^{+}_{k\sigma}$ $(a_{k\sigma})$ represents the creation (annihilation) operator of the s-electron of spin σ and momentum $\underline{k}$. ϵ_k is the energy of the conduction electrons relative to the Fermi energy of the host. H_{od} is the non-interacting Hamiltonian associated with the single d-orbital, i.e. the localized d-state of the transition metal impurity. This is written as

$$H_{od} = \sum_{\sigma} (+ \epsilon_d) \; c^{+}_{d\sigma} \, c_{d\sigma} \qquad 2.4$$

The energy ϵ_d is measured relative to the Fermi energy of the host and is negative. $c^{+}_{d\sigma}$, $c_{d\sigma}$ creates and annihilates, respectively, a d-electron of spin σ.

H_{sd} gives the mixing term between the conduction and localized states. The change in potential at the impurity site causes a d-electron to 'hop' into the conduction band and vice versa. H_{sd} is written in terms of the overlap matrix element $V_{kd} = V_{dk}^{*}$ as

$$H_{sd} = \sum_{k\sigma} (V_{kd}\, a_{k\sigma}^{+}\, c_{d\sigma} + \text{h.c.}) \qquad 2.5$$

Finally H_{dd} describes the intra-atomic Coulomb repulsion between localized spin-up and spin-down electrons and is given by

$$H_{dd} = \sum_{\sigma} U\, c_{d\sigma}^{+}\, c_{d\sigma}\, c_{d,-\sigma}^{+}\, c_{d,-\sigma} = \sum_{\sigma} U\, n_{d\sigma}\, n_{d,-\sigma} \qquad 2.6$$

where U is the atomic Coulomb repulsion which is given by

$$U = \iint d^3r_1\, d^3r_2\, \varphi_d^2(r_1)\, \frac{e^2}{|r_1 - r_2|}\, \varphi_d^2(r_2) \qquad 2.7$$

and $n_{d\sigma}$ is the occupation number for the d-electrons of spin σ. Non-resonance scattering has been ignored in the Hamiltonian of eq. (2.1), in view of the fact that contribution from resonance scattering plays the dominant role in these alloys [4-12].

An important consequence of the non-zero overlap integral V_{kd} between the conduction and localized

states is that the localized states are broadened into a resonance of width 2Γ, where

$$\Gamma = \pi N(0) \langle |V_{kd}|^2 \rangle_{FS} \quad \ldots \quad 2.8$$

as shown in Fig. (5). The average is taken over all all momenta at the Fermi level and will, henceforth be written as $|V|^2$.

In the absence of s-d admixture, H_{dd} causes a splitting of the d-level. As mentioned earlier, the position of the d-level as well as the size of U determines the magnetic or non-magnetic behaviour of the system.

Let us introduce the notation

$$\epsilon_{\pm} = (\epsilon_d + U/2) \pm U/2 \quad \ldots \quad 2.9$$

Then if $\epsilon_+, \epsilon_- < 0$ or $\epsilon_+, \epsilon_- > 0$, no magnetic moment is associated with the localized state. On the other hand, if $\epsilon_+ > 0$ and $\epsilon_- < 0$, then a moment appears on the localized state. These different situations are shown in Fig. (6). In the non-magnetic case, the s-d admixture is so strong that it swamps out the splitting of the d-level.

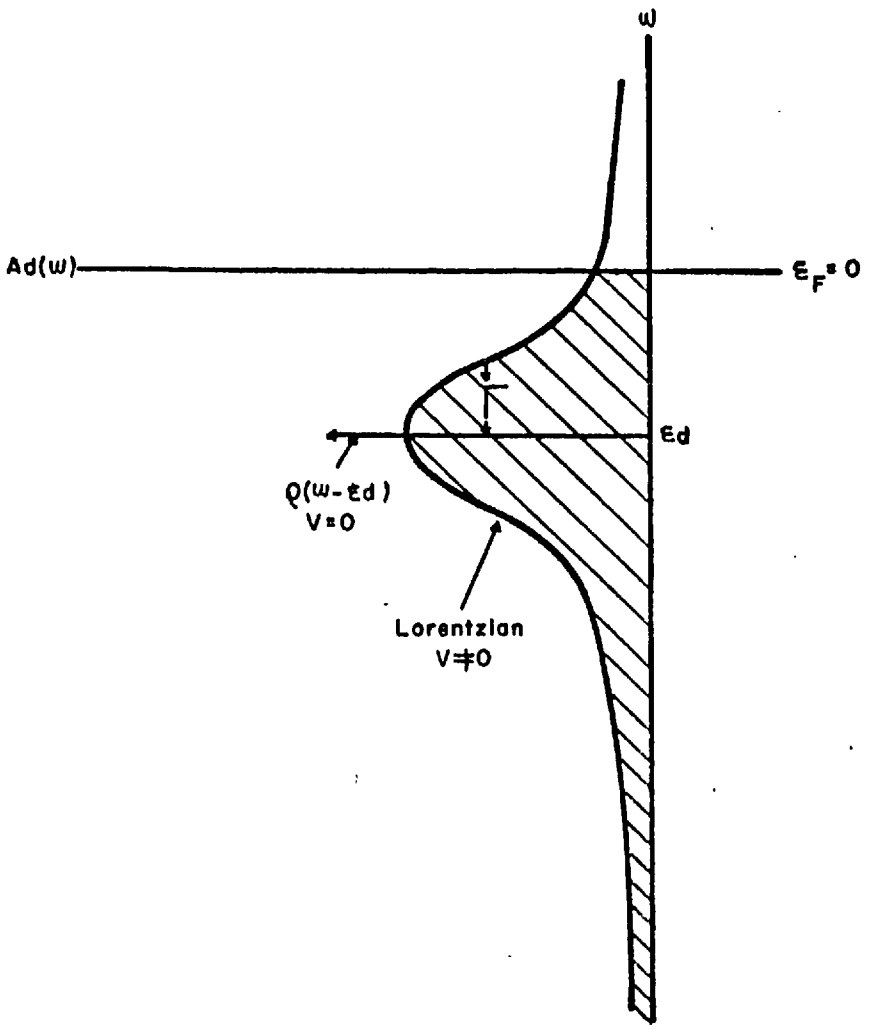
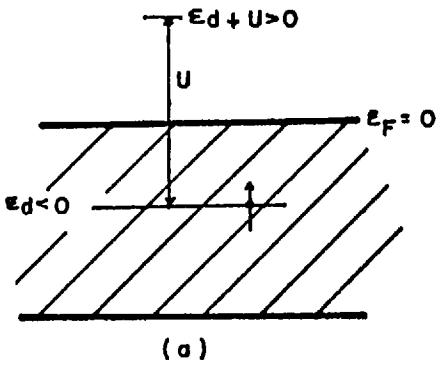
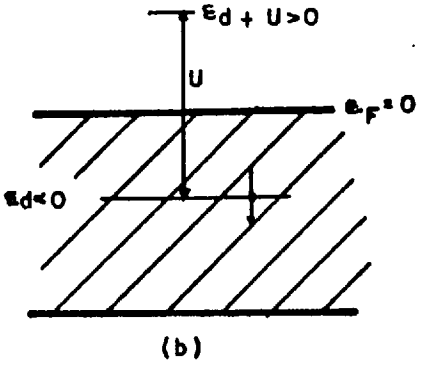


Fig. 5



(a)

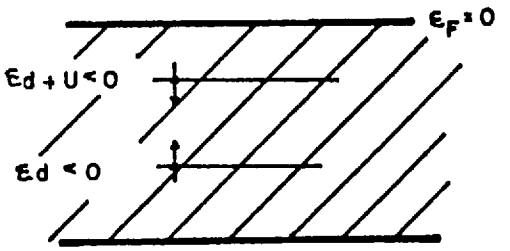
positive moment



(b)

negative moment

(a) and (b) time-reversed partners



(c)

no moment

Fig. 6

2.4 The Anderson Hamiltonian Extended to the Case of Many Impurities

In order to study transport properties, e.g. the resistivity of the alloy, the Anderson Hamiltonian has to be extended to the case of many impurities. The impurities are assumed to be distributed randomly at sites $\underline{R}_i$ $(i = 1, 2, 3, ...)$ and their concentration is assumed to be low. In this limit, impurity-impurity correlations are neglected. We also assume that the host matrix is isotropic. This assumption enables us to leave out all anisotropy as well as mean free path effects of Markovitz and Kadanoff[14]. The Hamiltonian now takes the form

$$H = H_{os} + H_{oi} + H_{si} + H_{ii} \qquad \ldots \qquad 2.10$$

where H_{os} remains the same as in eq. (2.3).

$$H_{oi} = \sum_{i=1}^{N_i} \sum_{\sigma} (+\epsilon_i)\, c_{i\sigma}^{+}\, c_{i\sigma} \qquad \ldots \qquad 2.11$$

having included the summation over the impurity sites i. $c_{i\sigma}^{+}$ $(c_{i\sigma})$ creates (annihilates) a d-electron of spin σ at the i-th impurity site and N_i is the number of impurities.

Similarly, we have

$$H_{si} = \sum_{i=1}^{N_i} \sum_{k\sigma} \left\{ V_{ki}\, e^{ikR_i}\, a^{+}_{k\sigma}\, c_{i\sigma} + \text{h.c.} \right\} \qquad 2.12$$

and

$$H_{ii} = \sum_{i=1}^{N_i} \sum_{\sigma} U\, n_{i\sigma}\, n_{i,-\sigma} \qquad \ldots \qquad 2.13$$

2.5 Virtual Recoil Contribution to the Normal State Hamiltonian

We now introduce virtual recoil processes into the Anderson scheme i.e. as a result of the resonance scattering the impurity atom recoils; hence there is a certain probability of a phonon being emitted. To second order in perturbation theory, the emitted phonon may be reabsorbed when the electron is scattered again at the same impurity site. This additional scattering channel leads to a modification of the s-d admixture term. The hopping of a d-electron into the conduction band is now described by

$$H'_{sd} = \sum_{k\sigma} V_{kd}\, e^{i\underline{k}(\underline{R}_o + \delta\underline{R})}\, a^{+}_{k\sigma}\, c_{d\sigma} \qquad 2.14$$

for the case of a single impurity located at the site $\underline{R}_o$.

Such a virtual phonon process is exhibited in the last diagram of Fig. 12a.

Here $\delta\underline{R}$ is the displacement of the impurity resulting from the recoil, and $\underline{R}_o$ is the equilibrium position. $\delta\underline{R}$ and the associated phonons are all virtual processes in nature.

To first order in the displacement, we have

$$H'_{sd} = \sum_{k\sigma} V_{kd}\, e^{i\underline{k}\underline{R}_o}\, (1 + i\underline{k}\cdot\delta\underline{R} + \ldots)\, a^+_{k\sigma}\, c_{d\sigma} \qquad 2.15$$

Phonon operators $b^+_{q\lambda}$ and $b_{q\lambda}$, are introduced and δR is written in terms of these operators as (G.7)

$$\delta\underline{R} = \sum_{q\lambda} \left(\frac{\hbar}{2MN\omega_{q\lambda}}\right)^{\frac{1}{2}} (b^+_{-q\lambda} + b_{q\lambda})\, \hat{e}_\lambda\, e^{iqR_o} \qquad 2.16$$

where $b^+_{q\lambda}$, $b_{q\lambda}$, respectively, creates and annihilates a phonon of frequency ω_q and polarization λ. $\hat{e}_\lambda$ is the unit polarization vector. Substitution for $\delta\underline{R}$ in eq. (2.15) gives :-

$$H'_{sd} = \sum_{k\sigma} V_{kd}\, a^+_{k\sigma} c_{d\sigma} \left[1 + i\underline{k} \sum_{q\lambda} |\alpha_{q\lambda}|\, (b^+_{-q\lambda} + b_{q\lambda}) \cdot \hat{e}_\lambda\right] \qquad 2.18$$

where the impurity site $\underline{R}_o$ has been chosen as zero, for convenience, and

$$|\alpha_{q\lambda}| = \left(\frac{1}{2MN\omega_{q\lambda}}\right)^{\frac{1}{2}} ; \quad \hbar = 1 \qquad 2.19$$

In the case of many impurities the modified admixture term becomes

$$H_{si}' = \sum_{i=1}^{N_i} \sum_{k\sigma} \Big\{ V_{ki} \, e^{i\underline{k}\underline{R}^o_i} \, a^+_{k\sigma} \, c_{i\sigma} \Big[1 + i\underline{k} \sum_{q\lambda} |\sigma_{q\lambda}| \times (b^+_{-q\lambda} + b_{q\lambda}) \cdot \hat{e}_\lambda \, e^{iqR^o_i} \Big] + \text{h.c.} \Big\} \qquad 2.19$$

In the q-summation over the phonon states, terms for which $q = k$ are omitted, since they lead to coherent scattering in which momentum is conserved. Momentum is not conserved in the recoil interaction H_{si}, since it is an impurity scattering mechanism.

CHAPTER THREE

3 GREEN'S FUNCTION FORMALISM

The successful application of Green's functions in quantum electrodynamics has motivated its extension to other quantum mechanical calculations: e.g. the study of solid state phenomena, nuclear physics and scattering problems in elementary particle physics.

The Green's function $G(x,x';\ t,t')$ describes the propagation of an excitation in a given system. In fact, it gives the probability that a particle (e.g. an electron) injected into a many-particle system, such as a metal, at a point x' at a time t' will be found at another point x at a later time t.

In practice, the Fourier transform of $G(x,t)$ to momentum-frequency space, i.e. $G(k,\omega)$, is mostly used for the calculation of various physical properties of a many-body system.

The Green's function or propagator formalism permits the description of various processes taking place in a many-body system in terms of Feynman diagrams[41]. Each diagram corresponds to an appropriate mathematical expression in a fixed order of perturbation theory.

3.1 The Diagram Technique

The Feynman diagram method will be reviewed in the following sections. In Section 3.2 the Interaction representation of the operators employed to describe a system of interacting particles is described, while in 3.3 the Green's function $G_{AB}(t,t')$ is defined and then expressed in terms of the Interaction representation operators. Wick's theorem is discussed in Section 3.4. Finally, the rules for constructing Feynman diagrams in coordinate-time as well as momentum-frequency space are given in Sections 3.5 and 3.6, respectively.

3.2 The Interaction representation

The time development of the states of an interacting system of particles can be described in one of three ways. The usual approach is to solve the Schrödinger equation

$$i \frac{\partial \Phi^S}{\partial t} = H \Phi^S \qquad \ldots \qquad 3.1$$

where Φ^S is the wave-function of the system in the Schrödinger representation, in which Φ^S changes with time, but the operator H does not. The above equation can be solved formally to yield

$$\Phi^S(t) = e^{-iHt} \Phi^H \qquad \ldots \qquad 3.2$$

where $\Phi^H = \Phi^S(0)$ is independent of time. Suppose now that we have an operator φ. Then using eq. (3.2), we can find time development of its matrix elements, viz.

$$\varphi_{ij}(t) = \langle \Phi_i^S(t) | \varphi | \Phi_j^S(t) \rangle$$

$$= \langle \Phi_i^H | e^{iHt} \varphi e^{-iHt} | \Phi_j^H \rangle \qquad 3.3$$

With respect to the wave-function Φ^H, we may interpret eq. (3.3) as the matrix elements of the time-dependent operator

$$\varphi(t) = e^{iHt} \varphi e^{-iHt} \qquad \ldots \qquad 3.4$$

This gives us a new representation in which the state vector is independent of tome, i.e. $\Phi^H = \Phi^S(0)$. The time development of the system is, therefore, pushed onto the operators which satisfy the Heisenberg equation of motion

$$\frac{\partial \varphi}{\partial t} = i (H\varphi - \varphi H) = i \left[H, \varphi \right]_- \qquad 3.5$$

where $[\cdot\,,\cdot]_-$ is the equal time commutator. Φ^H is the Heisenberg representation of the state vector and

is related to the Schrödinger representation through eq. (3.2).

The third representation, which proves to be of great importance in quantum field theoretic method, is the Interaction representation of the state vector. This is intermediate between the Schrödinger and the Heisenberg representations. The Hamiltonian of the system is divided into two parts :

$$H = H_o + H_1 \qquad \ldots \qquad 3.6$$

where H_o is the non-interacting Hamiltonian and H_1 gives the interactions taking place in the system and carries a time-dependence.

We now carry out the following transformation on the Schrödinger wave-function $\Phi^S(t)$:

$$\Psi(t) = e^{iH_o t} \Phi^S(t) \qquad \ldots \qquad 3.7$$

Differentiating eq. (3.7) with respect to time and making use of eqs. (3.1) and (3.2), we obtain :-

$$i \frac{\partial \Psi(t)}{\partial t} = H_1(t) \Psi(t) \qquad \ldots \qquad 3.8$$

$H_1(t)$ is given by

$$H_1(t) = e^{iH_o t} H_1 e^{-iH_o t} \qquad \ldots \qquad 3.9$$

Both the state vector and the operators are now time-dependent. Any Schrödinger operator φ^S can be transformed into the Interaction representation $\varphi^I(t)$ as follows:-

$$\varphi^I(t) = e^{iH_o t} \varphi^S e^{-iH_o t} \quad \ldots \quad 3.10$$

and its time development is given by the equation

$$\frac{\partial}{\partial t} \varphi^I(t) = i \left[H_o , \varphi^I(t) \right]_- \quad \ldots \quad 3.11$$

This differs from eq. (3.5) in that only the non-interacting Hamiltonian H_o is involved. Also eq. (3.8) is just the Schrödinger equation with the full Hamiltonian replaced by the interacting Hamiltonian H_1. Eq. (3.7) gives the Interaction representation of the wave-function.

We go back to eq. (3.8) and solve for $\Psi(t)$. The usual procedure is to suppose that the value of $\Psi(t)$ is known at some time $t = t_o$. The equation is then transformed into an integral equation by integrating both sides with respect to t and evaluating it between $t = t_o$ and $t\,(t > t_o)$. This yields

$$\Psi(t) = \Psi(t_o) - i \int_{t_o}^{t} dt' \, H_1(t') \, \Psi(t') \quad \ldots \quad 3.12$$

The best way of solving this integral equation is to introduce a time-development operator $U(t, t_o)$ defined by

$$U(t, t_0) \mid \Psi(t_0) > = \Psi(t) \qquad \ldots \qquad 3.13$$

$U(t, t_0)$ satisfies the integral equation

$$U(t,t_0) = 1 - i \int_{t_0}^{t} dt' \, H_1(t') \, U(t', t_0) \qquad 3.14$$

and has the following properties:

$$\begin{aligned} &\text{(i)} \quad \text{It is unitary, i.e. } U U^{+} = 1 \\ &\text{(ii)} \quad U^{-1}(t,t_0) = U(t_0,t) = U^{+}(t,t_0) \\ &\text{(iii)} \quad U(t,t') = U(t,t_0) \; U(t_0,t') \end{aligned} \qquad 3.15$$

Eq. (3.14) is solved by iteration to yield the series

$$\begin{aligned} U(t,t_0) = 1 + (-i) \int_{t_0}^{t} dt_1 \, H_1(t_1) + (-i)^2 \int_{t_0}^{t} dt_1 \\ \times \int_{t_0}^{t_1} dt_2 \, H_1(t_1) \, H_1(t_2) + \ldots\ldots \\ \ldots + (-i)^n \int_{t_0}^{t} dt_1 \int_{t_0}^{t_1} dt_2 \ldots \int_{t_0}^{t_{n-1}} dt_n \\ \times \quad H_1(t_1) \, H_1(t_2) \ldots\ldots \; H_1(t_n) \end{aligned} \qquad 3.16$$

The n-th integral

$$I_n = \int_{t_0}^{t} dt_1 \int_{t_0}^{t_1} dt_2 \ldots \int_{t_0}^{t_{n-1}} dt_n \, H_1(t_1) \, H_1(t_2) \ldots \, H_1(t_n) \qquad 3.17$$

can be converted into an integral over the whole time interval from t_o to t with the restriction that t_k be earlier than t_{k-1} $(k < n)$, i.e. $t > t_1 > t_2 > \ldots\ldots\ldots\ldots > t_n > t_o$.

This enables us to rewrite I_n in the form

$$I_n = \frac{1}{n!} \sum_p \int_{t_o}^{t} dt_1 \int_{t_o}^{t} dt_2 \ldots \int_{t_o}^{t} dt_n \; H_1(t_{p1}) \; H_1(t_{p2}) \ldots H_1(t_{pn}) \ldots \quad 3.18$$

where $\sum_p$ denotes the summation over all permutations of the variables $t_1, t_2, \ldots\ldots t_n$; i.e. $t_1, t_2 \ldots t_n \rightarrow t_{p1}, \ldots\ldots t_{pn}$, and the ordering of the operators H_1 is maintained from left to right in order of decreasing time.

Next, we introduce the Dyson time-ordering operator P [42] such that

$$P\left\{H_1(t_1) \ldots H_1(t_n)\right\} = H_1(t_i) \ldots\ldots H_1(t_j) \ldots\ldots H_1(t_k) \ldots \quad 3.19$$

where

$$t_i > \ldots\ldots > t_j > \ldots\ldots\ldots > t_k .$$

The operators are then said to be in chronological order. The time-ordering operator P has the property of rearranging a product of time-labelled operators in the same order as the time sequence of their labels, with the latest one in time appearing first in the product. For example,

$$P\left\{ H_1(t_1)\, H_1(t_2) \right\} = \begin{cases} H_1(t_1)\, H_1(t_2), & \text{for } t_1 > t_2 \\ H_1(t_2)\, H_1(t_1), & \text{for } t_1 < t_2 \end{cases}$$

So we recast the n-th integral into the new form

$$I_n = \frac{1}{n!} \int_{t_o}^{t} dt_1 \int_{t_o}^{t} dt_2 \cdots \int_{t_o}^{t} dt_n\, P\left\{ H_1(t) \cdots\cdots H_1(t_n) \right\} \qquad \cdots \quad 3.21$$

Then eq. (3.16) may be written as

$$U(t,t_o) = \sum_{n=0}^{\infty} \frac{(-i)^n}{n!} \int_{t_o}^{t} dt \cdots \int_{t_o}^{t} dt_n\, P\left\{ H_1(t) \cdots H_1(t_j) \cdots \cdots H_1(t_n) \right\}$$

$$= P \exp\left\{ -i \int_{t_o}^{t} H_1(t')\, dt' \right\} \qquad \cdots \quad 3.22$$

We now make the assumption of 'adiabatic switching' i.e. the interaction H_1 is assumed to be turned on adiabatically at time $t = -\infty$ and turned off at time $t = +\infty$. The S-matrix of scattering theory is then defined as follows

$$S = U(-\infty, +\infty) \qquad \ldots \qquad 3.23$$

The adiabatic switching assumes that the ground state of the non-interacting system goes over adiabatically to the ground state of the interacting system with the evolution of time. The energy shift in the ground state and the Green's functions of the system are also assumed to be expressible in a power series in the interaction strength.

The Wick's chronological operator T will be used instead of the Dyson chronological operator P. This is defined in the same way as P except for a (-1) due to each fermion permutation, i.e.

$$T\{A(t)\,B(t')\} = \begin{cases} A(t)\,B(t'), & \text{for } t > t' \\ \eta B(t')\,A(t), & \text{for } t' < t \end{cases} \qquad 3.24$$

where $\eta = +1$ for boson operators and $\eta = -1$ for fermion operators. The S-matrix is written as

$$S = T \exp \left\{ -i \int_{-\infty}^{\infty} dt\, H_1(t) \right\} \quad \ldots \quad 3.25$$

The operator e^{iHt} can now be written in terms of Interaction representation operators. From eq. (3.7),

$$\Phi^S(t) = e^{-iH_0 t}\, \Psi(t) = e^{-iH_0 t}\, S(t,0)\, \Phi^S(0) \quad 3.26$$

where $\Phi^S(0) = \Phi^H(0) = \Psi(0)$

Also from eq. (3.2)

$$\Phi(t) = e^{-iHt}\, \Phi^S(0)$$

Hence

$$e^{-iH(t_1 - t_2)} = e^{-iH_0(t_1 - t_2)}\, S(t_1, t_2) \quad 3.28$$

Similarly

$$e^{iH(t_1 - t_2)} = S(t_2, t_1)\, e^{iH_0(t_1 - t_2)} \quad \ldots \quad 3.29$$

3.3 The Green's function

The one-particle causal Green's function is defined as follows :-

$$G_{AB}(t,t') = -i \langle 0 | T\{A^H(t)\, B^H(t')\} | 0 \rangle \qquad 3.30$$

where $A^H(t)$, $B^H(t)$ are operators in the Heisenberg representation, (3.4), and the coordinate indices have been surpressed. The average $\langle .... \rangle$ is taken over the true ground state $|0\rangle$ of H. Using eqs. (3.4) and (3.29), $A^H(t)$ is written as

$$\begin{aligned} A^H(t) &= e^{iHt}\, A^S\, e^{iHt} \\ &= S(0)\, e^{iH_0 t}\, A^S\, e^{-iH_0 t}\, S(t,0) \\ &= S(0,t)\, A^I(t)\, S(t,0) \qquad \ldots \qquad 3.31 \end{aligned}$$

where A^S and A^I stand for the Schrödinger and the Interaction representation, respectively, of the operator A.

The true ground state is written as follows in terms of the non-interacting ground state Φ_0 :

$$|0> = \Phi^H(0) = \Phi^S(0) = S(0,-\infty)\,\Psi(-\infty)$$

$$= S(0,-\infty)\,\Phi_0 \qquad \ldots \quad 3.32$$

where adiabatic switching has been invoked

Similarly

$$<0| = \Phi^{H^*}(0) = \Psi(\infty)\,S(\infty,0) \qquad \ldots \quad 3.33$$

$\Psi(\infty)$ can only differ from $\Psi(-\infty)$ by a phase factor and in consequence :-

$$\Psi(\infty) = S(\infty,-\infty)\,\Psi(-\infty) = e^{i\theta}\,\Psi(-\infty) \qquad 3.34$$

Eq. (3.30), together with eqs. (3.31-3.34), gives the following equation for the Green's function:-

$$G_{AB}(t,t') = -i\,e^{i\theta}<\Phi_0|\,S(\infty,0)\,T\{S(0,t)\,A(t)$$

$$x\;\; S(t,0)\,S(0,t')\,B(t')\;x$$

$$x\;\; S(t',0)\,S(0,-\infty)\}|\Phi_0> \qquad \ldots \quad 3.35$$

The phase factor θ is related to the S-matrix as follows:

$$e^{i\theta} = <\Phi_0|S(\infty,-\infty)|\Phi_0> = <\Phi_0|S|\Phi_0> \qquad 3.36$$

The final form for the Green's function is now obtained from (3.35) and (3.36) :-

$$G_{AB}(t,t') \quad -i\frac{\langle \Phi_o | T\{ A(t)\, B(t')\, S \} | \Phi_o \rangle}{\langle \Phi_o | S | \Phi_o \rangle} \quad \ldots \qquad 3.37$$

The operators $A(t)$ and $B(t')$ are in the Interaction representation.

3.4 Wick's Theorem

The calculation of the Green's function involves a product of a number of time-ordered terms resulting from the perturbation expansion of the S-matrix which may be written in terms of creation and annihilation operators in the Interaction representation. The basic theorem which gives the systematic way of writing down the expectation value of any time-ordered product of the creation and annihilation operators in terms of free-particle Green's function is called the Wick's theorem. It states that the non-interacting ground state average of the T-product of identical numbers of creation and annihilation operators in the interaction representation is equal to the sum of all possible paired averages involving a creation and an annihilation operator. The following example illustrates the theorem:

$$<T\{a_1(t_1)\, a_2(t_2)\, a_3^+(t_3)\, a_4^+(t_4)\}>_0$$

$$= <T\{a_1(t_1)\, a_4^+(t_4)\}>_0 <T\{a_2(t_2)\, a_3^+(t_3)\}>_0$$

$$+ \eta <T\{a_1(t_1)\, a_3^+(1_3)\}>_0 <T\{a_2(t_2)\, a_4^+(t_4)\}>_0$$

... 3.38

where $<\ldots\ldots>_0$ represents the average over the non-interacting ground state. Thus the problem has been reduced to one of calculating products of free particle Green's functions, viz

$$<T\{a_1(t_1)\, a_2(t_2)\, a_3^+(t_3)\, a_4^+(t_4)\}>_0$$

$$= G_{14}^0(t_1,t_4)\, G_{23}^0(t_2,\, t_3) + \eta\, G_{13}^0(t_1,t_3)\, G_{24}^0(t_2,t_4)$$

... 3.39

This decomposition permits the assignation of simple diagrams to the paired averages. Moreover, the diagrams give a pictorial representation of the processes taking place in a many-body system.

The free particle Green's function $G^0(x,x')$ is represented diagramatically by the solid line shown in Fig. (7a), where x represents the space-time point (r,t).

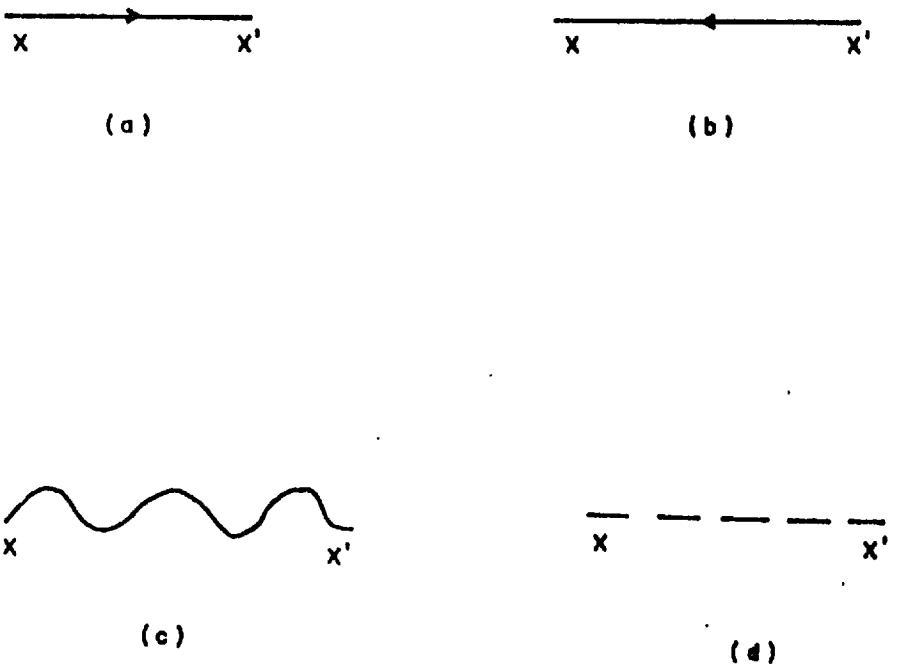


Fig. 7

The arrow indicates the direction of propagation. From now on $G^0(x,x')$ is used to represent a fermion propagator. Fig. (7 b) represents a free hole Green's function. The free phonon Green's function $D(x,x')$ is represented by the wavy lines shown in Fig. (7 c). The arrow is omitted since the phonon propagator is an even function of $(x-x')$. Finally an interaction line, e.g. the Coulomb interaction, is represented by the broken line shown in Fig. (7 d).

3.5

Rules for constructing Feynman diagrams occuring in the perturbation expansion of $G(x, x')$.

3.5.1 Diagrams in coordinate space

(i) Draw all topologically non-equivalent diagrams with $2n$ vertices and two external lines.

(ii) Denote by $G^0(x,x')$ a directed solid line from x to x' and by $v(x-x')$ the interaction (i.e. broken) line. The interaction line is assumed to be non-directional, viz, $v(r_1 - r_2) = v(r_2 - r_1)$ and instantaneous, that is, $v(x - x') = v(r-r')\,\delta(t-t')$.

(iii) Integrate over the coordinates of each vertex and sum over spin variables, viz. $\sum_{\sigma} \int d^3x$. Two solid lines and one broken line always meet at each vertex.

(iv) Multiply the expression obtained by the factor $(-1)^{n+F}$, where n is the order of the perturbation given by the number of interaction lines and F is the number of closed fermion loops in the diagram.

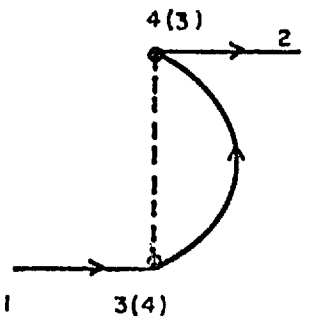
(v) Green's functions of the same time argument $G(0)$ are taken as $\lim_{t \to +0} G(-t)$.

Because of the homogeneity of space-time, the free particle propagators depend on $(x-x')$, i.e.

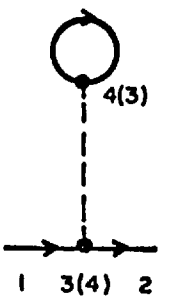
$$G^0(x,x') = G^0(x-x') = G^0(r-r' : t-t') \quad \ldots \quad 3.40$$

Examples of some typical diagrams are shown in Fig. (8). In Fig. (8 a), an electron undergoes exchange scattering against background particles. The analytical expression corresponding to this process is given by

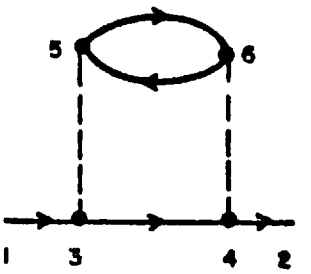
$$- \int d^4x_3 \, d^4x_4 \, G^0(1,3) \, G^0(3,4) \, G^0(4,2) \, v(3,4) \qquad 3.41$$



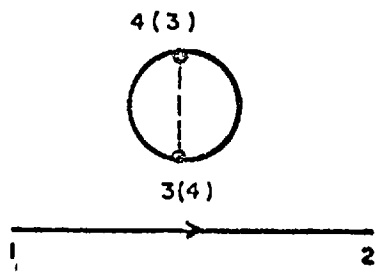
(a)



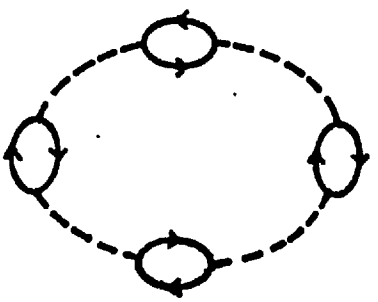
(b)



(c)



(d)



(e)

Fig. 8

where we have used the shorthand notation $i = x_i = (r_i, t_i)$; $i = 1,2,3,4$ and $d^4x = d^3r\, dt$.

In Fig. (8 b), the electron undergoes a forward scattering at (3) against the background and the corresponding expression is

$$\int d^4x_3\, d^4x_4\, G^0(1,3)\, G^0(3,2)\, v(3,4)\, G^0(0) \qquad \ldots \quad 3.42$$

The diagram representing $G^0(0)$ is particularly interesting. This represents a ground state - to - ground state excitation or a spontaneous rearrangement of the Fermi sea. All ground state diagrams do not have any particle or hole line in either the initial or final state, as is shown in Fig. (8 e). The mathematical expressions for all the other diagrams of Fig.(8) can be written down along the lines indicated. Fig. (8 d) is a typical example of a disconnected diagram. Figs. (8 a) - (8 c) are all connected diagrams.

3.6 Diagrams in momentum-frequency space for the perturbation expansion of $G(k,\omega)$

The evaluation of the integrals occurring in diagrams in coordinate-space is, generally, difficult since the free-particle functions are discontinuous functions of time. The Fourier transforms of these functions to momentum-

frequency space, however, are much simpler to compute. Hence actual applications of the diagrammatic method usually involve diagrams in momentum-frequency space. Another advantage is that conservation of momentum and energy (frequency) at each vertex is automatically built into the formalism.

3.6.1 Rules for evaluating diagrams in momentum-frequency space

(i) Draw all connected diagrams starting and ending with (k, ω, σ). When the system is not translationally invariant, the line starts with (k, ω, σ) and ends in (k', ω', σ'), say.

(ii) Associate a free particle Green's function $G^{o}_{\sigma}(k, \omega)$ with each solid line and $v(q)$ with each broken line.

(iii) Conserve all momenta, energy and spins at each vertex.

(iv) Integrate over all intermediate state momenta, and energies and sum over spins according to the prescription

$$\int \frac{d^3p}{(2\pi)^3} \quad , \int \frac{d\omega}{2\pi} \quad , \sum_{\sigma}$$

(v) Multiply by $(-1)^{n+F}$, where n is the order of the interaction (i.e. the number of broken lines) and F is the number of fermion loops.

We shall evaluate the diagrams shown in Fig. (9) as a demonstration of there rules - the results are as follows :

$$\text{Fig.9(a)} : \quad -\sum_{\sigma'} \int \frac{d^3k}{(2\pi)^3} \int \frac{d\Omega}{2\pi} v_k \, G^0_\sigma(p,\omega)\, G^0_\sigma(p,\omega) G^0_{\sigma'}(p-k,\, \omega-\Omega) \qquad \ldots \quad 3.40$$

$$\text{Fig.9(b)}: \quad v_0 G^0_\sigma(p,\omega)\, G^0_\sigma(p,\omega) \sum_{\sigma'} \int \frac{d^3p'}{(2\pi)^3} \int \frac{d\omega'}{2\pi} G^0_{\sigma'}(p',\, \omega') \qquad \ldots \quad 3.41$$

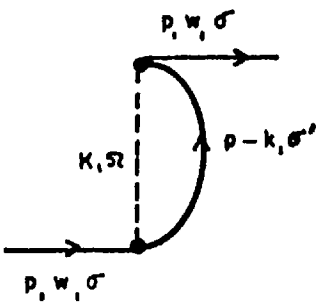
$$\text{Fig.9(c)}: \quad -G^0(p,\omega)G^0(p,\omega) \int \frac{d^3q}{(2\pi)^3} \int \frac{d\Omega}{2\pi} G^0(p-q,\, \omega-\Omega) \times$$

$$\times \int \frac{d^3p'}{(2\pi)^3} \int \frac{d\omega'}{2\pi} G^0(p',\omega')\, G^0(p'+q,\, \omega'+\Omega) \qquad 3.42$$

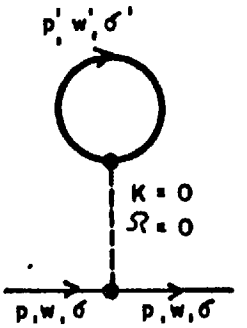
$$\text{Fig.9(d)} \quad -g^2 D^0(q,\Omega)\, D^0(q,\Omega) \int \frac{d^3p}{(2\pi)^3} \int \frac{d\omega}{2\pi}$$

$$\times \; G^0(p,\omega)\, G^0(p-q,\, \omega-\Omega) \qquad \ldots \quad 3.43$$

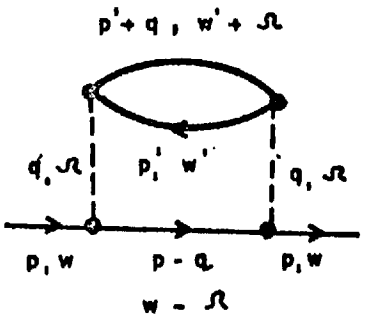
Each electron-phonon vertex is assigned a value g for


p, w, σ
K, Ω
p − k, σ'
p, w, σ

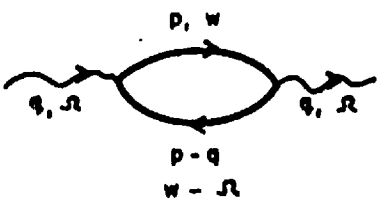
(a)


p', w', σ'
K = 0
Ω = 0
p, w, σ
p, w, σ

(b)


p' + q , w' + Ω
q, Ω
p', w'
q, Ω
p, w
p - q
p, w
w - Ω

(c)


p, w
q, Ω
q, Ω
p - q
w - Ω

(d)

Fig. 9

the coupling constant.

3.7 Dyson equation and the self-energy operator

In several applications of the diagramatic technique an infinite number of terms of the perturbation series has to be summed since several terms of the series give contributions of the same order of magnitude. Often the task is reduced to summing an infinite number of a particular class of diagrams.

All diagrams for the Green's function can be written in terms of the irreducible self-energy Σ. An irreducible diagram is one which cannot be split into two simpler diagrams by cutting a single fermion line.

The insertion of the self-energy parts leads to the modified or the full Green's function which is represented diagrammatically by Fig. (10) in momentum-frequency space. The mathematical expression corresponding to the diagrams is given by

$$G(k,\omega) = G^0(k,\omega) + G^0(k,\omega)\ \Sigma\ (k,\omega)\ G^0(k,\omega)$$

$$+ G^0(k,\omega)\ \Sigma\ (k,\omega)\ G^0(k,\omega)\ \Sigma\ (k,\omega)\ G^0(k,\omega)$$

$$+ \cdots\cdots\cdots$$

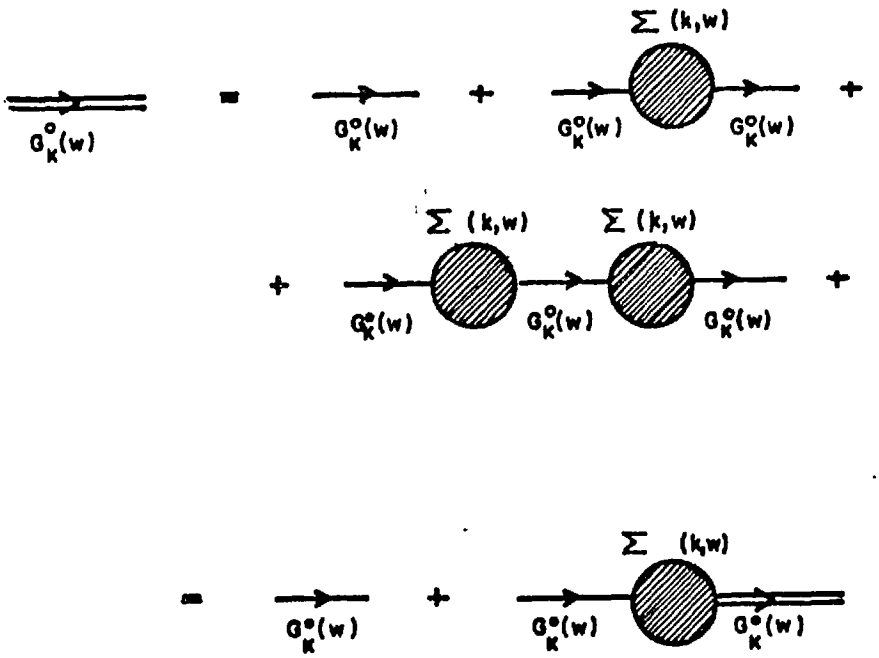

Σ (k,w)
$G^{\circ}_{K}(w)$
$G^{\circ}_{K}(w)$
$G^{\circ}_{K}(w)$
$G^{\circ}_{K}(w)$
Σ (k,w)
Σ (k,w)
$G^{\circ}_{K}(w)$
$G^{\circ}_{K}(w)$
$G^{\circ}_{K}(w)$
Σ (k,w)
$G^{\circ}_{K}(w)$
$G^{\circ}_{K}(w)$
$G^{\circ}_{K}(w)$

Fig. 10

or symbolically

$$G = G^0 + G^0 \Sigma G^0 + G^0 \Sigma G^0 \Sigma G^0 + \ldots\ldots\ldots$$

$$= G^0 + G^0 \Sigma G \qquad \ldots \qquad 3.44$$

where $\Sigma(k,\omega)$ is the sum of all irreducible self-energy parts, i.e.

$$\Sigma = \Sigma_1 + \Sigma_2 + \Sigma_3 + \Sigma_4 + \ldots\ldots \qquad \ldots \qquad 3.45$$

Eq. (3.34) is Dyson's equation. It is solved formally to give

$$G = \frac{G^0}{1 - G^0 \Sigma} = \frac{1}{(G^0)^{-1} - \Sigma} \qquad \ldots \qquad 3.46\,a$$

$$\text{i.e.} \quad G(k,\omega) = \frac{1}{\omega - \epsilon_k - \Sigma(k,\omega) + i\delta_k} \qquad \ldots \qquad 3.46\,b$$

where we used (G1, G2) the expression

$$G^0(k,\omega) = (\omega - \epsilon_k + i\delta_k)^{-1} \qquad \ldots \qquad 3.47\,a$$

$$\delta_k < 0, \text{ for } \epsilon_k > 0$$

$$\delta_k > 0, \text{ for } \epsilon_k < 0 \qquad \ldots \qquad 3.47\,b$$

The self-energy part $\Sigma(k,\omega)$ is, in general, a complex

function of ω and k. Its real part gives a shift in the energy ϵ_k of the electron while the imaginary part gives the life-time or the decay rate of the single electron state.

3.8 The Green's function of imaginary time (or the temperature-dependent Green's function)

At finite temperatures, any experimental observation is a statistical average over a large number of processes. As such, the Green's function is now defined in terms of the statistical average of the probability for all possible initial and final states of the system [43]. The definition of the Green's function involves a reformulation of the Heisenberg representation (see Matsubara [44])

An operator $\varphi(\tau)$ in the new interaction representation is given by

$$\varphi(\tau) = e^{\mathcal{H}_0 \tau} \varphi e^{-\mathcal{H}_0 \tau} \quad ; -\beta < \tau < \beta \qquad \ldots \qquad 3.48$$

where $\mathcal{H}_0 = H_0 - \mu N$ $\qquad \ldots \qquad 3.49$

The Hamiltonian $\mathcal{H}_0$ is now given in terms of the number

of particles in the system and the chemical potential μ, since our system is described by a grand canonical ensemble. The partition function Z is then given by

$$Z = e^{-\beta\Omega(\beta,\mu,V)} = Tr\, e^{-\beta(H-\mu N)} \quad \ldots \quad 3.50$$

where

$$\tilde{\Omega} = -\frac{1}{\beta} \ln Z(\beta,\mu,V) = -kT \ln Z(T,\mu,V) \quad 3.51$$

is the Landau thermodynamic function.

The S-matrix becomes

$$S(\tau_1, \tau_2) = T_\tau \exp\left\{-\int_{\tau_1}^{\tau_2} d\tau' H_1(\tau')\right\} \quad 3.52$$

where T_τ is the Wick's time-ordering operator at finite temperature.

Also we get

$$e^{-\mathcal{H}(\tau_1-\tau_2)} = e^{-\mathcal{H}_0(\tau_1-\tau_2)} S(\tau_1-\tau_2) \quad 3.53$$

By analogy with the zero temperature expressions of eqs. (3.24), (3.26) and (3.37) the expression for thermodynamic Green's function is given by :-

$$\mathcal{G}^{c}_{AB}(\tau\ \tau') = -\langle T_\tau \{ A^H(\tau)\ B^H(\tau') \} \rangle$$

$$= -\frac{\langle T_\tau \{ A(\tau)\ B(\tau')\ S(\beta) \} \rangle_0}{\langle S(\beta) \rangle_0} \quad \ldots \quad 3.54$$

where $A(\tau)$ and $B(\tau)$ are in the new interaction representation, and

$$\langle A \rangle_0 = Z^{-1}\, Tr \left\{ e^{-\beta \mathcal{H}_0} A \right\} \quad \ldots \quad 3.55$$

is the grand-canonical average over the non-interacting states, and Tr stands for the trace.

Also

$$S(\beta) = T_\tau \exp \left\{ -\int_0^\beta d\tau\, H_1(\tau) \right\} \quad \ldots \quad 3.56$$

Wick's theorem is again applicable to eq. (3.56) and diagrams are identical in form to zero temperature diagrams.

The Fourier transform of $\mathcal{G}_{AB}(\tau)$ is written :-

$$\mathcal{G}_{AB}(\tau) = \frac{1}{\beta} \sum_n e^{-i\omega_n \tau}\ \mathcal{G}_{AB}(\omega_n) \quad \ldots \quad 3.57$$

where [44]

$$\omega_n = (2n + 1)\frac{\pi}{\beta} \quad \text{for fermions}$$

and $$\omega_n = 2n\frac{\pi}{\beta} \quad \text{for bosons} \quad \ldots \quad 3.58$$

The rules for constructing diagram in the perturbation expansion of $_{AB}(\omega_n)$ are similar to those for the diagrams of Section 3.6.1 :

(i) Draw all connected, topologically non-equivalent diagrams, starting and ending with $(\underline{k}, \omega_n, \sigma)$. When the system is not translationally invariant, the diagrams start with $(\underline{k}, \omega_n, \sigma)$ and end up with $(\underline{k}', \omega_n', \sigma')$, say.

(ii) Associate a free particle Green's function $^{o}(\underline{k}, \omega_n)$ with each solid line, $v(\underline{q}, \omega_n)$ with each broken line and the free phonon Green's function $\mathfrak{D}^{o}(\underline{p}, \omega_n)$ with each wavy line.

(iii) Conserve all momenta and energies at each vertex.

(iv) Sum over all intermediate states according to the prescription.

$$\sum_{k} = \int \frac{d^3k}{(2\pi)^3} \; ; \quad \frac{1}{\beta} \sum_{m} \text{ and } \sum_{\sigma}$$

(v) Multiply by the factor $(-1)^{n+F}$ for n broken lines and F fermion loops.

The free particle Green's function $\mathcal{G}^{0}(\underline{k}, \omega_n)$ is given by (G1, G2)

$$\mathcal{G}^{0}(\underline{k}, \omega_n) = (i\omega_n - \tilde{\epsilon}_k)^{-1} \quad \ldots \quad 3.59\,a$$

where

$$\tilde{\epsilon}_k = \epsilon_k - \mu \quad \ldots \quad 3.59\,b$$

We shall write down the expressions for the self-energy diagrams shown in Fig. (11) :

$$11\,(a) \quad = \sum_{p} v(\underline{k}-\underline{p}) \frac{1}{\beta} \sum_{m} \sum_{\sigma'} \mathcal{G}^{0}_{\sigma'}(\underline{p}, i\omega_m) \quad \ldots \quad 3.60$$

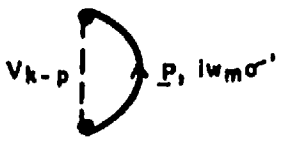
where the interaction is assumed to be instantaneous.

$$11\,(b) \quad = \frac{1}{\beta} \sum_{m} \frac{1}{\beta} \sum_{l} \sum_{q} \sum_{p'} \mathcal{G}^{0}(\underline{k}-\underline{q}, i\omega_n - i\omega_m)\, \mathcal{G}^{0}(\underline{p}', i\omega_l)$$

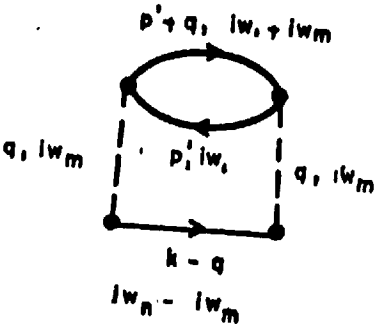
$$\times\, \mathcal{G}^{0}(\underline{p}' + q, i\omega_l + i\omega_m) \quad 3.61$$

$$11\,(c) \quad \Sigma(\underline{q}, i\omega_n) = \frac{1}{\beta} \sum_{m} \mathcal{D}^{0}(\underline{k}, i\omega_m)\, \mathcal{D}^{0}(\underline{k}-\underline{q}, i\omega_n - i\omega_m) \quad 3.62$$

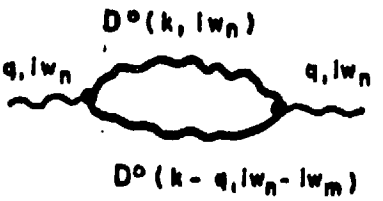
The frequency summation is performed by employing Poisson's summation formula. This formula converts the


V_{k-p}
$\underline{P}$, $iw_m\sigma'$

(a)


$p'+q$, $iw_{n'}+iw_m$
q, iw_m
p', $iw_{n'}$
q, iw_m
$k-q$
$iw_n - iw_m$

(b)


$D^o(k, iw_n)$
q, iw_n
q, iw_n
$D^o(k-q, iw_n - iw_m)$

(c)

Fig. II

summation over n into an integral over a contour C :

$$\frac{1}{\beta} \sum_{n} g(i\omega_n) = \int_C f(z)\, g(z)\, \frac{dz}{2\pi i} \qquad \ldots \qquad 3.63$$

$f(z)$ is the Fermi function which is given by $f(z) = (e^{\beta z} + 1)^{-1}$ where z is complex and $f(z)$ has poles at $z_n = (2n + 1)\frac{\pi}{\beta}$. The contour is taken around only the poles of $g(z)$.

CHAPTER FOUR

4. SELF ENERGIES OF THE s- AND d-ELECTRONS

The techniques outlined in Chapter Three are now employed to obtain the self-energies of the conduction(s) and localized (d) electrons in the normal state of the Al-iron group alloys.

The simple model of a parabolic band for the s-electrons of the host matrix, i.e. the nearly free electron approximation, is employed. The impurities are taken to be randomly distributed at sites $\underline{R}_i = 1, 2, \ldots\ldots N_i$) and their concentration n_i is low enough to neglect impurity-impurity correlations. Consequently all expressions must be linear in the parameter n_i. The Hamiltonian which describes the aluminium-iron group alloys is given in Sections 2.2-2.4.

The following thermodynamic Green's Functions for the problem are defined:

$$G^0(k,k';\tau) = -\langle T_\tau \{ a_k(\tau)\, a_{k'}^{\dagger}(0) \} \rangle$$

$$G^0(j,j';\tau) = -\langle T_\tau \{ c_j(\tau)\, c_{j'}^{\dagger}(0) \} \rangle$$

$$G^0(j,k;\tau) = -\langle T_\tau \{ c_j(\tau)\, a_k^{\dagger}(0) \} \rangle$$

$$G^0(k,j;\tau) = -\langle T_\tau \{ a_k(\tau)\, c_j^{\dagger}(0) \} \rangle \quad .. 4.1$$

where the statistical average is taken over the grand canonical ensemble. The operators a_k, a_k^+, c_j and c_j^+ are described in Sections 2.2 - 2.4.

Using the Hamiltonian of Sections 2.2 and 2.3, we set up equations of motion for the Fourier transforms of the Green's functions of eq. (4.1). In order to restore translational invariance to the system, averages are taken of all functions containing the impurity site vectors $\underline{R}_i$, assuming random impurity distribution[45]. In addition, the averages of a product of functions involving the impurity site vectors is replaced by a product of their averages. (See Abrikosov and Gorkov[33].)

A set of integral equations is then obtained for the Green's functions. The averaged Green's function for the s-electron becomes translationally invariant, i.e.

$$G(k,k' : i\omega_n) = G(k,i\omega_n)\,\delta_{kk'} \qquad \ldots \qquad 4.2$$

and that of the d-electron becomes independent of the impurity positions[5].

The self-energy parts Σ_s and Σ_d of the s- and d-electrons respectively are defined as follows in terms of the averaged Green's functions.

$$G_{\underline{k}}(i\omega_n) \equiv G(\underline{k},i\omega_n) = \left[i\omega_n - \epsilon_k - \Sigma_s(\underline{k},\, i\omega_n)\right]^{-1} \qquad 4.3$$

and

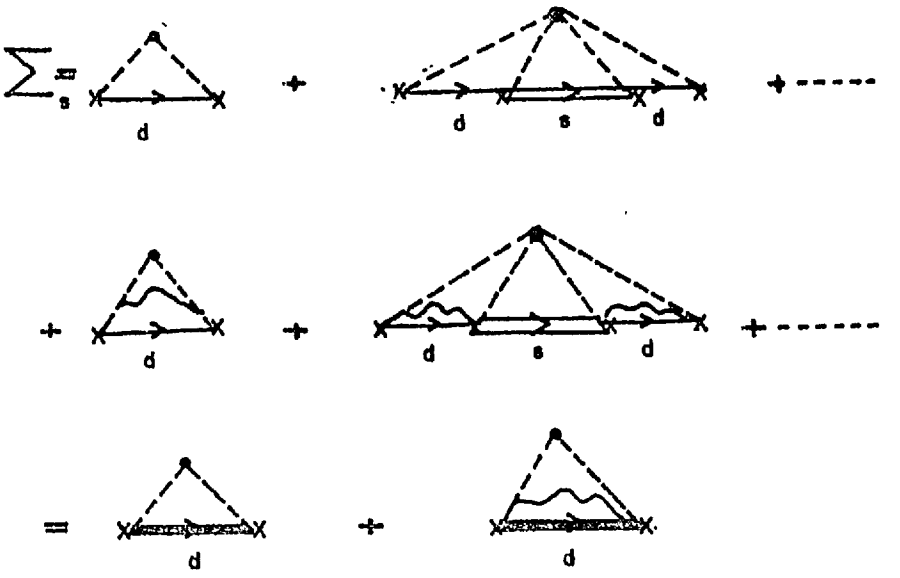
$$G_d\,(i\omega_n) = \left[i\omega_n - E_{d\sigma} - \Sigma_d\,(i\omega_n) \right]^{-1} \quad \ldots \quad 4.4$$

where $$E_{d\sigma} = -\epsilon_d + U \langle n_{d-\sigma} \rangle \quad \ldots \quad 4.5$$

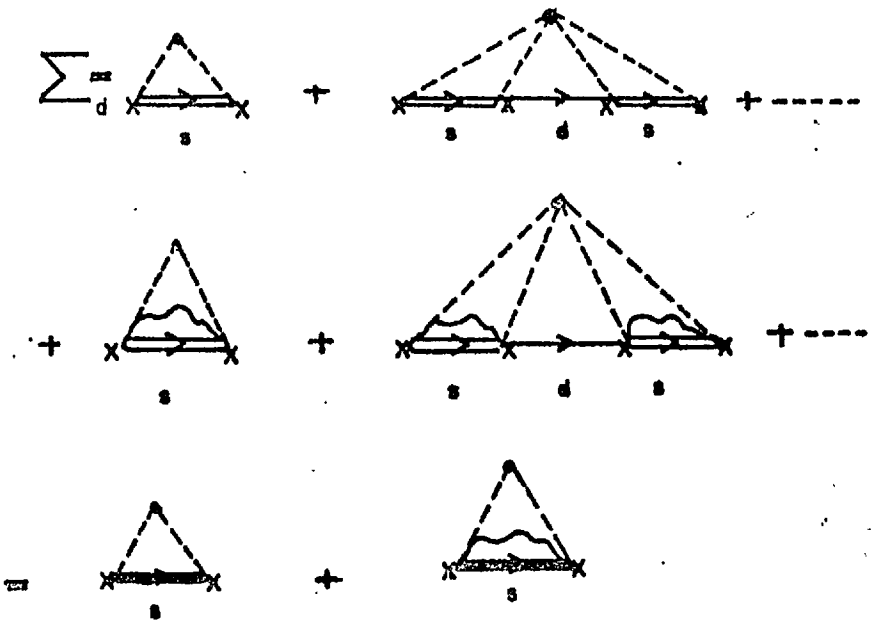
is the Hartree-Fock energy of the d-electron having spin σ. Here $G_{\underline{k}}(i\omega_n)$ and $G_d(i\omega_n)$ are the full s- and d-electron Green's functions, respectively. The self-energy diagrams are shown in Fig. (12). From the averaging procedure the significant contributions to the self-energy parts at low impurities concentration come from multiple scattering at the same impurity site. Hence diagrams such as Fig (12 c) can be neglected in our approximation (G1, and Reference 5).

Each self-energy part has two sub-diagrams: one is due to resonance scattering only and the other includes the virtual phonons due to the d-electron recoil. Only energy is conserved at the vertices where a virtual phonon line appears. Momentum is not conserved at these vertices because the interaction is local.

Analytical expressions for the self-energy parts are obtained from Fig (12). Fig. (12 a) gives

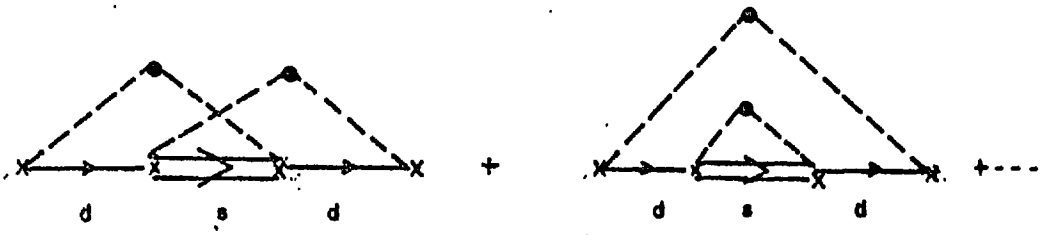


(a)



(b)

Fig. 12



(c)

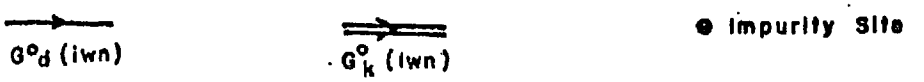




Fig. 12

This is possible in the non-magnetic limit for the following reason. The Anderson Hamiltonian for a degenerate impurity state includes an exchange interaction J between electrons of the same spin in different degenerate levels. The inclusion of such a term in a degenerate d-state gives rise to two new electronic levels (U - J) and (U + 4J). The state (U - J) is too low-lying and does not seem to affect the properties of the system. Only the level (U + 4J) is important and it is therefore sufficient to replace U by U + 4J or U_{eff} in the subsequent analysis. *

$$\Sigma_s(i\omega_n) = \Sigma_s^{res}(i\omega_n) + \Sigma_s^{rec}(i\omega_n)$$

$$= (2l+1)\, n_i |V|^2 G_d(i\omega_n) - (2l+1)\, n_i |V|^2$$

$$\times kT \sum_m G_d(i\omega_m)(i\underline{k}\cdot\hat{e}_\lambda) \sum_{q\lambda} |\alpha_{q\lambda}|^2$$

$$D_{q\lambda}(i\omega_n - i\omega_m) \qquad \ldots \quad 4.6$$

where the first term on the right hand side is due to resonance scattering only while the second term is due to the vertual phonons. $D_{q\lambda}$ is the phonon Green's function defined by

$$D_{q\lambda}(\tau) = -\langle T_\tau \{ \varphi_{q\lambda}(\tau)\ \varphi^+_{q\lambda}(0) \} \rangle \qquad \ldots \quad 4.7$$

It has been shown by Ratto and Blandin[7] that the effect of the degeneracy of the d-level is to introduce a factor $(2l + 1)$ into the expression for the self-energy of the s-electron.* For transition metal impurities, $l = 2$ and so the degeneracy factor is 5. The parameter n_i always goes with the degensracy factor $(2l+1)$, where l is the degeneracy.

* SEE ATTACHED INSET

The phonon field operator $\varphi_{q\lambda}$ is given by

$$\varphi_{q\lambda} = b_{q\lambda} + b^+_{-q\lambda} \qquad \ldots \quad 4.8.$$

$b^{+}_{q\lambda}$ ($b_{q\lambda}$) creates (annihilates) a bare phonon of wave vector q and polarization λ. Fig. (12 b) now gives Σ_d :-

$$\Sigma_d(i\omega_n) = \Sigma_d^{res}(i\omega_n) + \Sigma_d^{rec}(i\omega_n)$$

$$= |V|^2 \sum_k G_k(i\omega_n) - |V|^2 kT \sum_m \sum_k G_k(i\omega_m) \times$$

$$\times (i\underline{k}\cdot\hat{e}_\lambda)^2 \sum_{q\lambda} |\alpha_{q\lambda}|^2 D_{q\lambda}(i\omega_n - i\omega_m) \qquad 4.9$$

4.1. Recoil contribution to the d-electron self-energy, Σ_d^{rec}

The virtual recoil contribution to $\Sigma_d(i\omega_n)$ is given from eq. (4.9) by

$$\Sigma_d^{rec}(i\omega_n) = -|V|^2 kT \sum_m \sum_k G_k(i\omega_m) \sum_{q\lambda} |\alpha_{q\lambda}|^2 (i\underline{k}\cdot\hat{e}_\lambda)^2$$

$$\times D_{q\lambda}(i\omega_n - i\omega_m) \qquad \ldots \quad 4.10$$

Assuming an isotropic phonon spectrum for the host matrix, the electron-phonon coupling constant $\alpha_{q\lambda}$ and the phonon Green's function $D_{q\lambda}$ become independent of polarization. The sum over the polarization then gives

$$\sum_{\lambda} (\underline{k}\cdot\hat{e}_{\lambda})^2 = k^2 \approx k_F^2 \qquad \ldots \quad 4.11$$

where only electrons very close to the Fermi surface are taken into account and k_F is the Fermi momentum.

$\Sigma_d^{rec}(i\omega_n)$ becomes

$$\Sigma_d^{rec}(i\omega_n) = k_F^2 |V|^2 kT \sum_m \sum_k G_k(i\omega_m) \sum_q |\alpha_q|^2 D_q(i\omega_n - i\omega_m) \qquad \ldots \quad 4.12$$

The frequency summation is now converted into an integral along a contour C by use of the Poisson summation formula of eq. (3.63). It is also convenient to introduce the spectral representation for the phonon Green's function. This takes the form (G2):

$$D_{q\lambda}(i\nu_n) = \int d\nu\, B_{q\lambda}(\nu) \left(\frac{1}{i\nu_n - \nu} - \frac{1}{i\nu_n + \nu}\right) \qquad 4.13$$

where the spectral weight function $B_{q\lambda}(\nu)$ is given by

$$B_{q\lambda}(\nu) = Z^{-1}(1 - e^{\beta\nu}) \sum_{m,n} e^{-\beta E_m} |\langle m|\varphi_{q\lambda}|n\rangle|^2$$

$$\times\ \delta(\nu - E_n + E_m) \qquad \ldots \quad 4.14\,a$$

and

$$Z = \sum_m e^{-\beta E_m} \qquad 4.14\,b$$

is the grand partition function. Then Σ_d^{rec} becomes :

$$\Sigma_d^{rec}(i\omega_n) = k_F^2 |V|^2 \sum_k \int \frac{dz}{2\pi i} G_k(z) \sum_q |\alpha_q|^2 \int d\nu\, B_q(\nu)\, x$$

$$\left(\frac{f(-z)}{i\omega_n - z - \nu} + \frac{f(z)}{i\omega_n - z + \nu}\right) \quad \ldots \quad 4.15$$

The contour C is shown in Fig. (13). The complex variable z is then taken to the real axis by deforming the contour C into C', picking up the poles of the integrand at $z = i\omega_n \pm \nu$. Use of the relation

$$G_k(\omega + i\delta) - G_k(\omega - i\delta) = 2i\ \mathrm{Im}\ G_k(\omega + i\delta) \quad \ldots \quad 4.16$$

gives the following expression for Σ_d^{rec} from eq. (4.15) :

$$\Sigma_d^{rec}(i\omega_n) = k_F^2 |V|^2 \sum_k \int \frac{d\omega'}{2\pi i}\, 2i\ \mathrm{Im}\ G_k(\omega') \sum_q |\alpha_q|^2\ x$$

$$\int d\nu\, B_q(\nu) \left(\frac{f(-\omega')}{i\omega_n - \omega' - \nu} + \frac{f(\omega')}{i\omega_n - \omega' + \nu}\right)$$

$$+ k_F^2 |V|^2 \sum_k \sum_q |\alpha_q|^2 \int d\nu\, B_q(\nu)\ x$$

$$\left\{G_k(i\omega_n - \nu)\, f(\nu - i\omega_n) + G_k(i\omega_n + \nu)\, f(i\omega_n + \nu)\right\}$$

$$\ldots \quad 4.16$$

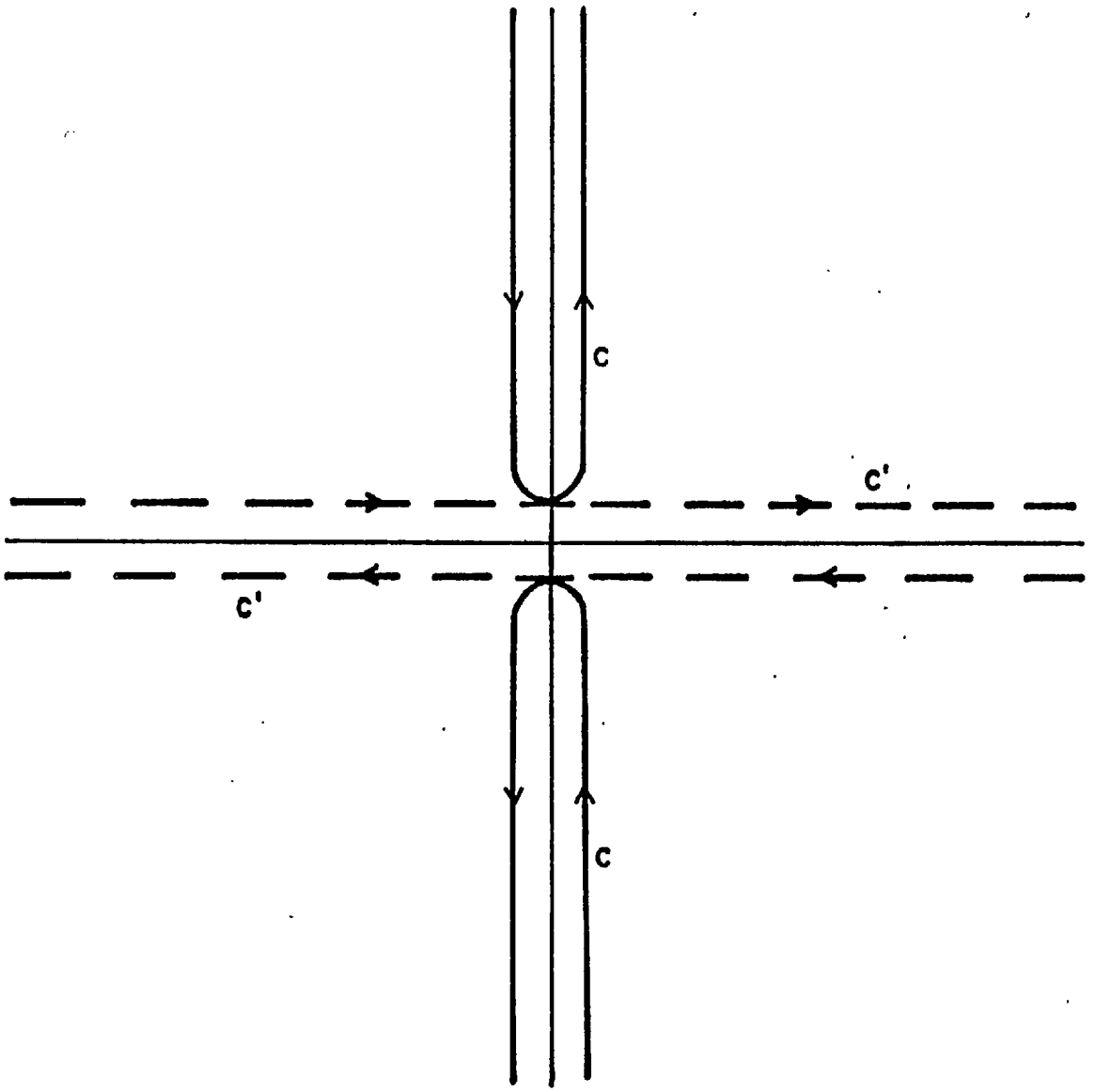


Fig. 13

The second term on the right comes from the pole contributions. But

$$f(\nu \pm i\omega_n) = (e^{\beta\nu} e^{\pm i\omega_n} + 1)^{-1} \quad \ldots \quad 4.17$$

and

$$\omega_n = (2n + 1)\pi/\beta \quad \ldots \quad 4.18$$

So

$$f(\nu \pm i\omega_n) = (e^{\beta\nu} - 1)^{-1} = b(\nu) \quad \ldots \quad 4.19$$

where $b(\nu)$ is the Bose factor.

From eqs. (4.16) and (4.19) :-

$$\Sigma_d^{rec}(i\omega_n) = k_F^2 |V|^2 \sum_k \int \frac{d\omega'}{\pi} \text{Im } G_k(\omega') \sum_q |\alpha_q|^2 \int d\nu\, B_q(\nu) \times$$

$$\times \left(\frac{b(\nu) + f(-\omega')}{i\omega_n - \omega' - \nu} + \frac{b(\nu) + f(\omega')}{i\omega_n - \omega' + \nu} \right) \quad 4.20$$

The next step is the analytical continuation of $\Sigma_d^{rec}(i\omega_n)$ onto the real axis from above i.e. $i\omega_n \longrightarrow \omega + i\delta$, $\delta \longrightarrow +0$, yielding the following result :

$$\Sigma_d^{rec}(\omega) = k_F^2 |V|^2 \sum_k \int \frac{d\omega'}{\pi} \text{Im } G_k(\omega') \sum_q |\alpha_q|^2 \int B_q(\nu) \; x$$

$$x \quad \left(\frac{b(\nu) + 1 - f(\omega')}{\omega - \omega' - \nu + i\delta} + \frac{b(\nu) + f(\omega')}{\omega - \omega' + \nu + i\delta} \right) \qquad 4.21$$

Use of the relation

$$f(-\omega) = 1 - f(\omega) \qquad \ldots \qquad 4.22$$

has been made to obtain eq. (4.21). From Appendix A

$$\sum_k G_k(i\omega_n) = -i\pi N(0) \qquad \ldots \qquad 4.23$$

From eqs. (4.21) and (4.23) the recoil contribution to the d-electron self-energy is given by

$$\Sigma_d^{rec}(\omega) = -\pi N(0) |V|^2 k_F^2 \int \frac{d\omega'}{\pi} \sum_q |\alpha_q|^2 \int d\nu \, B_q(\nu) \; x$$

$$x \left(\frac{b(\nu) + 1 - f(\omega')}{\omega - \omega' - \nu + i\delta} + \frac{b(\nu) + f(\omega')}{\omega - \omega' + \nu + i\delta} \right) \qquad 4.24$$

Now

$$\frac{1}{x \pm i\delta} = P \frac{1}{x} \mp i\pi\delta(x) \qquad \ldots \qquad 4.25$$

where P implies the principal part of the integral. Eqs. (4.24), (4.25) and the following simple form for the phonon spectral weight function (G.2)

$$B_q(\nu) = \delta(|\nu| - \omega_q)\ \mathrm{sgn}\ \nu \qquad \ldots \quad 4.26$$

where

$$\mathrm{sgn}\ \nu = \begin{cases} +1, & \text{for } \nu > 0 \\ -1, & \text{for } \nu < 0 \end{cases} \qquad \ldots \quad 4.27$$

then lead to the following expressions for the real and imaginary parts of $\Sigma_d^{rec}(\omega)$:

$$\mathrm{Re}\ \Sigma_d^{rec}(\omega) = -\pi N(0)|V|^2 k_F^2 P \int \frac{d\omega'}{\pi} \sum_q \left(\frac{1}{2NM\omega_q}\right) x$$

$$x \left(\frac{b(\omega_q) + 1 - f(\omega')}{\omega - \omega' - \omega_q} + \frac{b(\omega_q) + f(\omega')}{\omega - \omega' + \omega_q}\right) \qquad 4.28$$

$$\mathrm{Im}\ \Sigma_d^{rec}(\omega) = \pi N(0)|V|^2 k_F^2 \int d\omega' \sum_q \left(\frac{1}{2NM\omega_q}\right) x$$

$$\Big\{\left[b(\omega_q) + 1 - f(\omega')\right] \delta(\omega - \omega' - \omega_q) +$$

$$\left[b(\omega_q) + f(\omega')\right] \delta(\omega - \omega' + \omega_q)\Big\}$$

$$= \pi N(0)|V|^2 k_F^2 \sum_q \left(\frac{1}{2NM\omega_q}\right) \Big\{ 2b(\omega_q) + 1 - f(\omega - \omega_q)$$

$$+ f(\omega + \omega_q)\Big\}. \qquad 4.29$$

Now $$f(\omega+\omega_q) - f(\omega-\omega_q) = \frac{\sinh \beta\omega_q}{\cosh \beta\omega + \cosh \beta\omega_q} \qquad 4.30$$

Hence eq. (4.29) becomes

$$\text{Im } \Sigma_d^{rec}(\omega) = \Gamma k_F^2 \sum_q \left(\frac{1}{2NM\omega_q}\right) \left(2b(\omega_q) + 1 - \frac{\sinh \beta\omega_q}{\cosh \beta\omega + \cosh \beta\omega_q}\right) \quad \ldots \quad 4.31$$

where $\Gamma = \pi N(0)|V|^2$ is the half-width of the resonance, and $\alpha_q^2 = 1/2\, NM\omega_q$, M is the mass of the impurity atom and N is the number of atoms in the lattice, of which $N - N_i$ are the host atoms. The contribution to the life-time of the resonance level due to the virtual recoil processes is given by

$$\frac{1}{2\tau_d^{rec}(\omega)} = -\text{Im } \Sigma_d^{rec}(\omega) \qquad \ldots \quad 4.32$$

The relaxation time for $\omega = 0$ then becomes

$$\frac{1}{2\tau_d^{rec}(0)} = -\Gamma k_F^2 \sum_q \left(\frac{1}{2NM\omega_q}\right) \left\{ 2b(\omega_q) - 1 - \tanh\left(\frac{\beta\omega_q}{2}\right)\right\} \quad \ldots \quad 4.33$$

The zero frequency relaxation time is important for low temperatures since only electrons at the Fermi level take part in scattering processes at these temperatures. $\tau_d^{rec}(0)$ of eq. (4.33) is calculated using a Debye spectrum for the phonons. In this approximation,

the sum over q is replaced by an integral of the form .

$$\sum_q A(\omega_q) = N \int A(\omega) F(\omega) d\omega \quad \ldots \quad 4.34$$

where $F(\omega)$ is the phonon density of states given by :

$$F(\omega) d\omega = \frac{3\omega^2}{\omega_D^3} d\omega \quad (0 < \omega < \omega_D) \quad \ldots \quad 4.35$$

ω_D is the Debye frequency characteristic of the host matrix, and is related to the Debye temperature Θ_D by

$$\omega_D = k \Theta_D \quad (\hbar = 1) \quad \ldots \quad 4.36$$

Eqs. (4.33) to (4.36) give

$$\frac{1}{2\tau_d^{rec}(0)} = \frac{3\Gamma k_F^2}{2M\omega_D^3} \int_0^{\omega_D} d\omega \cdot \omega \left\{ 2b(\omega) + 2f(\omega) \right\} \quad 4.37$$

where $1 - \tanh(\beta\omega/2) = 2f(\omega)$ ... 4.38

Writing $z = \beta\omega$ and integrating with respect to z from 0 to Θ_D/T, gives

$$\frac{1}{2\tau_d^{rec}(0)} = 12\Gamma(m/M) \left(\frac{\epsilon_F}{k\Theta_D}\right) \left(\frac{T}{\Theta_D}\right)^2 G_1(\Theta_D/T) \quad 4.39$$

where $k_F^2 = 2m\epsilon_F$ and

$$G_1(x) = \int_0^x z e^z (e^{2z} - 1)^{-1} dz \quad \ldots \quad 4.40$$

The graph of $G_1(\Theta_D/T)$ as a function of T/Θ_D is plotted in Fig. (14).

We return to eq. (4.28) and convert the negative interval of the ω'- integral to the positive interval. Then for $\omega = 0$,

$$\mathrm{Re}\ \Sigma_d^{rec}(0) = 0 \qquad \ldots \qquad 4.42$$

This result implies that the virtual recoil of the impurity does not lead to any shift in the energy of the resonance level. Thus the d-electron propagator is

$$G_d(\omega) = \left[\omega - E_d + i\Gamma(1 + A\,T^2)\right]^{-1} \qquad 4.43$$

where

$$A = \frac{12}{\Theta_D^{\,2}} \frac{m}{M} \frac{\epsilon_F}{k\Theta_D} G_1(\Theta_D/T) \qquad \ldots \qquad 4.44$$

The Anderson resonance width Γ can be replaced by a temperature-dependent width $\Gamma_{eff}(T)$:

$$\Gamma_{eff}(T) = \Gamma(1 + AT^2) \qquad \ldots \qquad 4.45$$

The variation of $\Gamma_{eff}(T)$ with T is shown in Fig. (15) for Al-Cr and Al-Mn.

From the data of Table I, the inverse life-time for Al-Mn is given by

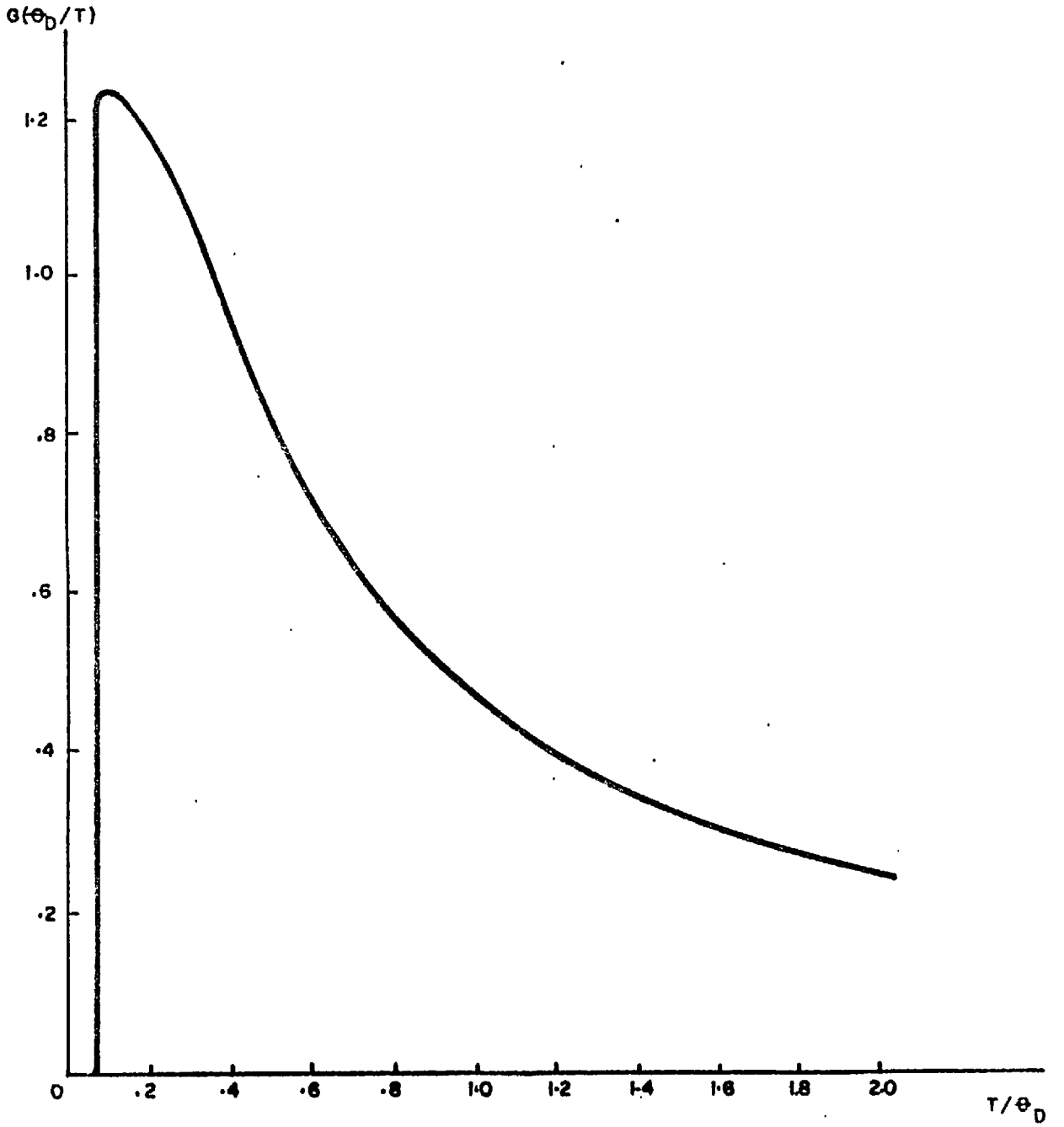


FIG. 14

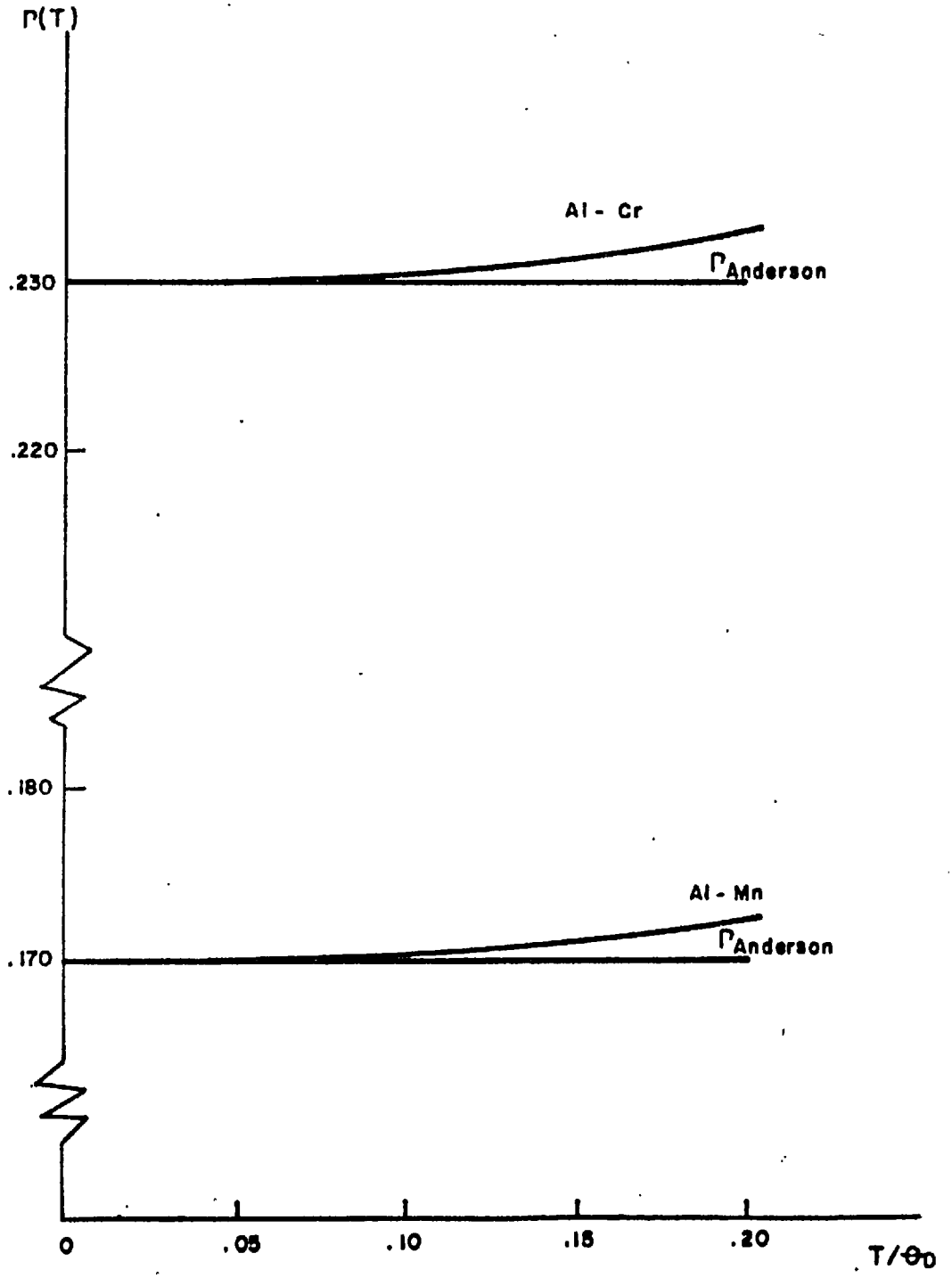

Γ(T)
Al - Cr
Γ Anderson
.230
.220
.180
Al - Mn
Γ Anderson
.170
0
.05
.10
.15
.20
T/ΘD

Fig. 15

TABLE I

Al

T_{co}	Θ_D	N(O)	α	N(O)|g|	ϵ_F	Δ_{00}
1.18°K (1, 4)	428°K (51)	0.29 (4)	6.046 (4)	0.1654	10 eV (G4)	1.78×10^{-4} eV (6)

TABLE II

	Al-Mn	Al-Cr
$\frac{\Delta \gamma_i}{n_i}$ mj/mol-deg^2 at.% (4)	0.44	0.32
$\frac{-\Delta T_c}{n_i}$ °K/at. % (4)	9.1	4.6
m/M (G4)	9.961×10^{-6}	1.056×10^{-5}

$U_{eff} = 0.24$ eV ; $U = 0.5$ eV.

$$\frac{1}{2\tau_d^{rec}(0)} = .02961\,(T/\Theta_D)^2\, G_1\,(\Theta_D/T) \qquad 4.45\,a$$

and for Al-Cr, we get

$$\frac{1}{2\tau_d^{rec}(0)} = .02793\,(T/\Theta_D)^2\, G_1\,(\Theta_D/T) \qquad 4.45\,b$$

The d-electron Green's function is now written :

$$G_d^{eff}(\omega) = (\omega - E_d + i\Gamma_{eff}(T))^{-1} \quad \ldots \qquad 4.46$$

The d-electron density of states at the Fermi level given by

$$N_d(0) = \frac{1}{\pi}\,\frac{\Gamma}{E_d^2 + \Gamma^2} \quad \ldots \qquad 4.47$$

becomes

$$N_d^{eff}(0) = \frac{1}{\pi}\,\frac{\Gamma_{eff}}{E_d^2 + \Gamma_{eff}^2} \quad \ldots \qquad 4.48$$

The effective d-density of states of eq. (4.48) shows up in the residual resistivity to be discussed in Chapter 5.

4.2. Recoil contribution to the s-electron self-energy, $\Sigma_s^{rec}(i\omega_n)$

$\Sigma_s^{rec}(i\omega_n)$ is given by

$$\Sigma_s^{rec}(i\omega_n) = (2l+1)\, n_i |V|^2 kT \sum_m G_d(i\omega_m) \sum_q |\alpha_{q\lambda}|^2$$

$$\times (i\underline{k}\cdot\hat{e}_\lambda)^2 D_{q\lambda}(i\omega_n - i\omega_m)$$

$$= (2l+1)\, n_i |V|^2 k_F^2 kT \sum_m G_d(i\omega_m) \sum_q |\alpha_q|^2$$

$$\times D_q(i\omega_n - i\omega_m) \quad \ldots \quad 4.49$$

after summation over the phonon polarizations. Use of the Poisson's summation formula of eq. (3.63) yields:-

$$\Sigma_s^{rec}(i\omega_n) = (2l+1)\, n_i |V|^2 k_F^2 \int \frac{dz}{2\pi i} G_d(z) \sum_q |\alpha_q|^2$$

$$\times \left\{ \frac{f(-z)}{i\omega_n - z - \omega_q} + \frac{f(z)}{i\omega_n - z + \omega_q} \right\} \ldots \quad 4.50$$

We follow the same procedure as in Section 4.1 and make use of the relation

$$G_d(\omega + i\delta) - G_d(\omega - i\delta) = 2i \text{ Im } G_d(\omega + i\delta) \qquad 4.51$$

Then $\Sigma_s^{rec}(i\omega_n)$ in eq.(4.50) becomes :-

$$\Sigma_s^{rec}(i\omega_n) = (2l+1)\, n_i |V|^2 k_F^2 \int \frac{d\omega'}{2\pi} \text{Im } G_d(\omega') \sum_q |\alpha_q|^2 \times$$

$$\times \left(\frac{b(\omega_q)+1-f(\omega')}{i\omega_n - \omega' - \omega_q} + \frac{b(\omega_q)+f(\omega')}{i\omega_n - \omega' + \omega_q} \right) \qquad 4.52$$

The d-electron spectral weight function $A_d(\omega)$ is defined as follows :

$$A_d(\omega) = \left| \frac{1}{\pi} \text{Im } G_d(\omega) \right| = \frac{1}{\pi} \frac{\Gamma}{(\omega - E_d)^2 + \Gamma^2} \qquad 4.53$$

Eq. (4.52) is then analytically continued (i.e. $i\omega_n \rightarrow \omega + i\delta$) to give :-

$$\Sigma_s^{rec}(\omega) = (2l+1)\, n_i |V|^2 k_F^2 \int d\omega' \, A_d(\omega') \sum_q |\alpha_q|^2 \times$$

$$\times \left(\frac{b(\omega_q)+1-f(\omega')}{\omega - \omega' - \omega_q + i\delta} + \frac{b(\omega_q)+f(\omega')}{\omega - \omega' + \omega_q + i\delta} \right) \qquad 4.54$$

Decomposition of $\Sigma_s^{rec}(\omega)$ into its real and imaginary parts gives :-

$$\mathrm{Re}\,\Sigma_s^{rec}(\omega) = (2l+1)\, n_i |V|^2 k_F^2 P \int d\omega' \, A_d(\omega') \sum_q |a_q|^2 \; x$$

$$x \left(\frac{b(\omega_q) + 1 - f(\omega')}{\omega - \omega' - \omega_q} + \frac{b(\omega_q) + f(\omega')}{\omega - \omega' + \omega_q} \right) \qquad 4.55$$

where P denotes the principal part of the integral.

$$\mathrm{Im}\,\Sigma_s^{rec}(\omega) = -(2l+1)\,\pi\, n_i |V|^2 k_F^2 \sum_q |a_q|^2 \; x$$

$$\left\{ A_d(\omega - \omega_q) \; (b(\omega_q) + 1 - f(\omega - \omega_q)) \right.$$

$$\left. + \; A_d(\omega + \omega_q) \; (b(\omega_q) + f(\omega + \omega_q)) \right\} \qquad 4.56$$

For excitations close to the Fermi surface (i.e. $\omega = 0$)

$\mathrm{Im}\,\Sigma_s^{rec}(0)$ becomes

$$\mathrm{Im}\,\Sigma_s^{rec}(0) = -(2l+1)\,\pi\, n_i |V|^2 k_F^2 \sum_q \frac{1}{2NM\omega_q} (b(\omega_q) - f(\omega_q)) x$$

$$(A_d(-\omega_q) + A(\omega_q)) \quad \ldots \qquad 4.57$$

Choice of a Debye spectrum for the host gives :-

$$\mathrm{Im}\,\Sigma_s^{rec}(0) = -5\pi n_i |V|^2 k_F^2 \int_0^{\omega_D} d\omega_q \frac{3\omega_q}{M\omega_D^3} (b(\omega_q) + f(\omega_q))$$

$$x\,(A_d(-\omega_q) + A_d(\omega_q)) \quad \ldots \quad 4.58$$

For the physical case in which the half-width of the resonance, Γ, is much larger than the Debye cut-off frequency ω_D, i.e. $\Gamma >> \omega_D$, we get

$$\mathrm{Im}\,\Sigma_s^{rec}(0) = -12\Gamma n_i (m/M)(\epsilon_F/k\Theta_D)(T/\Theta_D)^2 \; x$$

$$[N_d(0)/N(0)]\, G_1(\Theta_D/T) \quad 4.60$$

where $G_1(\Theta_D/T)$ is given by eq. (4.40). Also the recoil phonon does not produce any shift in the energy of the conduction electrons because from eq. (4.55)

$$\mathrm{Re}\,\Sigma_s^{rec}(0) = 0. \quad \ldots \quad 4.61$$

CHAPTER FIVE

5. ELECTRONIC PROPERTIES OF THE NORMAL STATE ALLOY

In this chapter a few of the electronic properties of the aluminium iron group alloys in the normal state will be calculated from the expression derived for the self-energy parts $\Sigma_s(\omega)$ and $\Sigma_s(\omega)$ in Chapter Four. In particular, the electronic specific heat, the residual resistivity and the mass enhacement of the s- and d-electrons will be calculated.

5.1. The Electronic Specific Heat

Contributions to the electronic specific heat ΔC comes from the s-and d-electrons. Because of the high density of d-electron states, the d-electron contribution to ΔC is much larger than the s-electron contribution which may be neglected.

The energy associated with the presence of the impurity is given by [46]

$$E(T) = \frac{1}{\beta} \sum_{n\sigma} \left\{ i\omega_n - \Sigma_d^{\sigma}(i\omega_n) \right\} G_d(i\omega_n)$$

$$= -\sum_{\sigma} \int \frac{d\omega}{\pi} f(\omega)\, \mathrm{Im} \left\{ G_d(\omega)\, (\omega - \Sigma_d^{\sigma}(\omega)) \right\} \qquad 5.1$$

where $f(\omega) = (e^{\beta\omega} + 1)^{-1}$ is the Fermi distribution function and the summation over spin variable σ is also included in eq. (5.1). $\Sigma_d(\omega)$ is the total self-energy of the d-electron and it is made up of the partial self-energies $\Sigma_d^{res}(\omega)$, Σ_d^{rec} and $\Sigma_{dd}(\omega)$. The first two contributions are due to resonance scattering only and virtual recoil processes, respectively. $\Sigma_{dd}(\omega)$ is the self-energy due to the d-d intra-atomic Coulomb repulsion. Hence

$$\Sigma_d(\omega) = \Sigma_d^{res}(\omega) + \Sigma_d^{rec}(\omega) + \Sigma_{dd}(\omega) \quad \ldots \quad 5.2$$

In the Hartree-Fock (H.F.) approximation, $\Sigma_{dd}(\omega)$ is given by the diagram shown in Fig. 16. This yields

$$\Sigma_{dd}^{\sigma}(\omega) = U \int \frac{d\omega'}{2\pi i} G_{d,-\sigma}(\omega') = U\, n_{-\sigma} \quad \ldots \quad 5.3$$

Kjollerstron et al[46] have shown that only the real part of $\Sigma_d^{\sigma}(\omega)$ plays an important role in the calculation of the specific heat. Consequently, $\Sigma_d^{res}(\omega)$ drops out, since it is purely imaginary. The integral in eq. (5.1) is performed over the d-electron spectral weight function $A_d^{\sigma}(\omega)$, which is defined by

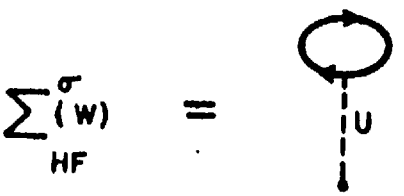


Fig. 16

$$A_d^{\sigma}(\omega) = \left| \frac{1}{\pi} \operatorname{Im} G_d^{\sigma}(\omega) \right| \qquad \ldots \qquad 5.4$$

Then eq. (5.1) becomes

$$E(T) = \sum_{\sigma} \int d\omega\, f(\omega)\, A_d^{\sigma}(\omega)\, (\omega - \xi^{\sigma}(\omega)) \qquad 5.5$$

where $\xi^{\sigma}(\omega) = \operatorname{Re} \Sigma_d^{\sigma}(\omega) = U n_{-\sigma} + \operatorname{Re} \Sigma_d^{rec}(\omega)$ 5.6

~~Kjollerstrom et al[46] obtained a contribution to the~~ specific heat by evaluating the expression

$$E_1(T) = \sum_{\sigma} \int d\omega\, f(\omega)\, A_d^{\sigma}(\omega)\, (\omega - \tfrac{1}{2} U n_{-\sigma}) \qquad 5.7$$

The factor $\frac{1}{2}$ prevents double counting in the two-particle interaction. Eq. (5.7) leads to the electronic specific heat contribution

$$C_1(T) = \frac{1}{3} \pi^2 k^2 T \sum_{\sigma} A_d^{\sigma}(0) \qquad \ldots \qquad 5.8$$

The contribution from the virtual recoil processes is now evaluated, from eq. (5.5), viz:

$$E^{rec}(T) = -\sum_{\sigma} \int d\omega\, f(\omega)\, A_d^{\sigma}(\omega)\, \operatorname{Re} \Sigma_d^{rec}(\omega)$$

$$= -\frac{\pi^2}{6} (kT)^2 \sum_{\sigma} A_d^{\sigma}(\omega) \frac{\partial}{\partial \omega} \operatorname{Re} \Sigma_d^{rec}(\omega)\Big|_{\omega=0} \qquad 5.9$$

In obtaining the above expression, the Sommerfeld formula for integrals involving the Fermi function and the result $\Sigma_d^{rec}(0) = 0$ were used. From eq. (4.29).

$$\frac{\partial}{\partial\omega} \mathrm{Re}\, \Sigma_d^{rec}(\omega)\Big|_{\omega=0} = \frac{\Gamma}{\pi} k_F^2 \int d\omega' \sum_q (1/2NM\omega_q)\, (-\partial f/\partial\omega') \times \left(\frac{1}{\omega' + \omega_q} - \frac{1}{\omega - \omega_q}\right) \qquad 5.10$$

Assuming a Debye spectrum for the host matrix and neglecting ω' compared with ω_q in the denominators of the curly brackets for $T << \Theta_D$, eq. (5.10) becomes

$$\frac{\partial}{\partial\omega} \mathrm{Re}\, \Sigma_d^{rec}(\omega)\Big|_{\omega=0} = -\frac{3\Gamma k_F^2}{\pi M \omega_D^2} \int d\omega' \left(-\frac{\partial f}{\partial\omega'}\right)$$

$$= -\frac{6}{\pi} \left(\frac{m}{M}\right) \left(\frac{\epsilon_F}{k\Theta_D}\right) \left(\frac{\Gamma}{k\Theta_D}\right) \qquad 5.11$$

Eqs. (5.9) and (5.11), therefore, give the virtual recoil contribution to the electronic specific heat to be

$$C^{rec}(T) = \frac{\partial}{\partial T} E^{rec}(T)$$

$$= \frac{1}{3}\pi^2 k^2 T \frac{6}{\pi} \left(\frac{m}{M}\right) \left(\frac{\epsilon_F}{k\Theta_D}\right) \left(\frac{\Gamma}{k\Theta_D}\right) \sum_\sigma A_d^\sigma(0) \qquad 5.12$$

Hence the total impurity contribution to the electronic

specific heat of the d-electrons is:

$$\Delta C_{imp}(T) = \frac{2}{3}\pi^2 k^2 T (1+a) A_d(0) \quad \ldots \quad 5.13$$

where $a = \frac{6}{\pi}\left(\frac{m}{M}\right)\left(\frac{e_F}{k\Theta_D}\right)\left(\frac{\Gamma}{k\Theta_D}\right)$ ... 5.14

and $\frac{2}{3}\pi^2 k^2 T A_d(0)$ is the contribution from the d-electrons obtained by Kjollerstrom et al[46].

The inclusion of the impurity concentration n_i and the degeneracy factor $(2l+1) = 5$ yields

$$\Delta C_{imp}^{tot}(T) = \frac{2}{3}\pi^2 k^2 T n_i \tilde{N}_d(0) \quad \ldots \quad 5.15$$

where $\tilde{N}_d(0) = (1+a) N_d(0)$ is phonon-enhanced d-electron density of states at the Fermi level and $N_d(0) = 5 A_d(0)$ is the bare d-electron density of states at the Fermi level.

The contribution to the electronic specific heat from the conduction electrons is given by (G.7, G.8).

$$\Delta C(T) = \frac{2}{3}\pi^2 k^2 T N(0) = \gamma T \quad \ldots \quad 5.16$$

To order n_i, we need not calculate the effect of the change in the s-electron self-energy since this is small

Therefore, the electronic specific heat of the alloy becomes

$$\Delta C_{alloy}(T) = \frac{2}{3}\pi^2 k^2 T (N(0) + n_i \tilde{N}_d(0)) \quad 5.17$$

and the electronic specific heat coefficient for the alloy is

$$\gamma_{alloy} = C_{alloy}(T)/T = \frac{2}{3}\pi^2 k^2 \left(N(0) + n_i \tilde{N}_d(0)\right)$$

i.e. $\gamma_{alloy} = \gamma + \Delta\gamma$ ... 5.18

where $\Delta\gamma = \frac{2}{3}\pi^2 k^2 n_i \tilde{N}_d(0)$ ... 5.19

is the enhancement of γ due to the impurity. Thus the measurement of the specific heat of the alloy gives information on the enhancement of the conduction electron density of states due to the presence of the impurity. The observed density of states of the alloy $N_{obs}(0)$ is given by

$$N_{obs}(0) = N(0) + n_i \tilde{N}_d(0) \quad \ldots \quad 5.20$$

From eq.(5.19) and Table II, $N_d(0)$ is found to be 9.11 states/eV-atom for Al-Mn and 6.74 states/eV-atom for Al-Cr. The calculated size of 'a' appearing in $\tilde{N}_d(0)$ is 0.017 for Al-Mn and 0.003 for Al-Cr. In consequence, the change in the density of d-states due to recoil is negligible.

5.2. Residual Resistivity

The impurity contribution to the resistivity of the alloy is given by [47]

$$\rho_{res}(T) = \frac{m}{ne^2} \int d\omega \left(-\frac{\partial f}{\partial \omega}\right) \frac{1}{\tau_s(\omega)} \quad \ldots \quad 5.21$$

where $f(\omega)$ is the Fermi distribution function, m is the mass of the conduction electron, n is the conduction electron density, e is the electronic charge and $\tau_s(\omega)$ is given by

$$\frac{1}{2\tau_s(\omega)} = - \text{Im}\ \Sigma_s(\omega) \qquad \ldots \qquad 5.22$$

At low temperatures, the Fermi distribution function reduces to the step function $\Theta(\omega)$ and its derivative with respect to ω yields the delta function $\delta(\omega)$. The frequency-dependent relaxation time $\tau_s(\omega)$ is, therefore, replaced by the zero frequency relaxation time $\tau_s(0)$. Consequently, eq. (5.21) becomes

$$\rho_{res}(T) = \frac{m}{ne^2} \frac{1}{\tau_s(0)} \qquad \ldots \qquad 5.23$$

* See INSERT ATTACHED →

Replacing $G_d(0)$ by $G_d^{eff}(0)$ and the vertex $|V|$ by $|V_{eff}|$, we may write

$$\Sigma_s(0) = 5 n_i \frac{\Gamma_{eff}}{\pi N(0)} G_d^{eff}(0)$$

where $\Gamma_{eff} = \pi N(0) |V_{eff}|^2$.

$$\frac{1}{2\tau_s(0)} = \frac{5 n_i \Gamma_{eff}}{N(0)} N_d^{eff}(0) \quad \ldots \quad 5.25\,a$$

$$= \frac{5 n_i}{\pi N(0)} \frac{\Gamma_{eff}^2}{E_d^2 + \Gamma_{eff}^2} \quad \ldots \quad 5.25\,b$$

Eq. (5.23) therefore yields

$$\rho_{res}(T) = 2(m/ne^2)\,(5 n_i/\pi N(0)\,\Gamma_{eff}^2/(E_d^2 + \Gamma_{eff}^2) \quad 5.26$$

where Γ_{eff} is given by eq. (4.45).

It is observed that $\rho_{res}(T) \to (m/ne^2)\,(5n_i/\pi N(0))$ as $E_d \to 0$ and is independent of the phonons and of temperature. This is the unitarity limit where maximum scattering is obtained and it is true for Al-Mn and Al-Cr. $\rho_{res}(T)$ is given as function of T for different values of E_d in Fig. 17. From eq.(4.45), the percentage change in impurity resistivity as a function of temperature for the alloy is :-
$2.96\,(T/\Theta_D)^2\,G_1(\Theta_D(T)$ for Al-Mn and $2.79\,(T/\Theta_D)^2\,G_1(\Theta_D/T)$ for Al-Cr.

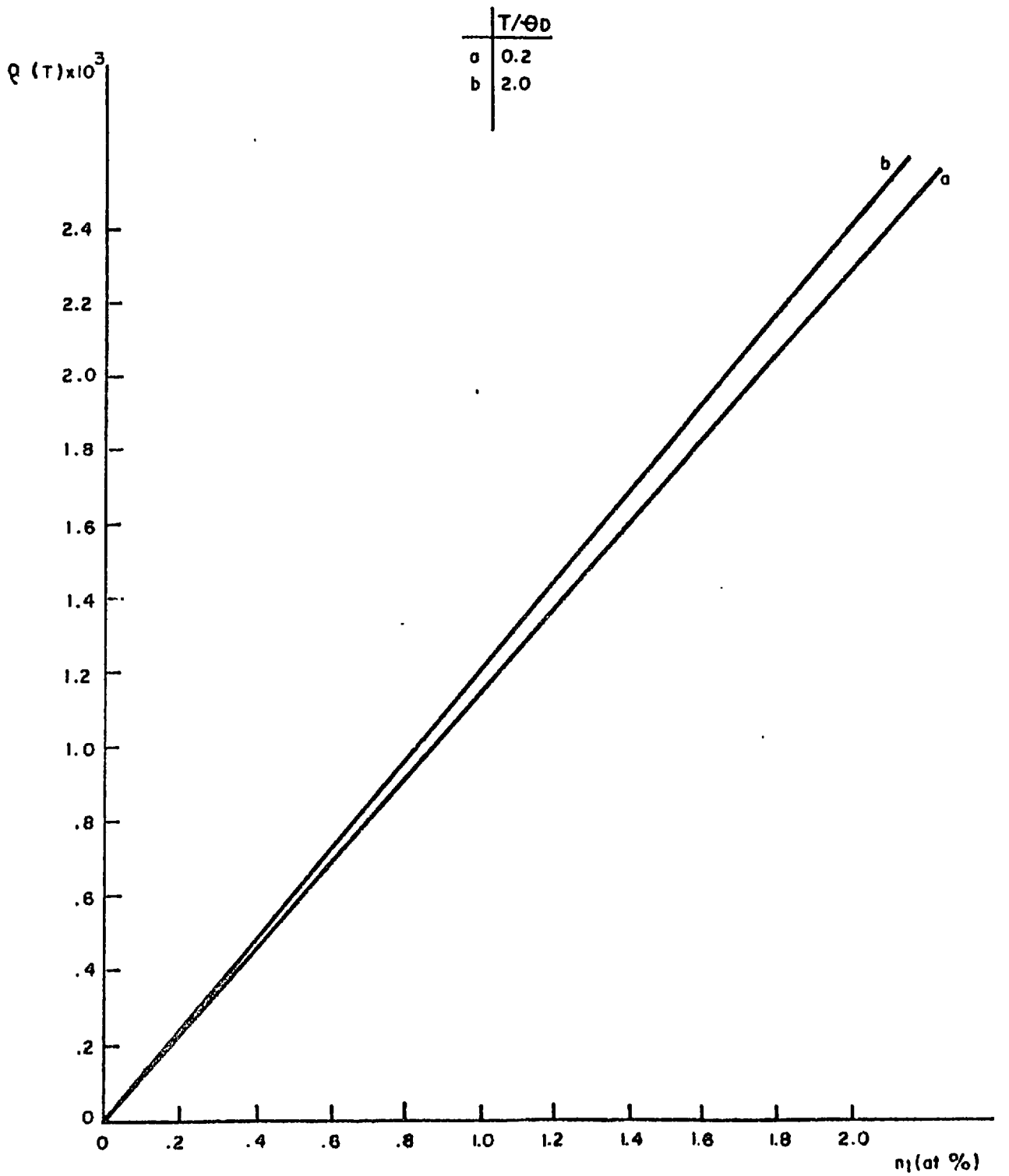

Ed = 0.5 eV
T/ΘD
a 0.2
b 2.0
Q (T)x10^3
2.4
2.2
2.0
1.8
1.6
1.4
1.2
1.0
.8
.6
.4
.2
0
0 .2 .4 .6 .8 1.0 1.2 1.4 1.6 1.8 2.0
n1(at %)
b
a

Fig. 17 a.

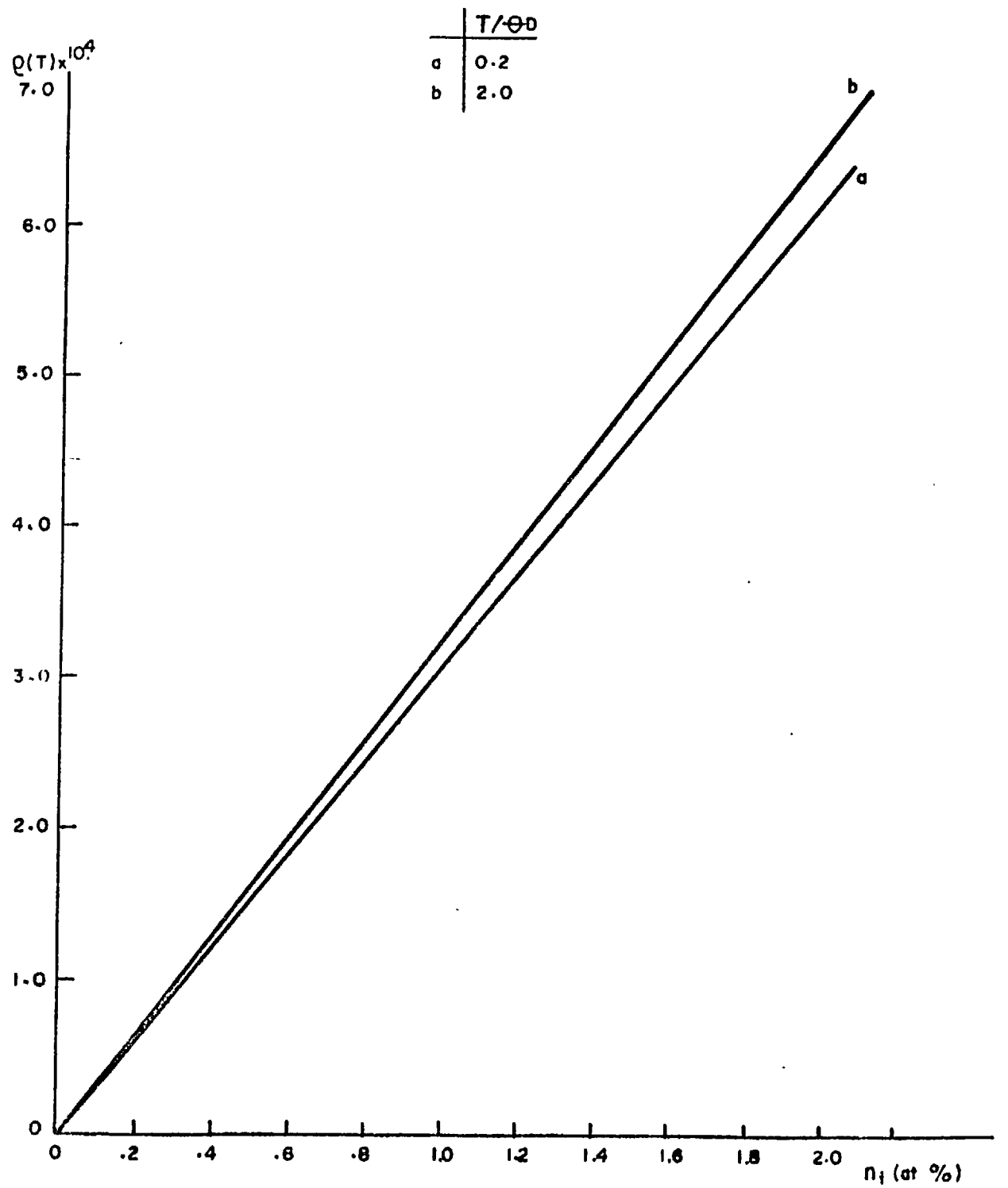

T/ΘD
a 0.2
b 2.0
ρ(T)x10⁴
7.0
6.0
5.0
4.0
3.0
2.0
1.0
0
b
a
0
.2
.4
.6
.8
1.0
1.2
1.4
1.6
1.8
2.0
nᵢ (at %)

Fig. 17. b

T/ΘD	G1(ΘD/T	Γeff(T)
0.2	1.19	0.1732 eV

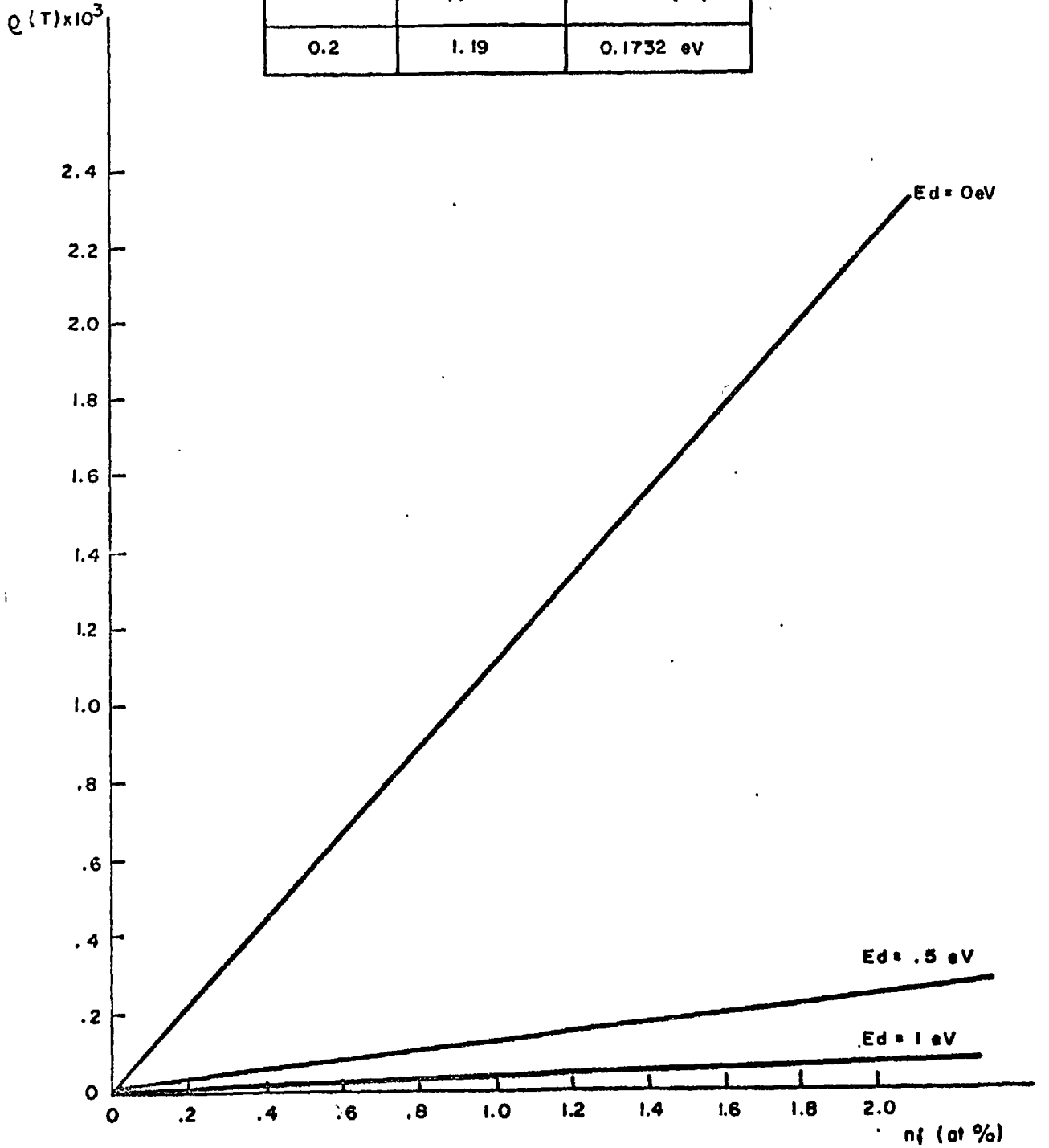


Fig. 17 c

5.3 Concluding Remarks

The analysis shows that virtual recoil of the impurity leads to a change in the normal state properties of the alloy. In particular, a T^2-dependence is found for the width of the resonance level at low temperatures. This leads to a percentage change in the impurity resistivity of the alloy, which for Al-Mn was found to be 2.96 $f(T/\Theta_D)$ and for Al-Cr it came to 2.79 $f(T/\Theta_D)$, where $f(T/\Theta_D) = (T/\Theta_D)^2 G_1(\Theta_D/T)$ and $G_1(\Theta_D/T)$ is given in eq. (4.40)

The d-electron contribution to the specific heat of the alloy was also found to be increased by the factor 'a' given by eg (5.14). This implies an increase in the d-electron density of states. The increase in the electronic specific heat is reflected in the mass enhancement of the electrons through the equation

$$\frac{\gamma}{\gamma_0} = \frac{m_s^*}{m_s} \qquad \ldots \qquad 5.27$$

where $\gamma_0 = \frac{2}{3}\pi^2 k^2 N(0)$ is the band structure value of the electronic specific heat coefficient and k is the Boltzmann constant. It should be noted, however, that the effects are small in aluminium-iron group alloys and will probably not be observed in these alloys.

PART TWO

THE SUPERCONDUCTING STATE

CHAPTER SIX

6. INTRODUCTION

It is well known from Bardeen-Cooper-Schrieffer (BCS) theory [49] that the basic mechanism which gives rise to superconductivity is the phonon-mediated attractive interaction between conduction electrons of opposite momenta and spins. In this model, only electrons within a shell of thickness $2\omega_D$ about the Fermi surface partake in superconductivity.

Generally, a phonon can carry a large momentum of of order of Fermi momentum k_F ($\hbar = 1$), but its energy is small compared to the Fermi energy ϵ_F. This difference in energy comes about because the Debye temperature of most metals is or order $10^2\ ^oK$ while the Fermi temperature is of order $10^4\ ^oK$ or higher. A consequence of the low energy of the phonons is that they can be most easily emitted or absorbed by electrons close to the Fermi surface.

The BCS theory is referred to as the 'weak coupling theory' because the superconducting transition temperature is very much smaller than the Debye temperature of the host, i.e. $T_c << \theta_D$. The electron-electron interaction

is taken as constant for electron energies less than the Debye energy, i.e. for $|\omega| < \omega_D$ and it is taken to be zero for $|\omega| > \omega_D$.

It is proposed here that the phonons originating from the virtual recoil of the impurity atom also lead to pairing interaction between conduction and localized electrons; i.e. we conjecture that the phonon generated as a result of an s-electron hopping onto the d-level may be absorbed by a d-electron and vice versa. Thus, as an s-electron in the $(\underline{k}\uparrow)$ state is resonantly scattered at the impurity site to a $d\uparrow$ state, a phonon may be simultaneously emitted as the impurity recoils. The phonon may be absorbed by a $d\downarrow$ electron which is then scattered to a $(-\underline{k}\downarrow)$ state. The total momentum of the pairs remains zero.

It is proposed that this mechanism may lead to pairing (attractive) interaction between conduction and localized electrons. The weak coupling limit is assumed and the strength of the constant interaction for the s-d pairs is denoted by g^{rec}, where the superscript stands for recoil and only recalls the origin of the attractive interaction.

In order to analyse the system of dilute non-magnetic superconducting alloys, the Hamiltonian used

by Ratto and Blandin is extended to include contributions from the virtual recoil processes. The Hamiltonian is based on the Anderson model for transition metal impurities in simple metals. See Part One of this thesis. Superconductivity and the virtual recoil processes are now introduced through the BCS Hamiltonian H_{BCS} and H_{rec} respectively. The full Hamiltonian is written as:

$$H = H_{os} + H_{od} + H_{sd} + H_{dd} + H_{BCS} + H_{rec} \quad \ldots \qquad 6.1$$

H_{os}, H_{od}, H_{dd} and H_{sd} have already been defined in Chapter 4. H_{BCS} describes the pairing interaction between conduction electrons of opposite momenta and spins in the superconducting host. It is written as:*

$$H_{BCS} = -|g| \sum_{kk'} a^{+}_{k\uparrow} a^{+}_{-k'\downarrow} a_{-k'\downarrow} a_{k'\uparrow} \qquad 6.2$$
$$= -|g| \sum_{kk'} \Psi^{+}_{k} \tau_{1} \Psi_{k'}$$

where g is the coupling strength of the attractive BCS interaction.

H_{rec} describes the proposed additional attractive interaction between the s- and d-electrons due to recoil effects.

In eqs.(5.39) and (5.40) of Part One, it was shown that the recoil phonons lead to a mass enhancement of

* $\Psi_{k} = \begin{pmatrix} c_{k\uparrow} \\ c^{+}_{-k\downarrow} \end{pmatrix}$ is a spinor field operator for the s-electron pair, and $\Psi^{+}_{k} = (c^{+}_{k\uparrow}, c_{-k\downarrow})$ is its conjugate.

both the conduction and localized electrons. This is expressed in terms of the factor 'a' given in eq. (5.14). The coupling strength g^{rec} of H_{rec} is derived for a Debye model of the host matrix in Section 6.7 and it is found to be exactly the same as the expression for the enhancement factor 'a' of Part One, that is

$$N(0)\,|\,g^{rec}\,|\;=\;a\;=\;\left(\frac{6}{\pi}\right)\left(\frac{m}{M}\right)\left(\frac{\epsilon_F}{k\Theta_D}\right)\left(\frac{\Gamma}{k\Theta_D}\right) \qquad 6.3$$

We, therefore, conclude that the same mechanism is responsible in both the normal and superconducting states. Thus H_{rec} is a pairing interaction between the conduction and localized electrons which takes place via the recoil phonons, and is written, in the weak coupling limit, as follows: *

$$H_{rec} = -\,|\,g^{rec}\,|\sum_j\sum_k a^+_{k\uparrow}\,a^+_{-k\downarrow}\,c_{j\downarrow}\,c_{j\uparrow} \qquad 6.4$$
$$= -\,|g^{rec}\,|\sum_j\sum_k \Psi^+_k\,\tau_1\,\Psi_j$$

In the pairing approximation, H_{dd}, H_{BCS} and H_{rec} are factorized self-consistently by the generalized Hartree-Fock approximation due to Gorkov [31]. This yields the following results :

* where Ψ_j is the spinor field operator for the jth localized d-electron, and is given by $\Psi_j = \begin{pmatrix} c_{j\uparrow} \\ c^+_{j\downarrow} \end{pmatrix}$

$$\tilde{H}_{BCS} = - \Delta_s \sum_k \left\{ a_{k\uparrow}^+ \, a_{-k\downarrow}^+ + a_{-k\downarrow} \, a_{k\uparrow} \right\} \quad \ldots \quad 6.4$$

$$\tilde{H}_{dd} = - \Delta_d \sum_j \left\{ c_{j\uparrow}^+ \, c_{j\downarrow}^+ + c_{j\downarrow} \, c_{j\uparrow} \right\} \quad \ldots \quad 6.5$$

Eq. (6.5) is due to Ratto and Blandin [7], who argued that as a result of the admixture of the localized and conduction states, part of the d-d Coulomb repulsion shows up in the interaction of the conduction states. This leads to a weakening in the binding energy of the Cooper pairs.

Zuckermann [5], in his work on resonance scattering in dilute superconducting alloys, did not extend the generalized Hartree-Fock factorization to H_{dd}. Finally, H_{rec} yields

$$\tilde{H}_{rec} = - \Delta_s \, t_{ds} \sum_j \left\{ c_{j\downarrow} \, c_{j\uparrow} + c_{j\uparrow}^+ \, c_{j\downarrow}^+ \right\}$$

$$- \Delta_d \, t_{sd} \sum_k \left\{ a_{k\uparrow}^+ \, a_{-k\downarrow}^+ + a_{-k\downarrow} \, a_{k\uparrow} \right\} \quad 6.6\,a$$

or

$$\tilde{H}_{rec} = (\Delta_s / \Delta_d) \, t_{ds} \, \tilde{H}_{dd} + (\Delta_d / \Delta_s) \, t_{sd} \, \tilde{H}_{BCS} \quad 6.6\,b$$

where

$$t_{ds} = |g^{rec}| \, / \, |g|$$

and

$$t_{sd} = |g^{rec}| / U \quad \ldots \quad 6.7$$

Δ_s is the order parameter of the pure superconductor and it is given by

$$\Delta_s = |g| \sum_{k'} < a_{-k'\downarrow} \; a_{k'\uparrow} > \quad \ldots \quad 6.8$$

and Δ_d gives the induced pairing in the d-state. This is written as:

$$\Delta_d = - U < c_{j\downarrow} \; c_{j\uparrow} > \quad \ldots \quad 6.9$$

Also the Hartree-Fock energy of a d-electron of spin σ is given by

$$E_d^{\sigma} = - \epsilon_d + U \; < n_{j,-\sigma} > \quad \ldots \quad 6.10$$

In the non-magnetic limit, E_d^{σ} becomes

$$E_{d\uparrow} = E_{d\downarrow} = E_d \quad \ldots \quad 6.11$$

6.1 The Nambu-Schrieffer Method

The Green's function formalism is extended to the superconducting state, and the Nambu-Schrieffer method (G.2) is employed for the calculations. In this formalism, the propagators for the electron pairs are represented by 2 x 2 matrices. Thus the conduction electrons are represented by the matrix Green's

function $\hat{G}_{kk'}(t)$, which is given by

$$\hat{G}_{k\,k'}(t) = \begin{pmatrix} G_{kk'}(t) & F_{kk'}(t) \\ F^{*}_{kk'}(t) & G_{kk'}(t) \end{pmatrix} \quad \ldots \quad 6.12$$

where

$$G_{kk'}(t) = -i < T \left\{ a_{k\uparrow}(t) \;\; a^{+}_{k'\uparrow}(0) \right\} >$$

and

$$F^{*}_{kk'}(t) = -i < T \left\{ a^{+}_{-k\downarrow}(t) \;\; a^{+}_{k'\uparrow}(0) \right\} > \quad 6.13$$

The matrix Green's function of the localized d-state is written as :

$$\hat{G}_{j}(t) = \begin{pmatrix} G_{j}(t) & F_{j}(t) \\ F^{*}_{j}(t) & G_{j}(t) \end{pmatrix} \quad \ldots \quad 6.14$$

where

$$G_{j}(t) = -i < T \left\{ c_{j\uparrow}(t) \;\; c^{+}_{j\uparrow}(0) \right\} >$$

and

$$F^{*}_{j}(t) = -i < T \left\{ c^{+}_{j\downarrow}(t) \;\; c^{+}_{j\uparrow}(0) \right\} > \quad 6.15$$

T is the Wick's time-ordering operator and $< \ldots\ldots >$ denotes the statistical average over the ground state

defined by the Hamiltonian H.

In order to obtain the expression for the superconducting transition temperature T_c and the thermodynamic properties of the superconducting alloy, the finite temperature Green's functions are employed. Accordingly, the matrix Green's functions of imaginary time τ are introduced, namely, $\hat{\mathcal{G}}_{kk'}(\tau)$ and $\hat{\mathcal{G}}_j(\tau)$. Their Fourie transforms $\hat{\mathcal{G}}_{kk'}(i\omega_n)$ and $\hat{\mathcal{G}}_j(i\omega_n)$ with respect to imaginary times are given by:

$$\hat{\mathcal{G}}_{kk'}(i\omega_n) = \frac{1}{\beta}\sum_n e^{-\beta\omega_n}\,\hat{\mathcal{G}}_{kk'}(\tau)$$

and

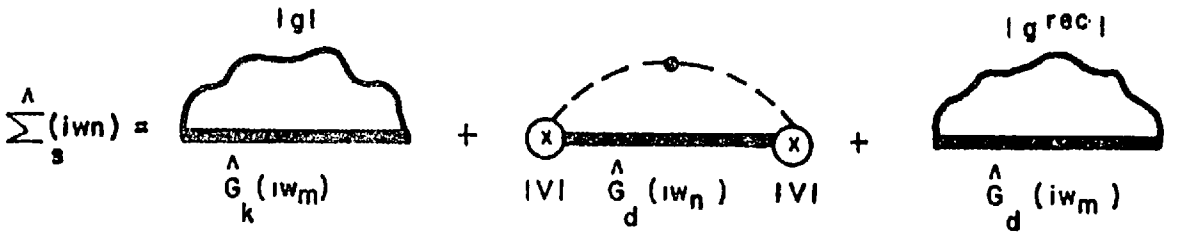
$$\hat{\mathcal{G}}_j(i\omega_n) = \frac{1}{\beta}\sum_n e^{-\beta\omega_n}\,\hat{\mathcal{G}}_j(\tau) \quad \ldots \quad 6.16$$

where

$$\omega_n = (2n+1)\pi kT \;;\; \beta = 1/kT \quad \ldots \quad 6.17$$

6.2 The s- and d-electron self-energies

The self-energy diagrams of the conduction and localized electron pairs are shown in Fig. (19). Non-resonant scattering effects are neglected, since the dominant contributions to the properties of aluminium-



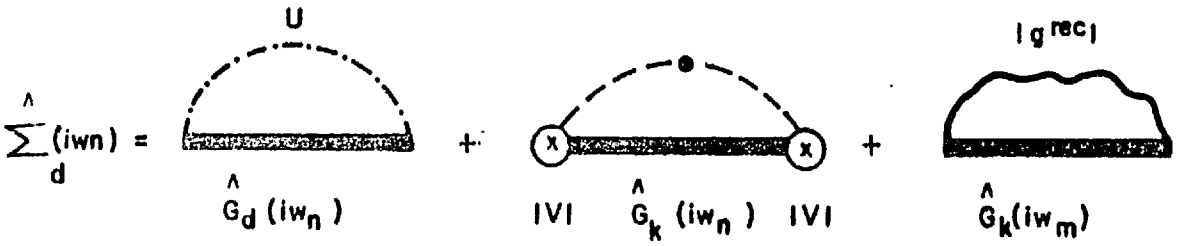


Fig. 19

iron group alloys come from resonant scattering[1-10]. Within the weak-coupling approximation, where the dynamics of the phonons is neglected, the following finite temperature expressions for the self-energies are obtained :

$$\hat{\Sigma}_s(i\omega_n) = |g| \frac{1}{\beta} \sum_m \sum_{k'} \tau_3 \hat{\mathcal{G}}_{k'}(i\omega_n)\tau_3 \Big|_{o.d}$$

$$+ \; 5n_i |V|^2 \tau_3 \hat{\mathcal{G}}_d(i\omega_n)\tau_3 +$$

$$+ \; 5n_i |g^{rec}| (1/\beta) \sum_m \tau_3 \hat{\mathcal{G}}_d(i\omega_m)\tau_3 \Big|_{o.d}$$

$$\hat{\Sigma}_d(i\omega_n) = - U (1/\beta) \sum_m \tau_3 \hat{\mathcal{G}}_d(i\omega_m)\tau_3 \Big|_{o.d} + |V|^2 \sum_{k'} \tau_3 \hat{\mathcal{G}}_{k'}(i\omega_n)\tau_3$$

$$+ |g^{rec}| (1/\beta \sum_m \sum_{k'} \tau_3 \hat{\mathcal{G}}_{k'}(i\omega_m)\tau_3 \Big|_{o.d} \qquad 6.19$$

where translational invariance has been restored to the system by averaging over the impurity positions. Hence

$$\hat{\mathcal{G}}_{kk'}(i\omega_n) = \hat{\mathcal{G}}_k(i\omega_n) \; \delta_{kk'} \qquad \ldots \qquad 6.20$$

$\hat{\Sigma}_s$ and $\hat{\Sigma}_d$ are the 2 x 2 matrix self-energies of the

s- and d-electrons, respectively; $\hat{\mathcal{G}}_k$ and $\hat{\mathcal{G}}_d$ are their full propagators, respectively. τ_i is a Pauli matrix, and $\mathbb{1}$ is the unit matrix, viz. :-

$$\tau_1 = \begin{pmatrix} 0 & 1 \\ 1 & 0 \end{pmatrix}; \quad \tau_3 = \begin{pmatrix} 1 & 0 \\ 0 & -1 \end{pmatrix}; \quad \mathbb{1} = \begin{pmatrix} 1 & 0 \\ 0 & 1 \end{pmatrix} \qquad 6.21$$

Takanaka and Takano [9] obtained similar expressions for the self-energies of the s- and d-electrons. However, they did not specify the mechanism which produced the s-d pairing. In addition, the cut-off on the m summation in eq. (6.19) was neglected.

The well-known ansatz for the Green's function (G.2) is now employed:

$$\hat{\mathcal{G}}_k(i\omega_n) = \left[i\omega_n \mathbb{1} - \epsilon_k \tau_3 - \hat{\Sigma}_s(i\omega_n) \right]^{-1} \quad \ldots \quad 6.22\,a$$

$$= \left[iZ_s(i\omega_n)\omega_n \mathbb{1} - \epsilon_k \tau_3 - \phi_s(i\omega_n)\tau_1 \right]^{-1} \qquad 6.22\,b$$

and

$$\hat{\mathcal{G}}_d(i\omega_n) = \left[i\omega_n \mathbb{1} - E_d \tau_3 - \hat{\Sigma}_d(i\omega_n) \right]^{-1} \qquad 6.23\,a$$

$$= \left[Z_d(i\omega_n) i\omega_n \mathbb{1} - E_d \tau_3 - \phi_d(i\omega_n)\tau_1 \right]^{-1} \quad \ldots \quad 6.23\,b$$

where $Z_s(i\omega_n)$ and $Z_d(i\omega_n)$ are the s- and d-electron

renormalization parameters, respectively; $\phi_s(i\omega_n)$ and $\phi_d(i\omega_m)$ are the unrenormalized gap functions and the subscript o.d stands for the off-diagonal part of the matrix.

The self-energies are now written in the following form (G.2):

$$\hat{\Sigma}_s(i\omega_n) = [1 - Z_s(i\omega_n)]\, i\omega_n \mathbb{1} + \phi_s(i\omega_n)\,\tau_1$$

$$\hat{\Sigma}_d(i\omega_n) = [1 - Z_d(i\omega_n)]\, i\omega_n \mathbb{1} + \phi_d(i\omega_n)\,\tau_1 \qquad 6.24$$

Eqs. (6.22) to (6.24) then yield the following self-consistent relations:

$$Z_{sn} = 1 + 5\, n_i\, |V|^2\, Z_{dn}/A_n \qquad \ldots \qquad 6.25\,a$$

$$\phi_{sn} = \Delta_s + 5\, n_i\, |V|^2\, \phi_{dn}/A_n + 5\, n_i\, |g^{rec}|\, (1/\beta) \sum_m \phi_{dm}/A_m \qquad 6.25\,b$$

$$Z_{dn} = 1 + |V|^2 \sum_{k'} Z_{sn}/B_{k'n} \qquad \ldots \qquad 6.25\,c$$

$$\phi_{dn} = \Delta_d + |V| \sum_{k'} \phi_{sn}/B_{k'n} + |g^{rec}|\, (1/\beta) \sum_{|m_m|<\omega_D} \sum_{k'} \phi_{sm}/B_{k'm} \qquad \ldots \quad 6.25\,d$$

where n_i is the impurity concentration in atomic fraction; Z_{sn} is written instead of $Z_s(i\omega_n)$, etc. The functions A_n and $B_{k'n}$ are given by:

$$A_n = A(i\omega_n) = Z_{dn}^2 \omega_n^2 + E_d^2 + \phi_{dn}^2$$

$$B_{k'n} = B_{k'}(i\omega_n) = Z_{sn}^2 \omega_n^2 + \epsilon_{k'}^2 + \phi_{sn}^2 \quad \ldots \quad 6.26$$

Since the electron energies of interest are restricted to $|\epsilon_k|$, $|\epsilon_{k'}| < \omega_D$, the limits of the integral over the conduction electron energies can be extended to infinity after the k'-summation has been converted into an integration over ϵ. The cutt-off on the m-summation in eq. (6.25 d) is essential, since only the electrons in the energy shell $2\omega_D$ about the Fermi surface partake in superconductivity.

Eq. (6.25) then becomes

$$Z_{sn} = 1 + 5\, n_i |V|^2 Z_{dn} / A_n \quad \ldots \quad 6.27\,a$$

$$\phi_{sn} = \Delta_s^{eff} + 5\, n_i |V|^2 \phi_{dn} / A_n \quad \ldots \quad 6.27\,b$$

$$Z_{dn} = 1 + \Gamma Z_{sn} / (Z_{sn}^2 \omega_n^2 + \phi_{sn}^2)^{\frac{1}{2}} \quad \ldots \quad 6.27\,c$$

$$\phi_{dn} = \Delta_d^{eff} + \Gamma \phi_{sn} / (Z_{sn}^2 \omega_n^2 + \phi_{sn}^2)^{\frac{1}{2}} \quad \ldots \quad 6.27d$$

where Δ_s^{eff} and Δ_d^{eff} are given by

$$\Delta_s^{eff} = \Delta_s - 5\, n_i\, t_{sd}\, \Delta_d$$

$$\Delta^{eff} = \Delta_s + t_{ds}\, \Delta_s \qquad \ldots \qquad 6.28$$

and Γ is the half-width of the resonance.

The finite temperature expressions for Δ_s and Δ_d are given by :

$$\Delta_s = \pi N(0) |g|\, kT \sum_{|\omega_n| < \omega_D} \frac{\phi_{sn}}{(Z_{sn}^2\, \omega_n^2 + \phi_{sn}^2)^{\frac{1}{2}}} \qquad 6.29$$

and

$$\Delta_d = - U\, kT \sum_n \frac{\phi_{dn}}{Z_{dn}^2\, \omega_n^2 + E_d^2 + \phi_{dn}^2} \qquad \ldots \qquad 6.30$$

6.3 The effect of recoil on the superconducting transition temperature of Al-Mn and Al-Cr

In order to obtain an expression for the superconducting transition temperature T_c, eqs. (6.27 a) - (6.27 d) are linearized with respect to quantities which characterize superconductivity of the alloy, namely, Δ_s, Δ_d, ϕ_{sn} and ϕ_{dn}. Near T_c, these quantities are small; hence the justification

for the linearization. Also $E_d = 0$ for Al-Mn and Al-Cr. Thus the set of self-consistent equations becomes:

$$Z_{sn} = 1 + 5\, n_i \frac{\Gamma}{\pi N(0)\, \eta_n^2\, \omega_n^2} \qquad \ldots \qquad 6.31\,a$$

$$\phi_{sn} = \Delta_s^{eff} + 5\, n_i \frac{\Gamma \phi_{dn}}{\pi N(0)\, \eta_n^2\, \omega_n^2} \qquad \ldots \qquad 6.31\,b$$

$$Z_{dn} = \eta_n \qquad \ldots \qquad 6.31\,c$$

$$\phi_{dn} = \Delta_d^{eff} + \frac{\Gamma\, \phi_{sn}}{Z_{sn} |\omega_n|} \qquad \ldots \qquad 6.31\,d$$

where

$$\eta_n = 1 + \frac{\Gamma}{|\omega_n|} \qquad \ldots \qquad 6.32$$

Eq. (6.31) gives ϕ_{sn} to the lowest order in n_i as :

$$\phi_{sn} \left\{ 1 - \frac{5\, n_i\, \Gamma^2}{\pi N(0) Z_{sn} \eta_n^2\, \omega_n^3} \right\} = \Delta_s^{eff} + \frac{5\, n_i\, \Gamma\, \Delta_d^{eff}}{\pi N(0) \eta_n^2\, \omega_n^2} + O(n_i^2)$$

$$\ldots \qquad 6.33$$

The superconducting transition temperature T_c is given by

$$\ln(T_{c0}/T_c) = \lim_{\Delta \to 0} \pi k T_c \sum_{\substack{n \\ |\omega_n^c| < \omega_D}} \left\{ Z_{sn}^c - \phi_{sn}^c/\Delta_s \right\} \Big/ Z_{sn}^c \, |\omega_n^c|$$

$$= \lim_{\Delta \to 0} \pi k T_c \sum_{\substack{n \\ |\omega_n^c| < \omega_D}} \left\{ \frac{1}{|\omega_n^c|} - \frac{\phi_{sn}^c/\Delta_s}{Z_{sn}^c \, |\omega_n^c|} \right\} \qquad 6.34$$

where T_{c0} and ω_D are, respectively, the superconducting transition temperature and the Debye frequency of the host metal. Substituting for Z_{sn} and ϕ_{sn} from eqs. (6.31a) and (6.33) yields the result :

$$\ln(T_{c0}/T_c) = K \pi k T_c \sum_{\substack{n \\ |\omega_n^c| < \omega_D}} \frac{(1-t_{ds}) + \phi(T_c)\,(1 + 5\, n_i\, t_{sd})}{|\omega_n^c| \left\{ (\eta_n^c \omega_n^c)^2 + K \right\}}$$

$$- 5\, n_i\, t_{sd}\, \phi(T_c)\, \pi k T_c \sum_{\substack{n \\ |\omega_n^c| < \omega_D}} \frac{1}{|\omega_n^c|} \qquad 6.35$$

where

$$K = 5\, n_i\, \Gamma / \pi N(0) \qquad \ldots \qquad 6.36$$

and

$$\phi(T) = -\Delta_d/\Delta_s \qquad \ldots \qquad 6.37$$

At $T = T_c$, Δ_d is given by

$$\Delta_d = - U\, kT \sum_n \frac{\phi_{dn}}{Z_{dn}^2\, \omega_n^2}$$

$$= - U\, kT \sum_n \left(\frac{\Delta_d + t_{ds}\, \Delta_s}{\eta_n^2\, \omega_n^2}\right) - U\, kT \sum_{|\omega_n| < \omega_D} \frac{\Gamma\, \phi_{sn}}{Z_{sn}\, \eta_n^2\, \omega_n^3} \qquad \ldots \quad 6.38$$

($E_d = 0$)

Substituting for ϕ_{sn}, eq. (6.38) becomes

$$\Delta_d \left(1 + U\, kT \sum_n \frac{1}{\eta_n^2\, \omega_n^2}\right) = - \Delta_s\, t_{ds}\, U\, kT \sum_n \frac{1}{\eta_n^2\, \omega_n^2} -$$

$$- U \Gamma kT \sum_{|\omega_n| < \omega_D} \left\{ \frac{\Delta_s\, (\eta_n^2\, \omega_n^2 + K t_{ds})}{(\eta_n \omega_n + K)\, \eta_n^2\, \omega_n^3} \right.$$

$$\left. + \frac{\Delta_d (K - 5 n_i\, t_{sd}\, \eta_n^2\, \omega_n^2)}{(\eta_n \omega_n + K)\, \eta_n^2\, \omega_n^3} \right\} \qquad 6.39$$

Putting

$$U_{eff} = \frac{U}{1 + U\, kT \sum_n \frac{1}{\eta_n^2\, \omega_n^2}} \qquad \ldots \quad 6.40$$

eq. (6.39) becomes

$$\Delta_d \left\{ 1 + U_{eff}\, \Gamma kT \left[K \sum_{\substack{n \\ |\omega_n| < \omega_D}} \frac{1}{(\eta_n^2 \omega_n^2 + K)\, \eta_n^2 \omega_n^3} - \right. \right.$$

$$\left. \left. - 5\, n_i\, t_{sd} \sum_{\substack{n \\ |\omega_n| < \omega_D}} \frac{1}{(\eta_n^2 \omega_n^2 + K)\, |\omega_n|} \right] \right\}$$

$$= - U_{eff}\, \Delta_s\, kT \left\{ t_{ds} \sum_n \frac{1}{\eta_n^2 \omega_n^2} + \Gamma \left[\sum_{\substack{n \\ |\omega_n| < \omega_D}} \frac{1}{\eta^2 \omega_n^3} - \right. \right.$$

$$\left. \left. - K(1 - t_{ds}) \sum_{\substack{n \\ |\omega_n| < \omega_D}} \frac{1}{(\eta_n^2 \omega_n^2 + K)\, \eta_n^2 \omega_n^3} \right] \right\} \qquad 6.41$$

The sums appearing in eq. (6.41) are evaluated in Appendix B.

$\phi(T)$ is obtained to be

$$\phi(T) = U_{eff} \left\{ t_{ds} \frac{\xi(2,\lambda)}{2\pi^2 kT} + \frac{\alpha}{\pi\Gamma} \left[1 - \frac{5n_i(1 - t_{ds})}{\pi N(0)\, \Gamma} \right] \right\}$$

$$\times \left\{ 1 + 5n_i\, U_{eff} \frac{\alpha}{\pi\Gamma} \left[\frac{1}{\pi N(0)\, \Gamma} + t_{ds} \right] \right\} \qquad 6.42$$

where

$$\alpha = \ln \left(\frac{1.14\ \omega_D}{kT} \right) \qquad \ldots \quad 6.43$$

Hence

$$\phi(T) = U_{eff} \left\{ t_{ds} \frac{\zeta(2,\lambda)}{2\pi^2 kT} + \frac{\alpha}{\pi \Gamma} \right\} + O(n_i) \qquad \ldots \quad 6.44$$

and $\zeta(2, \lambda)$ is the generalized Riemann zeta function of order 2.

Eq. (6.35), therefore, becomes

$$\ln(T_{c0}/T_c) = \frac{5 n_i \Gamma}{\pi N(0)} \left\{ \left[(1 - t_{ds}) + \phi(T_c) \right] \frac{\alpha}{\pi \Gamma^2} \right\} - 5\, n_i\, t_{sd}\, \phi(T_c)\, \frac{\alpha}{\pi}$$

$$= n_i \frac{N_d(0)}{N(0)} \alpha \left\{ (1 - t_{ds}) + \frac{1}{5} U_{eff}\, N_d(0)\, \alpha + U_{eff}\, t_{ds}\, \frac{\zeta(2, \lambda_c)}{2\pi^2\, kT_c} \right\}$$

$$- n_i\, N_d(0)\, \Gamma\, t_{sd}\, \alpha \left\{ \frac{1}{5} U_{eff}\, N_d(0) + U_{eff}\, t_{ds}\, \frac{\zeta(2, \lambda_c)}{2\pi^2\, kT_c} \right\} + O(n_i^2) \qquad 6.45$$

where $N_d(0) = 5/\pi\Gamma$ is the bare d-electron density

of states at the Fermi surface. Use of the approximation $\zeta(2, \lambda_c) \approx 2\pi kT_c$ (see Appendix B) gives the result :

$$\ln (T_{c0}/T_c) = n_i \frac{N_d(0)}{N(0)} \alpha \left\{ (1-t_{ds}) + \frac{1}{5} U_{eff} N_d(0)(\alpha + t_{ds}) \right\}$$

$$- n_i N_d(0) \Gamma t_{sd} \alpha \left\{ \frac{1}{5} U_{eff} N_d(0)(1 + t_{ds}) \right\} \quad \ldots \quad 6.46$$

The initial decrease of T_c with respect to n_i is from eq. (6.46)

$$\left. \frac{\partial T_c}{\partial n_i} \right|_{n_i = 0} = - T_{c0} \frac{N_d^{eff}(0)}{N(0)} \alpha \left\{ 1 + \frac{1}{5} \tilde{U}_{eff} N_d^{eff}(0) \alpha \right\} \quad 6.47$$

where

$$N_d^{eff}(0) = N_d(0) (1 - t_{ds}) \quad \ldots \quad 6.48$$

and

$$\tilde{U}_{eff} = U_{eff}(1 - t_{ds})^{-2} \left\{ (1 + \alpha^{-1} t_{ds}) \left[1 - \frac{5N(0)}{N_d^{eff}(0)} t_{sd}(1 - t_{ds}) \right] \right\}$$

$$\ldots \quad 6.49$$

The expression of Ratto and d'Agliano[18] for the initial decrease is obtained by putting $t_{sd} = t_{ds} = 0$. Their result is

$N_d^{eff}(0)$ is an effective superconducting density of states which is different from the phonon-enhanced density of states in the normal alloy.

$$\left.\frac{\partial T_c}{\partial n_i}\right|_{n_i=0}^{RA} = - T_{c0} \frac{N_d(0)}{N(0)} \alpha \left\{ 1 + \frac{1}{5} U_{eff} N_d(0) \alpha \right\} \qquad 6.50$$

We note that eq. (6.47) has the same form as eq. (6.50) with U_{eff} replacing U and $N_d^{eff}(0)$. The recoil effects are implicit in the two quantities U_{eff} and $N_d^{eff}(0)$.

6.4 The energy gap equation

The renormalized energy gap function Δ_{Gn} is given by (G.2)

$$\Delta_{Gn} = \phi_{sn} / Z_{sn} \qquad \ldots \qquad 6.51$$

Eqs. (6.31a), (6.31b) and (6.51) yield the following result :

$$\Delta_{Gn} \left\{ 1 + 5 n_i \frac{|V|^2}{A_n} \left(1 + \frac{\Gamma Z_{sn}}{(Z_{sn}^2 \omega_n^2 + \phi_{sn}^2)^{\frac{1}{2}}} \right) \right\}$$

$$= \Delta_s^{eff} + 5 n_i \frac{|V|^2}{A_n} \Delta_d^{eff} + \frac{\Gamma Z_{sn} \Delta_{Gn}}{(Z_{sn}^2 \omega_n^2 + \phi_{sn}^2)^{\frac{1}{2}}}$$

$$\ldots \qquad 6.52$$

which reduces to

$$\Delta_{Gn} (1 + K_n) = \Delta_s^{eff} + K_n \Delta_d^{eff} \qquad \ldots \qquad 6.53$$

where

$$K_n = 5\, n_i\, |V|^2 / A_n = 5\, n_i\, \Gamma / \pi N(0)\, A_n \qquad 6.54$$

From eqs. (6.28) and (6.53) the expression for the energy gap function is

$$\Delta_{Gn} = \Delta^K_{Gn} + \frac{5\, n_i\, t_{sd}\, \Delta_d + K_n\, t_{ds}\, \Delta_s}{1 + K_n} \quad \ldots \qquad 6.55$$

Δ^K_{Gn} is given by [16]

$$\Delta^K_{Gn} = \frac{\Delta_s + K_n\, \Delta_d}{1 + K_n} \quad \ldots \qquad 6.56$$

For non-magnetic alloys, $\Gamma >> kT_c >> \Delta_s, \Delta_d$. Hence

$$A_n = \eta_n\, \omega_n = (\Gamma + |\omega_n|)^2 \quad \ldots \qquad 6.57$$

Thus when $\omega_n < \omega_D$ and $\Gamma >> \omega_D$, A_n and hence K_n are independent of ω_n, i.e.

$$K_n = C = n_i \frac{N_d(0)}{N(0)} \quad \ldots \qquad 6.58$$

Consequently, the energy gap function Δ_{Gn} is real. Hence, eq. (6.55) becomes

$$\Delta_{Gn} = \Delta^K_G + \frac{5\, n_i\, t_{sd}\, \Delta_d + C\, t_{ds}\, \Delta_s}{1 + C} \qquad 6.59$$

where [16]

$$\Delta_G^K = (\Delta_s + C\,\Delta_d)/(1 + C) \quad \ldots \quad 6.60$$

Eqs. (6.37), (6.44) and (6.59) lead to the result

$$\Delta_G = f\Delta_s \quad \ldots \quad 6.61$$

f is given by

$$f = f_1 + f_{ds} + f_{sd} \quad \ldots \quad 6.62\,a$$

where

$$f_1 = (1 - Cd)/(1 + C) \quad \ldots \quad 6.62\,b$$

$$f_{ds} = C\,t_{ds}/(1 + C) \quad \ldots \quad 6.62\,c$$

$$f_{sd} = -5\,n_i\,dt_{sd}/(1 + C) \quad \ldots \quad 6.62\,d$$

and

$$\Delta_d = -\phi(T)\,\Delta_s = -d\,\Delta_s \quad \ldots \quad 6.62\,e$$

Also

$$f_K = (1 - Cd_K)/(1 + C) \quad \ldots \quad 6.63a$$

where

$$d_K = \frac{1}{5}\,\frac{N_d(0)\,U_{eff}}{N(0)\,|g|} \quad \ldots \quad 6.63\,b$$

The factor (1 + C) represents an increase in the density of conduction electron states due to the participation of the d-electrons near the Fermi level. On the other hand, (1-Cd) gives the pair weakening effect of the Coulomb repulsion U between spin-up and spin-down d-electrons in the non-magnetic limit. Consequently f_1 represents a weakening of the superconducting pairing in the absence of recoil effects.

It is not clear at the moment what physical interpretation can be given to f_{ds} and f_{sd}.

Superconductivity is quenched at the critical impurity concentration n_i^c which is given by $\Delta_G = 0$, i.e. $f = 0$. Thus eq. (6.62) gives

$$n_i^c = N(0) \left\{ N_d(0) (d - t_{ds}) + 5 d t_{sd} \right\}^{-1} \qquad 6.64$$

For Al-Mn the critical impurity concentration is found to be 1.01 at.% and for Al-Cr, it is 1.68 at.%.

6.5 The superconducting density of states

The density of states of the conduction electrons in the excitation spectrum of a superconductor $N(\omega)$, is given by [37]

$$N(\omega) = \frac{1}{\pi} \mathrm{Im} \sum_m \hat{G}_k(\omega) \Big|_{\mathrm{diag}}$$

$$= N(0) \, \mathrm{Re} \left\{ \frac{\omega}{(\omega^2 - \Delta_G^2)^{\frac{1}{2}}} \right\} \qquad \ldots \qquad 6.65$$

where the subscript "diag" stands for the diagonal part of the conduction electron matrix Green's function $\hat{G}_k(\omega)$. There are no single electron states below the gap edge, i.e. $\omega < \Delta_G$. Since the gap is purely real, eq.(6.65) is identical with the BCS density of states, and

$$\frac{N(\omega)}{N(0)} = \frac{\left(\frac{\omega}{\Delta_{00}}\right)}{\left\{\left(\frac{\omega}{\Delta_{00}}\right)^2 - \left(\frac{\Delta_G}{\Delta_{00}}\right)^2\right\}^{\frac{1}{2}}} \quad \ldots \quad 6.66$$

Δ_{00} is the order parameter of the pure superconductor at $0^{\circ}K$. The superconducting density of states normalized with respect to the density of states of the normal metal at the Fermi level plotted against (ω/Δ_{00}) is shown in Fig. (20). For a fixed value of Δ_{00}, the normalized density of states tends to unity as ω/Δ_{00} becomes large. The similarity of the plot with the BCS density of states is not surprising, since Δ_G is real. Also Kaiser [16] has shown that the dilute non-magnetic superconducting alloys behave essentially like BCS superconductors. The sharp peak shifts towards lower frequencies as the impurity concentration increases. The figures written against the curves denote the impurity concentration in at.% Kiwi and Zuckermann [6] obtained a similar density of states curve.

6.6 Calculation of the energy gap Δ_G at zero temperature

The gap function is readily calculated through the order parameter Δ_s of the alloy. Eqs. (6.29) and (6.51) give the following result :

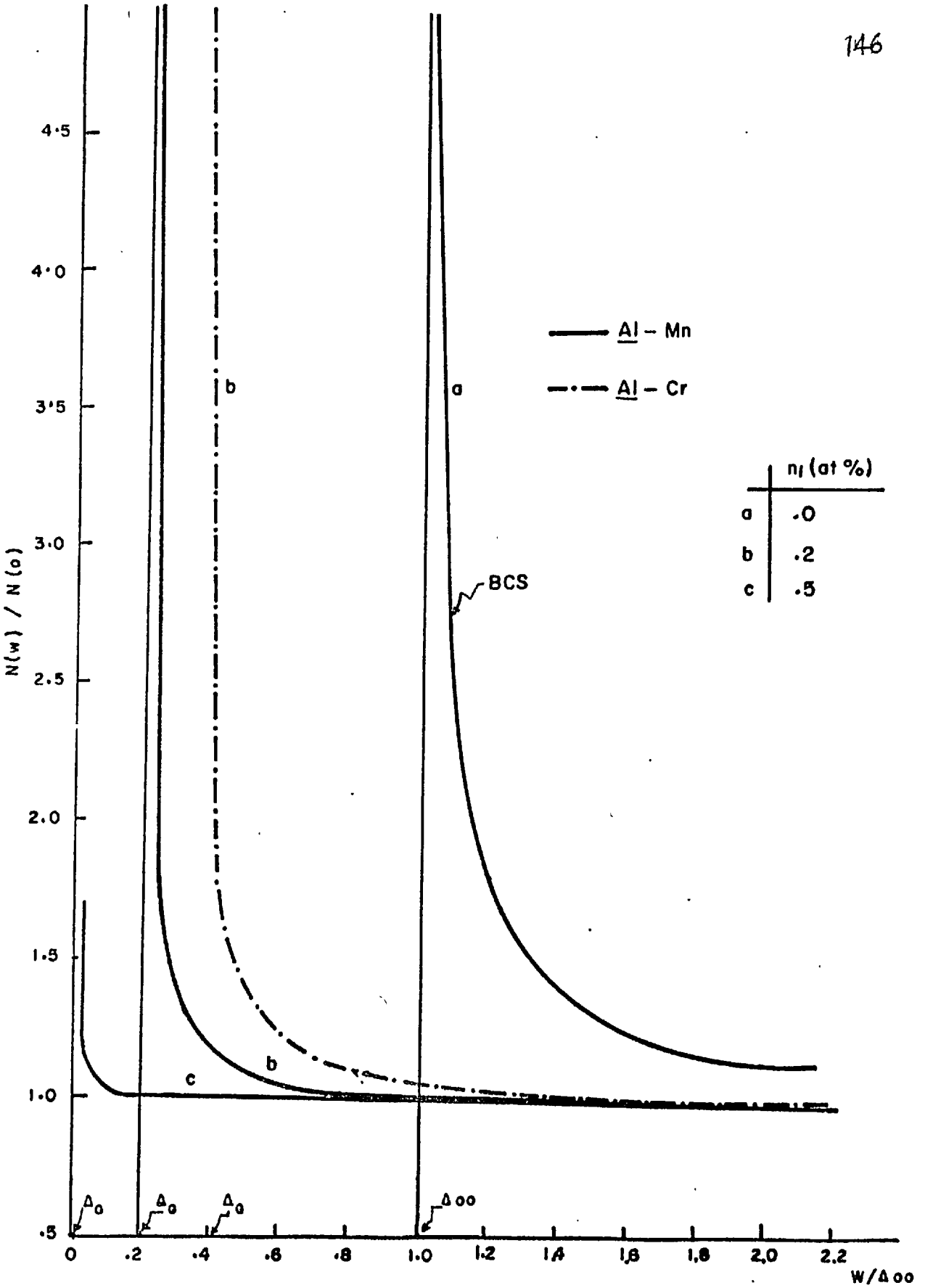

4·5
4·0
3·5
3·0
2.5
2.0
1.5
1.0
·5
N(w) / N(o)
Al – Mn
Al – Cr
b
a
BCS
c
b
n_I (at %)
a .0
b .2
c .5
Δ_o
Δ_o
Δ_o
Δ_∞
0
.2
.4
.6
.8
1.0
1.2
1.4
1.6
1.8
2.0
2.2
W/Δ_∞

Fig. 20

$$\Delta_s = \pi N(0) |g| kT \sum_{|\omega_n| < \omega_D} \frac{\Delta_G}{(Z_{sn}^2 \omega_n^2 + \Delta_G^2)^{\frac{1}{2}}} \quad \ldots \quad 6.67$$

At $T = 0$, the sum over ω_n is replaced by an integral over ω (G.1), i.e.

$$kT \sum_{|\omega_n| < \omega_D} \rightarrow \int_{-\omega_D}^{\omega_D} \frac{d\omega}{2\pi} \quad \ldots \quad 6.68$$

Thus the zero temperature expression for the order parameter is

$$\Delta_s(T\ 0) = \Delta_{s0} = N(0) |g| \Delta_{G0} \ln \left(\frac{2\omega_D}{\Delta_{G0}}\right) \quad \ldots \quad 6.69\,a$$

or

$$\frac{1}{f\lambda_s} = \ln \left(\frac{2\omega_D}{\Delta_{G0}}\right) \quad \ldots \quad 6.69\,b$$

where $\lambda_s = N(0) |g|$. Eq. (6.69 b), therefore, gives the energy gap as

$$\Delta_{G0} = 2\omega_D e^{-1/f\lambda_s} \quad \ldots \quad 6.70$$

For the pure superconductor the order parameter (which is the same as the energy gap) at zero degree is

---

f is a renormalization of the BCS coupling constant due to both the Coulomb repulsion U and the virtual recoil effect (see eq. (6.62)).

$$\Delta_{00} = 2\omega_D \, e^{-1/\lambda_s} \qquad \ldots \quad 6.71$$

Hence

$$\Delta_{G0}/\Delta_{00} = \exp\left\{(f-1)/f\lambda_s\right\} \qquad \ldots \quad 6.72$$

Also the ratio of the order parameter of the dilute alloy to that of the pure superconductor at $T = 0$ is given by

$$\Delta_{s0}/\Delta_{00} = (1/f)\exp\left\{(f-1)/f\lambda_s\right\} \qquad 6.73$$

Both Δ_{G0} and Δ_{S0} depend on n_i. This dependence is shown in Fig. (21) for Al-Mn and Al-Cr.

The superconducting transition temperature T_c may also be written in the BCS form, if the following replacements are carried out :

$$\lambda_s \rightarrow f\lambda_s$$
$$\Delta_0 \rightarrow \Delta_G = f\Delta_s \qquad \ldots \quad 6.74$$

Thus the BCS expression

$$T_{c0} = 1.14\,\omega_D \, e^{-1/\lambda_s} = 1.14\,\omega_D \, e^{-1/N(0)|g|} \qquad 6.75$$

is replaced by

$$T_c = 1.14\omega_D \, e^{-1/f\lambda_s} = 1.14\omega_D \, e^{-1/N(0)|g_{eff}|} \qquad 6.76$$

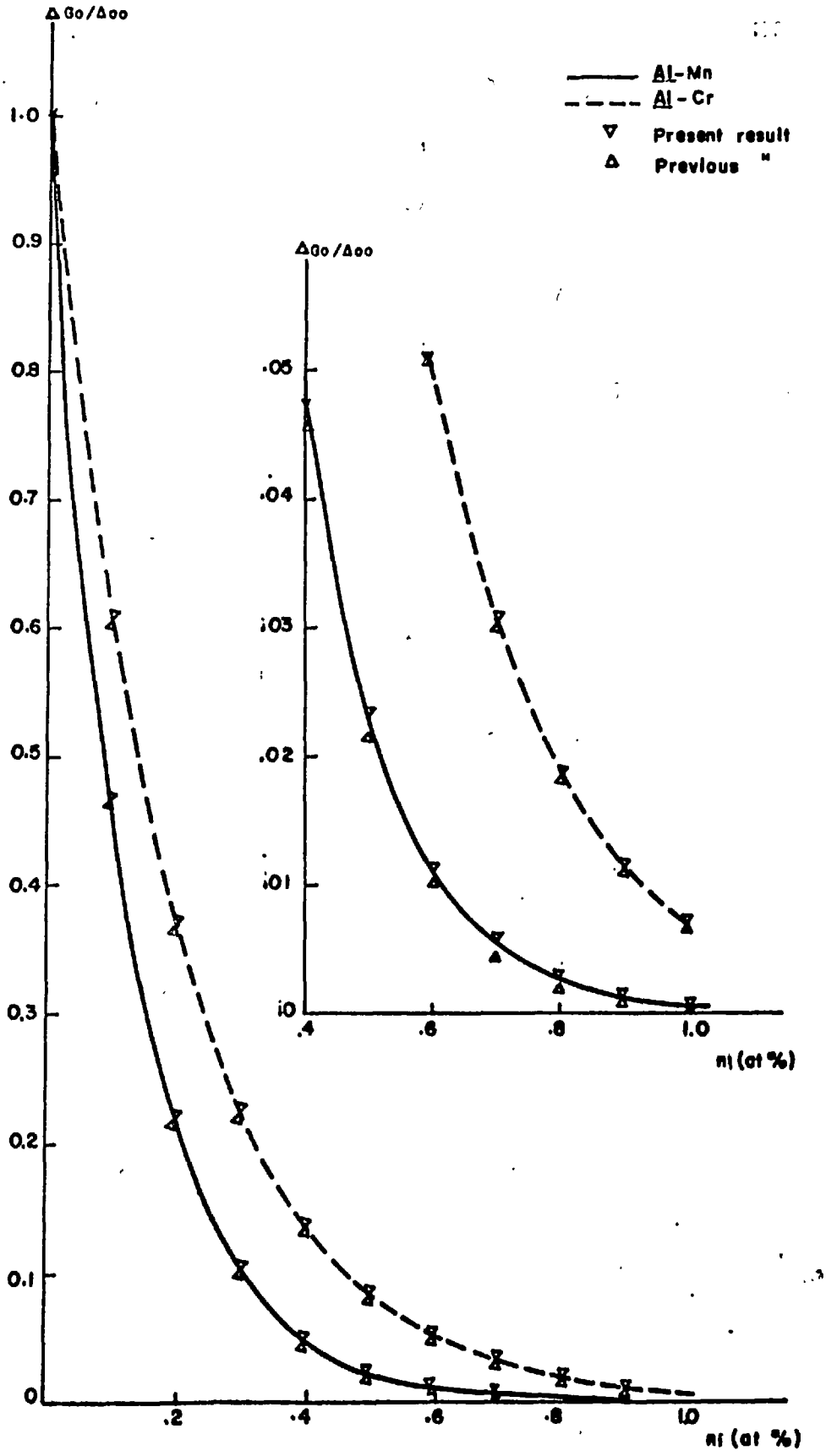

Δ Go/Δoo
Al-Mn
Al - Cr
Present result
Previous "
1.0
0.9
0.8
0.7
0.6
0.5
0.4
0.3
0.2
0.1
0
.2
.4
.6
.8
1.0
at (at %)
Δ Go/Δoo
.05
.04
.03
.02
.01
.0
.4
.6
.8
1.0
at (at %)

Fig. 21

where g_{eff} is an effective coupling strength. Eqs. (6.72), (6.75) and (6.76) give the relation

$$T_c / T_{c0} = \Delta_{G0} / \Delta_{00} = \exp \{ (f-1) / f\lambda_s \} \quad \ldots \quad 6.77\,a$$

i.e.

$$T_c / T_{c0} = 1 + (f-1) / f\lambda_s \quad \ldots \quad 6.77\,b$$

The change ΔT_c in the transition temperature of the host metal due to the presence of the impurity is, therefore, given by

$$\Delta T_c / T_{c0} = (f-1) / f\lambda_s$$

$$= - n_i \frac{N_d(0)}{N(0)} \alpha \left\{ 1 + \frac{1}{5} N_d(0)\, U_{eff}\, \alpha \right.$$

$$- t_{ds} \left(1 - \frac{1}{5} N_d(0)\, x \right.$$

$$\left. \left. x\, U_{eff}\, \alpha \right\} - n_i\, t_{sd}\, N_d(0)\, U_{eff}\, \alpha\, (\alpha + t_{ds}) \right.$$

$$\ldots \quad 6.78$$

where

$T_c = T_{c0} + \Delta T_c$. Eq. (6.78) agrees with eqs. (6.46) and (6.47) obtained earlier. $\Delta T_c / \Delta T_{c0}$

is plotted as a function of n_i in Fig. (22). The plot shows that the impurity recoil leads to an enhancement of T_c obtained by Ratto and d'Agliano [18] and Kaiser [16]. In addition, eq. (6.77) yields the law of corresponding states, namely

$$\Delta_{GO}/kT_c = \Delta_{OO}/kT_{cO} = 1.76 \quad \ldots \quad 6.79$$

In order to obtain a measure of the effect of the recoil on T_c, it is desirable to link the s-d interaction strength g^{rec} with the system parameters α_q and Γ, which appeared in Part One of the thesis. From Fig. (19), $g^{rec}(\omega)$ is given by

$$g^{rec}(\omega_n - \omega_m) = |V|^2 k_F^2 \sum_q |\alpha_q|^2 D_q(\omega_n - \omega_m) \qquad 6.80a$$

Hence

$$g^{rec}(\omega - \omega') = |V|^2 k_F^2 \sum_q |\alpha_q|^2 D_q(\omega - \omega') \quad \ldots \quad 6.80b$$

It is convenient, at this stage, to use the spectral representation for the phonon Green's function. This is given by

$$D_q(\omega) = \int \frac{B_q(\omega')\, d\omega'}{\omega - \omega' + i\delta}, \quad \delta \to +0 \qquad 6.81$$

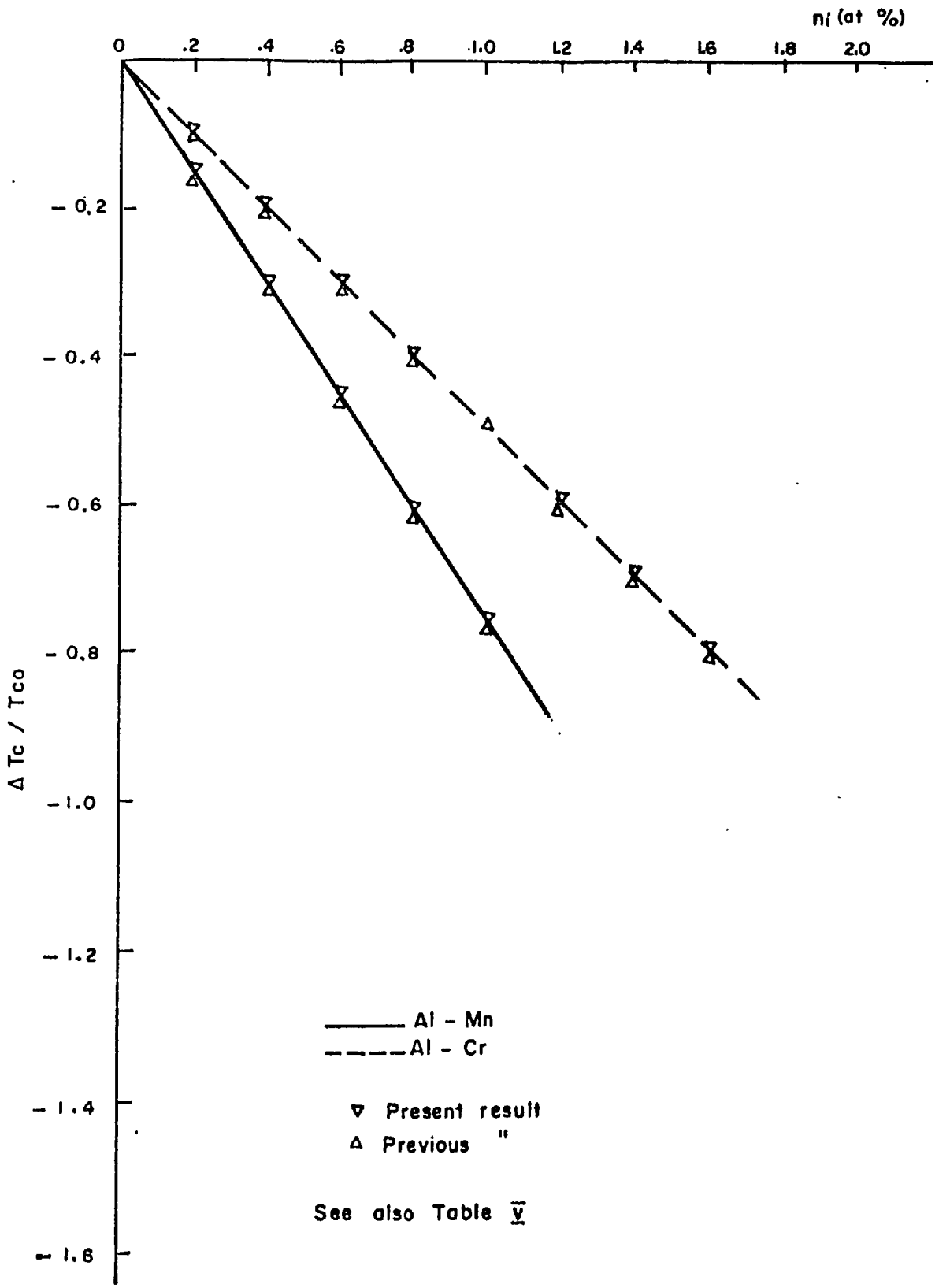

ni (at %)
0
.2
.4
.6
.8
1.0
1.2
1.4
1.6
1.8
2.0
- 0.2
- 0.4
- 0.6
- 0.8
- 1.0
- 1.2
- 1.4
- 1.6
Δ Tc / Tco
Al - Mn
Al - Cr
▽ Present result
△ Previous "
See also Table V

Fig. 22

TABLE III

Al-Mn

n_i (at.%)	$-\Delta T_c / T_{co}$ (present)	$-\Delta T_c / T_{co}$ (previous)
0	0.00000000	0.00000000
.02	0.153013174	0.15315363
.04	0.30606349	0.30630727
.06	0.45909524	0.45946091
.08	0.61212701	0.61261457
.10	0.76515874	0.76576819
.12	0.91819052	0.91892182
.14	1.0712222	1.0720754
.16	1.2242539	1.2252290
.18	1.3772857	1.3783827
.20	1.5303174	1.5315363

Al-Cr

0	0.00000000	0.00000000
.02	0.10010099	0.10019576
.04	0.20020200	0.20039153
.06	0.30030299	0.30058729
.08	0.40040399	0.40078305
.10	0.50050501	0.50097884
.12	0.60060601	0.60117460
.14	0.70070701	0.70137037
.16	0.80080798	0.80156614
.18	0.90090900	0.90176185
.20	1.0010099	1.0019576

where the spectral weight function $B_q(\varpi)$ is antisymmetrical with respect to frequency, i.e.

$$B_q(-\varpi) = -B_q(\varpi) \qquad \ldots \quad 6.82$$

If the negative frequencies are converted to positive frequencies, eq. (6.81) becomes

$$D_q(\varpi) = \int_0^\infty d\varpi' \; B_q(\varpi') \left\{ \frac{1}{\varpi - \varpi' + i\delta} - \frac{1}{\varpi + \varpi' + i\delta} \right\}$$

Assuming that the phonons have small decay rates at the low temperatures of interest, we put $B_q(\omega) = \delta(\omega - \omega_q)$ into eq. (6.80) and take the interaction to be constant for

and zero otherwise, i.e. BCS approximation. Consequently only the zero frequency value of $g^{rec}(\omega)$ is to be calculated. Thus

$$|g^{rec}| \equiv |g^{rec}(o)| = \frac{|V|^2 k_F^2}{MN} \sum_q (1/\omega_q^2) \qquad \ldots 6.84$$

where $\alpha_q = (1/2MN\omega_q)^{1/2}$.

The sum over the phonon frequencies is now written as an integral by introducing the phonon density of states $F(\omega)$. (See eqs. (4.34) and (4.35)).

For a Debye spectrum the sum in eq. (6.84) yields $1/\omega_D^2$.

Hence

$$N(0)\,|g^{rec}| = \frac{6}{\pi}\left(\frac{m}{M}\right)\left(\frac{\epsilon_F}{k\Theta_D}\right)\left(\frac{\Gamma}{k\Theta_D}\right) \qquad \ldots \quad 6.86$$

The calculated values of $N(0)\,|g^{rec}|$ as well as t_{sd} and t_{ds} for Al-Mn and Al-Cr are given in Table V.

From eq. (6.76), $|g_{eff}|$ is expressed in terms of $|g|$ by

$$|g_{eff}| = |g| - n_i \frac{N_d^2(0)\,U_{eff}}{5\,N^2(0)}\left[1 - \frac{5\,N(0)|g|\,t_{ds}}{N_d(0)\,U_{eff}}\right]$$

$$- n_i \frac{N_d^2(0)\,U_{eff}}{5\,N^2(0)} \cdot N(0)\,|g|\,t_{ds}$$

$$- n_i \frac{N_d(0)\,U_{eff}}{N(0)|g|}\,\frac{t_{sd}}{N(0)}\left[1 + \frac{t_{ds}}{N(0)|g|}\right] \qquad 6.87$$

When $t_{sd} = t_{ds} = 0$, the result of Ratto and d'Agliano is retrieved, viz. :

$$|g'_{eff}| = |g| - n_i \frac{N_d^2(0)\,U_{eff}}{5\,N^2(0)} \qquad \ldots \quad 6.88$$

$$|g^{rec}| = |V|^2 k_F^2 \frac{3}{M\omega_D^3} \int_0^{\omega_D} d\omega$$

i.e. $$N(0)|g^{rec}| = \frac{6}{\pi}\left(\frac{m}{M}\right)\left(\frac{\epsilon_F}{k\Theta_D}\right)\left(\frac{\Gamma}{k\Theta_D}\right) \quad \ldots \quad 6.90$$

The calculated values of $N(0)|g^{rec}|$ as well as t_{sd} and t_{ds} for Al-Mn and Al-Cr are given in Table V.

From eq. (6.76), $|g_{eff}|$ is expressed in terms of $|g|$ by

$$|g_{eff}| = |g| - n_i \frac{N_d^2(0)\, U_{eff}}{5\, N^2(0)} \left[1 - \frac{5\, N(0)|g|\, t_{ds}}{N_d(0)\, U_{eff}}\right]$$

$$- n_i \frac{N_d^2(0)\, U_{eff}}{5\, N^2(0)} \cdot N(0)|g|\, t_{ds}$$

$$- n_i \frac{N_d(0)\, U_{eff}}{N(0)|g|} \frac{t_{sd}}{N(0)} \left[1 + \frac{t_{ds}}{N(0)|g|}\right] \quad 6.91$$

When $t_{sd} = t_{ds} = 0$, the result of Ratto and d'Agliano is retrieved, viz. :

$$|g'_{eff}| = |g| - n_i \frac{N_d^2(0)\, U_{eff}}{5\, N^2(0)} \quad \ldots \quad 6.92$$

TABLEIV

	Al-Mn	Al-Cr
$\tilde{N}_d(0)$ states/eV-atom	9.26	6.74
a	0.017	0.003
$N_d(0)$ states/eV-atom	9.11	6.72
Γ eV	0.17	0.23
E_d eV	0	0
$N(0)\|g^{rec}\|$	0.017	0.003
t_{ds}	0.103	0.018
t_{sd}	0.120	0.020
$\phi(T) = d$	2.97	2.48
+ $N_d(0)$	9.87	6.52

+ From depression of superconducting transition temperature.

Fig. (23 a) shows the dependence of g_{eff} on n_i. The plot indicates that, for Al-Mn, superconductivity is quenched at the critical impurity concentration n_i^c of 0.99 at.%. The corresponding value of n_i^c for Al-Cr is obtained from Fig. (23 b) to be 1.67 at.%. These figures are in good agreement with 1.01 at.% and 1.68 at.% obtained using eq. (6.64) for Al-Mn and Al-Cr, respectively.

The formula of Ratto and d'Agliano gives n_i^c equal to 1.10 at.% and 1.76 at.% for Al-Mn and Al-Cr, respectively.

The ratio

$$\Lambda = \frac{|g_{eff}| - |g|}{|g'_{eff}| - |g|}$$

has been computed for Al-Mn and Al-Cr, where $g'_{eff} = g_{eff} \mid t_{sd} = 0 = t_{ds}$. The computed values are :

Al-Mn : $\Lambda = 1.164$, with $t_{ds} = .103$ and $t_{sd} = .120$.

Al-Cr : $\Lambda = 1.024$, with $t_{ds} = .018$ and $t_{sd} = .020$.

These values confirm the assertion that the recoil phonons play some role in the superconductivity of the

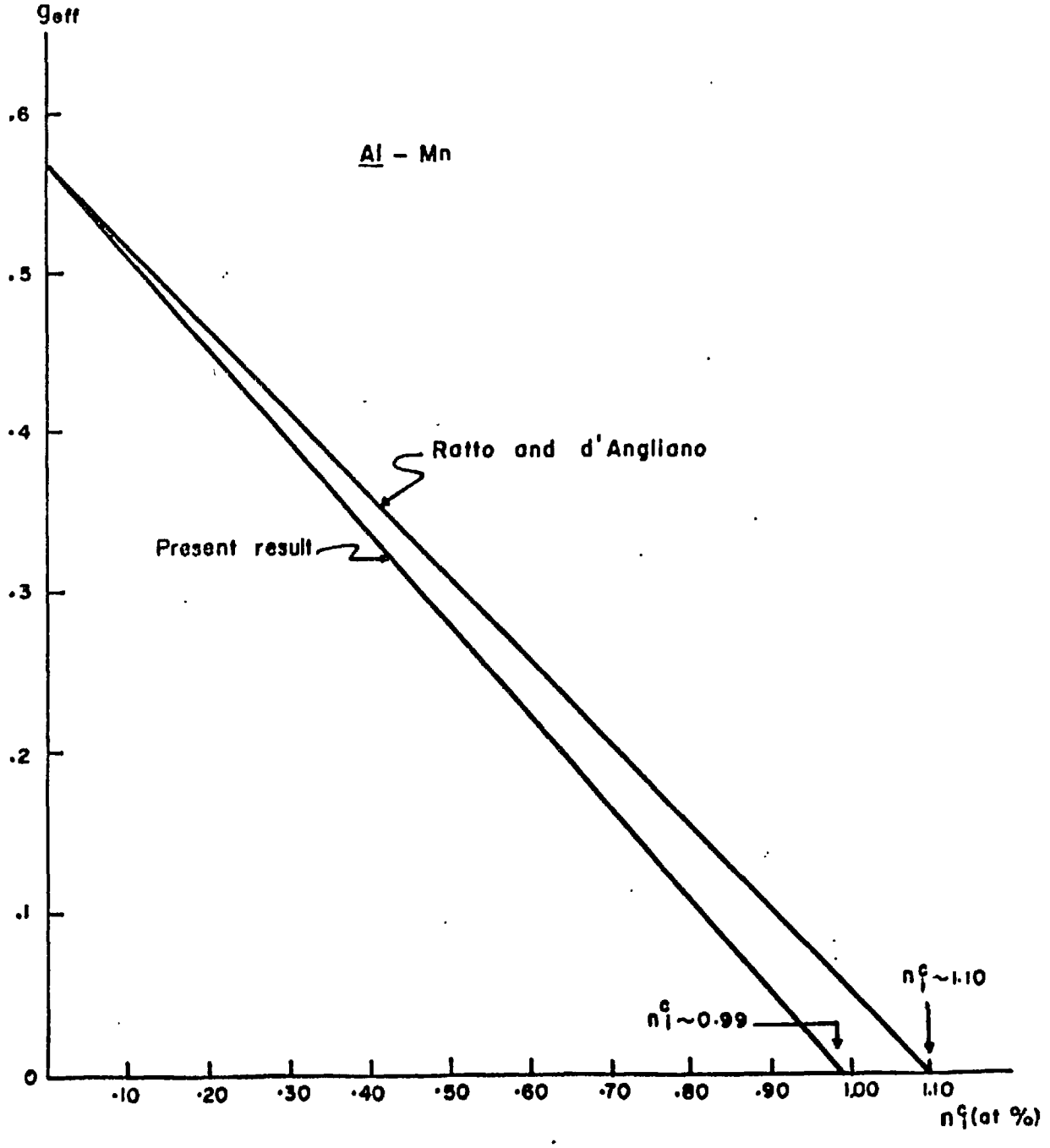

g_{eff}
.6
.5
.4
.3
.2
.1
0
Al – Mn
Rotto and d'Angliano
Present result
$n_i^c \sim 1.10$
$n_i^c \sim 0.99$
·10
·20
·30
·40
·50
·60
·70
·80
·90
1.00
1.10
n_i^c (at %)

Fig. 23.a

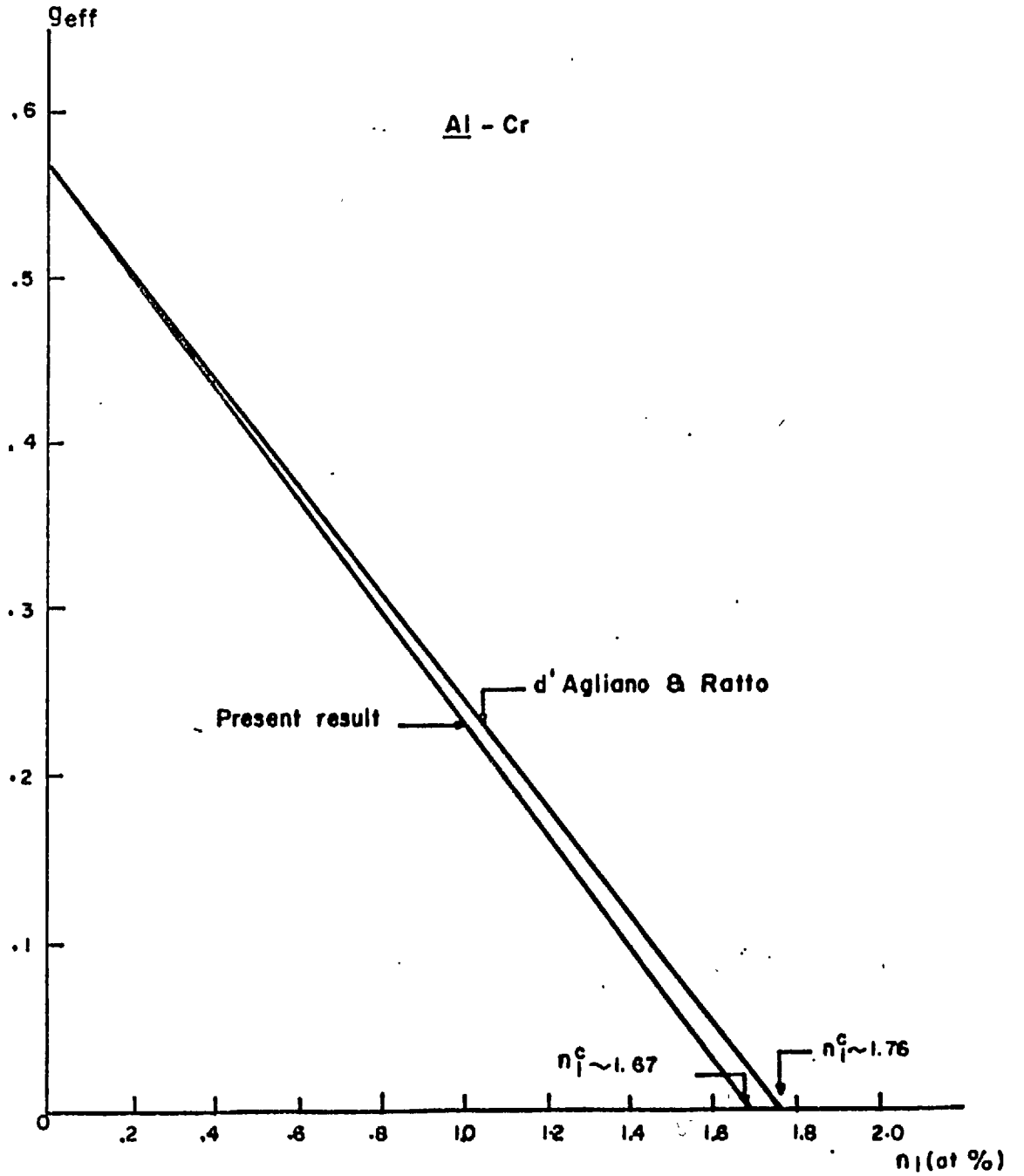

g_{eff}
.6
.5
.4
.3
.2
.1
0
Al - Cr
d' Agliano & Ratto
Present result
$n_l^c \sim 1.67$
$n_l^c \sim 1.76$
.2
.4
.6
.8
1.0
1.2
1.4
1.6
1.8
2.0
n_l (at %)

Fig. 23.b

aluminium-iron group alloys, especially when there is a strong resonance scattering, as in Al-Mn.

It is also useful to compare the strengths of the s-d and the s-s (BCS) coupling constants. Writing $\mu = |g^{rec}| / |g|$, the respective sizes of μ for Al-Mn and Al-Cr are

$$\mu_{Al\text{-}Mn} = 0.12 \quad \text{and} \quad \mu_{Al\text{-}Cr} = 0.02$$

that is, the recoil contributions to the superconductivity of these alloys are 12% and 2%, respectively, of the BCS contribution.

CHAPTER SEVEN

7. THERMODYNAMIC FUNCTIONS

In this chapter the effects of the impurity recoil on the thermodynamic properties of dilute non-magnetic superconducting alloys of Al-Mn and Al-Cr are examined. The expressions for the temperature dependence of the energy gap $\Delta_G(T)$, the electronic specific heat $C_s(T)$ and the critical magnetic field $H_c(T)$ are derived from temperatures close to T_c and 0^oK.

7.1 Thermodynamic properties of the superconducting alloy for temperatures close to the transition temperature : $T = T_c$

7.1.1 The energy gap

In order to obtain the temperature dependence of the energy gap $\Delta_G(T)$, the self-consistent equation for the order parameter Δ_s is expanded in powers of the energy gap. For temperatures close to T_c, i.e. $(T_c - T) << T_c$, eq. (6.67) gives the following result:

$$\frac{1}{\lambda_s} = \pi kTf\left\{\sum_{\substack{n \\ |\omega_n| < \omega_D}} \frac{1}{|\omega_n|} - \frac{\Delta_G^2(T)}{2} \sum_n \frac{1}{|\omega_n|^3}\right\} \qquad 7.1$$

Recalling that at $T = T_c$, the gap is zero, eq. (7.1) becomes (for this case)

$$\frac{1}{\lambda_s} = \pi k T_c \, f \sum_{\substack{n \\ |\omega_n^c| < \omega_D}} \frac{1}{|\omega_n^c|} \qquad \ldots \quad 7.2$$

Combining eqs. (7.1) and (7.2) yields

$$\ln\left(\frac{T}{T_c}\right) = - \frac{\pi k T f}{2} \Delta_G^2(T) \sum_n \frac{1}{|\omega_n|^3} \qquad \ldots \quad 7.3\,a$$

$$= - \frac{f \Delta_G^2(T)}{(\pi k T)^2} \sum_{n=0}^{\infty} \frac{1}{(2n+1)^3} \qquad \ldots \quad 7.3\,b$$

where $|\omega_n| = (2n + 1)\pi k T$ and the summation over n is extended to infinity, since the sum converges rapidly (G.1). The result is expressed in terms of Riemann zeta function $\zeta(z)$, which is given by

$$\sum_{n=0}^{\infty} \frac{1}{(2n+1)^z} = \frac{2^z - 1}{2^z} \zeta(z) \qquad \ldots \quad 7.4$$

Hence eq. (7.3 b) becomes

$$\ln\left(\frac{T}{T_c}\right) = - \frac{7}{8} \zeta(3) \, f \frac{\Delta_G^2(T)}{(\pi k T)^2} \qquad \ldots \quad 7.5$$

Rewriting the left hand side of eq. (7.5) as

$$\ln\left(\frac{T}{T_c}\right) = \ln\left(1 + \frac{T - T_c}{T_c}\right) \approx -\left(1 - \frac{T}{T_c}\right) \quad \ldots \quad 7.6$$

and substituting back into eq. (7.5) gives the temperature dependence of the gap in the form :

$$\Delta_G(T) = \frac{\pi k T_c}{\sqrt{f}} \sqrt{\frac{8}{7\zeta(3)}} \sqrt{1 - \frac{T}{T_c}} \quad 7.7$$

where it is assumed that T is not too different from T_c in the first factor on the right hand side of eq. (7.7). The corresponding expression for the pure metal is given by (G.1) :

$$\Delta_0(T) = \pi k T_{c0} \sqrt{\frac{8}{7\zeta(3)}} \sqrt{1 - \frac{T}{T_{c0}}} \quad \ldots \quad 7.8$$

Hence eqs. (7.7) and (7.8) together give

$$\frac{\Delta_G(T)}{\Delta_0(T)} = \frac{1}{\sqrt{f}} \left(\frac{T_c - T}{T_{c0} - T}\right)^{\frac{1}{2}} \left(\frac{T_c}{T_{c0}}\right) \quad \ldots \quad 7.9$$

From eqs. (6.62) and (6.63),

$$\frac{1}{f} = (1 + C)\left[1 - C(d - t_{ds}) - 5\, n_i\, d\, t_{sd}\right]^{-1}$$

$$= 1 + C\,(1 + d - t_{ds}) + 5\, n_i\, d\, t_{sd} + O(n_i^2) \quad 7.10$$

Thus the expression for $\Delta_G(T)$ becomes

$$\Delta_G(T) = \pi k T_c \sqrt{\frac{8}{7\zeta(3)}} \left\{ 1 + n_i \frac{N_d(0)}{2N(0)} (1 + d - t_{ds}) + \right.$$

$$\left. + \frac{5}{2} n_i d\, t_{sd} \right\} \left(1 - \frac{T}{T_c}\right)^{\frac{1}{2}} \qquad 7.11$$

At an impurity concentration of 0.05 at.% and a reduced temperature T/T_{c0} equal to 0.75, the size of the ratio of the gap function with and without recoil contribution

$$\Pi = \left[\frac{\Delta_G(T)}{\Delta_G(T) \mid t_{ds} = 0 = t_{sd}} \right]$$

is computed to be :

$$\Pi_{\underline{Al}\text{-}Mn} = 1.00022 \quad \text{and} \quad \Pi_{\underline{Al}\text{-}Cr} = 1.0079$$

7.1.2 The electronic specific heat

The discontinuity in the electronic specific heat at the transition temperature T_c is obtained from the difference between the Helmholtz free energies of the superconducting and normal states. This is given by [6,10]

$$F_S - F_N = \int_o^{\Delta_G} \left(\frac{\partial |g|^{-1}}{\partial \Delta_G} \right) \Big|_{T = T_c} \Delta_G^2 \, d\Delta_G \qquad 7.12$$

From eq. (7.1),

$$|g|^{-1} = N(0)\,\pi f\,kT \left\{ \sum_{|\omega_n|<\omega_D} \frac{1}{|\omega_n|} - \frac{\Delta_G^2}{2} \sum_n \frac{1}{|\omega_n|^3} \right\} \qquad 7.13$$

i.e.

$$\left.\frac{\partial |g|^{-1}}{\partial \Delta_G}\right|_{T=T_c} = -\pi N(0) f kT_c\, \Delta_G \sum_n \frac{1}{|\omega_n^c|^3}$$

$$= -\frac{7}{4}\zeta(3)\frac{N(0)f}{(\pi kT_c)^2}\Delta_G \qquad \ldots \qquad 7.14$$

Hence the difference between the Helmholtz free energies of the superconducting and normal states is

$$F_S - F_N = -\frac{7\zeta(3)}{16(\pi k T_c)^2} N(0) f \Delta_G^4$$

$$= -\frac{4N(0)}{7\zeta(3)} \frac{(\pi k T)^2}{f} \left(1 - \frac{T}{T_c}\right)^2 \qquad 7.15$$

by eq. (7.7).

The discontinuity in the specific heat, i.e. the specific heat jump, is obtained from [6,10]

$$C_S - C_N = -T \frac{\partial^2}{\partial T^2} (F_S - F_N) \qquad \ldots \qquad 7.16\,a$$

i.e. $$(C_S - C_N)_{T=T_c} = \frac{8N(0)}{7\zeta(3)} \frac{\pi^2 k^2}{f} T_c \qquad \ldots \qquad 7.16\,b$$

Also the ratio of the specific heat discontinuity of the alloy to that of the pure metal is

$$S = \frac{(C_S - C_N)_{\text{alloy}}}{(C_S - C_N)_{\text{pure metal}}} = \frac{1}{f} \frac{T_c}{T_{c0}} \quad \ldots 7.17\,a$$

$$\text{i.e.} \quad S = \left\{ 1 + n_i \frac{N_d(0)}{N(0)} (1 + d - t_{ds}) + 5\, n_i\, d\, t_{sd} \right\} \frac{T_c}{T_{c0}} \quad \ldots 7.17\,b$$

The ratio S is calculated using the following experimental results of Martin [52] for Al-Mn ; Martin took $T_{c0} = 1.174^{\circ}K$ and $T_c = 0.84^{\circ}K$ at impurity concentration of 0.045 at.%, and obtained S = 0.73. The analysis of Kiwi and Zuckermann [6] gave S = 0.72.

Using the data of Table IV, the transition temperature T_c corresponding to an impurity concentration of 0.045 at.% is calculated to be $T_c = 0.769^{\circ}K$ for Al-Mn and $T_c = 0.910^{\circ}K$ for Al-Cr. The corresponding values of the ratio of the specific heat discontinuity of the alloy to that of the pure metal are obtained as $S_{Al\text{-}Mn} = 0.69$ and $S_{Al\text{-}Cr} = 0.80$. In order to compare these results with the experimental result of Martin [52] on Al-Mn, $S_{Al\text{-}Mn}$ is recalculated using the values given in Table VI. The computed values are $S_{Al\text{-}Mn} = 0.73$, which agrees exactly with Martin's result and $S_{Al\text{-}Cr} = 0.76$.

TABLE V

Al-Mn

Γ	N(O)	N(O) |g|	T_{co}	ϵ_F	U
1 eV	.19	.167	1.174	10eV	10eV

Calculated values:

t_{ds}	t_{sd}
0.054	0.619

7.1.3 The critical magnetic field H_c

At temperature $T < T_c$, a metal placed in a magnetic field may be in both the normal and superconducting phases. An extra magnetic energy of magnititude $H^2/8\pi$ is produced by the surface currents on the superconductor. Thus the free energy of a superconductor in a magnetic field is $F_S = F_N + H^2/8\pi$. Also a critical magnetic field H_c exists at which superconductivity is destroyed. The transition from the superconducting to the normal phase is determined from the relation (G.9):

$$-\frac{H_c^2(T)}{8\pi} = F_S - F_N \qquad \ldots \qquad 7.18$$

Using eq. (7.15), $H_c(T)$ becomes

$$H_c(T) = 4\pi kT_c \sqrt{\frac{2N(0)\pi}{7\zeta(3)}} \left\{ 1 + n_i \frac{N_d(0)}{2N(0)} (1 + d - t_{ds}) + \frac{5}{2} n_i d\, t_{sd} \right\} \left(1 - \frac{T}{T_c}\right) \qquad 7.19$$

In terms of the critical magnetic field $H_{c0}(T)$ for the pure superconductor, the critical field for the alloy is

$$H_c(T) = \left\{ 1 + n_i \frac{N_d(0)}{2N(0)} (1 + d - t_{ds}) + \frac{5}{2} n_i d\, t_{sd} \right\} \left(\frac{T_c - T}{T_{c0} - T} \right) H_{c0}(T) \qquad \ldots \qquad 7.20$$

The ratio of the critical magnetic field with and without recoil effects

$$\nu = \left[\frac{H_c(T)}{H_c(T)\big|_{t_{sd} = 0 = t_{ds}}} \right]$$

is also calculated for the alloys at an impurity concentration of 0.05 at.%. The values obtained are :

$$\nu_{\underline{Al}\text{-}Mn} = 2.00064 \quad \text{and} \quad \nu_{\underline{Al}\text{-}Cr} = 1.99998.$$

The effect of the recoil phonons is seen to be very pronounced here.

7.2 Thermodynamic properties of the superconducting alloy for temperature much lower than the transition temperature: $T << T_c$

7.2.1 The energy gap

To calculate the energy gap in the temperature range $0 < T << T_c$, the temperature dependence of all the parameters in eq. (7.67) is retained. $\Delta_G(T)$ is no longer negligible compared to the thermal energy kT and so it is not dropped out from the denominator. Eq. (6.67) is now written as

$$\Delta_S(T) = \lambda_S \pi k T \sum_{|\omega_n| < \omega_D}^{n} \frac{\Delta_G(T)}{\left[\omega_n^2 + \Delta_G^2(T)\right]^{\frac{1}{2}}} \quad \ldots \quad 7.21$$

Putting $\Delta_G(T) = f\,\Delta_S(T)$ gives the result

$$1 = f \lambda_S \pi k T \sum_{|\omega_n| < \omega_D}^{n} \frac{1}{\left[\omega_n^2 + \Delta_G^2(T)\right]^{\frac{1}{2}}} \quad \ldots \quad 7.22$$

Converting the summation over ω_n into an integral of ω, yields

$$\frac{1}{\lambda_s} = f \int_0^{\omega_D} \frac{d\omega \tanh\left(\frac{\sqrt{\omega^2 + \Delta_G^2(T)}}{2kT}\right)}{\left[\omega^2 + \Delta_G^2(T)\right]^{\frac{1}{2}}} \quad 7.23$$

or

$$\frac{1}{f\lambda_s} = \int_o^{\omega_D} \frac{d\omega}{\Omega} + \int_o^{\omega_D} \frac{d\omega}{\Omega} \left(\tanh \frac{\Omega}{2kT} - 1\right) \quad 7.24$$

where

$$\Omega = \sqrt{\omega^2 + \Delta_G^2(T)} \quad \ldots \quad 7.25$$

Eq. (7.24) together with eq. (6.69) gives

$$\ln \frac{\Delta_G(T)}{\Delta_{GO}} = -2 \int_o^{\omega_D} \frac{d\omega}{\Omega} \frac{1}{e^{\Omega/2kT} + 1} \quad 7.26$$

The transformation

$$\omega \rightarrow \Omega = \sqrt{\omega^2 + \Delta_G^2(T)} \qquad \ldots \qquad 7.27$$

and eq. (7.26) then lead to the following result :

$$\ln \frac{\Delta_G(T)}{\Delta_{GO}} = \ln \frac{\Delta_S(T)}{\Delta_{SO}} = -2 \int_{\Delta_G(T)}^{\omega_D} \frac{d\Omega}{[\Omega^2 - \Delta_G^2(T)]^{\frac{1}{2}} (e^{\Omega/2kT} + 1)}$$

Since the right hand side of eq. (7.28) is convergent, the upper limit of integration is extended to infinity. Then the transformation

$$\Omega = \Delta_G(T) \cosh \xi \qquad \ldots \qquad 7.29$$

converts the integral into a series solution in terms of Bessel function of the second kind of order zero, $K_0(z)$, (see G(1)), i.e.

$$\ln \frac{\Delta_{GO}}{\Delta_G(T)} = 2 \sum_{n=1}^{\infty} (-1)^{n+1} K_o \left(\frac{n \Delta_G(T)}{k T} \right) \qquad 7.30$$

At very low temperatures where $\Delta_G(T) >> kT$, the asymptotic form of the Bessel function is used, viz. (G5) :

$$K_m(z) \sim \sqrt{\frac{\pi}{2z}} e^{-z}, \quad z \rightarrow \infty \qquad \ldots \qquad 7.31$$

Hence, eq. (7.30) becomes

$$\ln \frac{\Delta_{GO}}{\Delta_G(T)} = 2 \sum_{n=1}^{\infty} (-1)^{n+1} \sqrt{\frac{\pi k T}{2n \Delta_G(T)}}\, e^{-\frac{n\Delta_G(T)}{kT}} \qquad 7.32$$

The main contribution to this expression comes from the $n = 1$ term, i.e.

$$\ln \frac{\Delta_{GO}}{\Delta_G(T)} = \sqrt{\frac{2\pi k T}{\Delta_G(T)}}\, e^{-\frac{\Delta_G(T)}{kT}} \quad \ldots \qquad 7.33$$

It is desirable to express this result in terms of the energy gap at $0^{\circ}K$, i.e. $\Delta_G(T)$ is written as $\Delta_G(T) = \Delta_{GO} + \delta\Delta_G$. Then

$$\ln \frac{\Delta_{GO}}{\Delta_G(T)} = -\ln\left(1 + \frac{\delta\Delta_G}{\Delta_{GO}}\right) = \frac{\Delta_{GO} - \Delta_G(T)}{\Delta_{GO}} \qquad 7.34$$

Consequently, eq. (7.33) becomes

$$\Delta_G(T) = \Delta_{GO} - \Delta_{GO} \sqrt{\frac{2\pi k T}{\Delta_{GO} + \delta\Delta_G}}\, e^{-\frac{\Delta_{GO} + \delta\Delta_G}{kT}}$$

$$\approx \Delta_{GO} - \sqrt{2\pi k T \Delta_{GO}}\, e^{-\frac{\Delta_{GO}}{kT}} \quad \ldots \qquad 7.35$$

For the pure superconductor, the equivalent expression is given by (G.1)

$$\Delta_0(T) = \Delta_{00} - \sqrt{2\pi k T \Delta_{00}}\; e^{-\frac{\Delta_{00}}{kT}} \quad \ldots \quad 7.36$$

The temperature dependence of the normalized energy gap $\Delta_G(T)/\Delta_{00}$ is shown as a function of the reduced temperature T/T_{c0} in Fig. (24) for Al-Mn and Al-Cr.

At the impurity concentration of 0.05 at.% and the reduced temperature T/T_{c0} of 0.123, the ratio of the energy gap with and without recoil Π is found to be $\Pi_{\text{Al-Mn}} = 1.0001$. Similarly, for Al-Cr at $n_i = 0.05$ at.% and $T/T_{c0} = 0.112$, $\Pi_{\text{Al-Cr}} = 1.0003$.

The zero temperature values for $n_i = 0.2$ at.% are

$$\Pi_{\text{Al-Mn}} = 1.023 \quad \text{and} \quad \Pi_{\text{Al-Cr}} = 1.004.$$

	n_1 (at %)
a	0
b	0.05
c	0.10

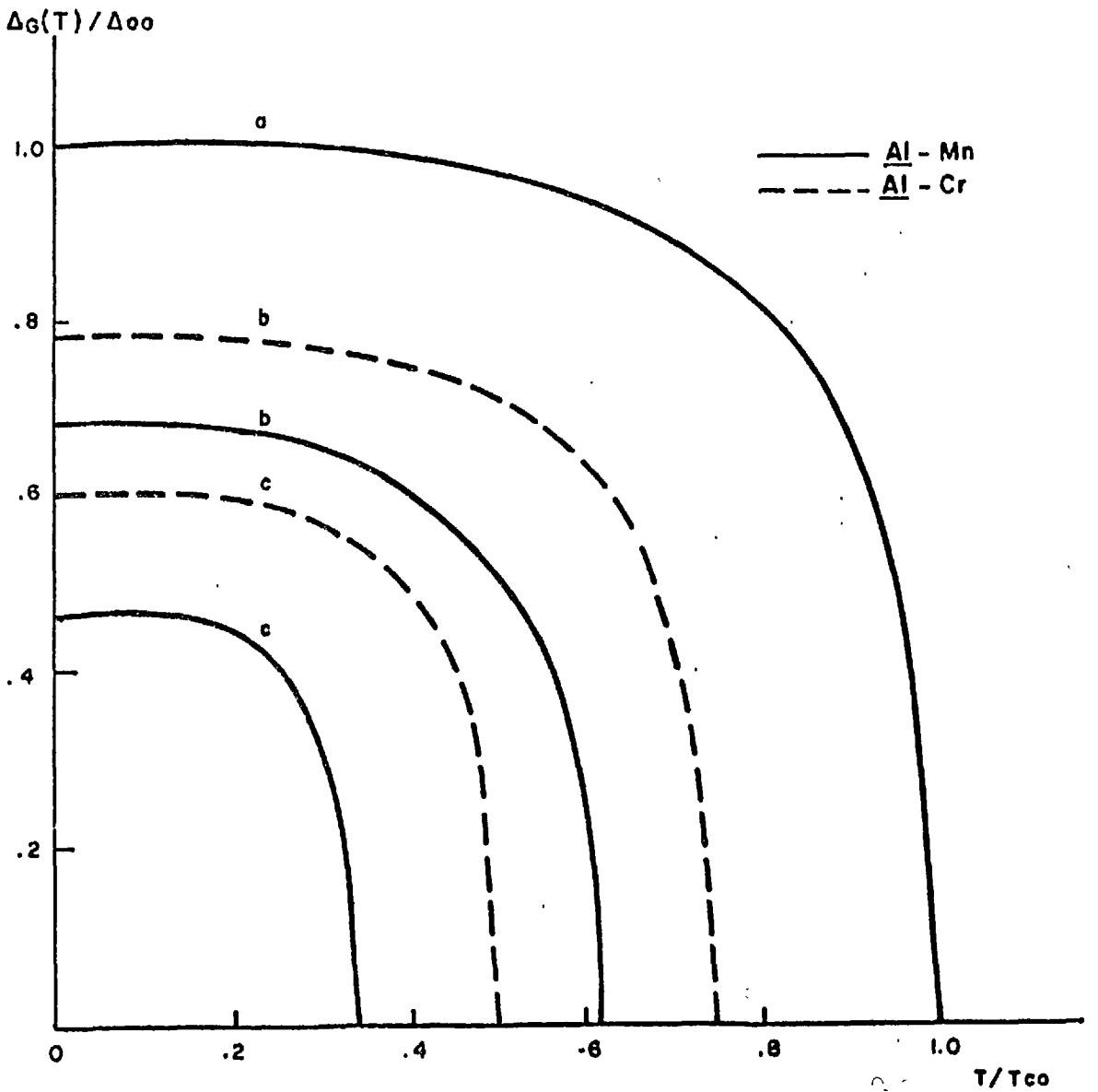


Fig. 24

7.2.2 Specific Heat

From eqs. (7.26) and (7.28),

$$\frac{1}{f\lambda_s} = \ln \frac{2\omega_D}{\Delta_G(T)} + \ln \frac{\Delta_G(T)}{\Delta_{GO}} \qquad \ldots \qquad 7.37$$

Eqs. (7.40) and (7.33) give

$$\frac{1}{|g|} = N(0) f \left\{ \ln \frac{2\omega_D}{\Delta_G(T)} - 2 \sum_{n=1}^{\infty} (-)^{n+1} K_o \left(\frac{n \Delta_G(T)}{kT} \right) \right\} \quad 7.38$$

So

$$\frac{\partial |g|^{-1}}{\partial \Delta_G(T)} = N(0) f \left\{ - \frac{1}{\Delta_G(T)} - 2 \sum_{n=1}^{\infty} (-)^{n+1} \frac{n}{kT} K_o' \left(\frac{n \Delta_G(T)}{kT} \right) \right\}$$

$$= N(0) f \left\{ - \frac{1}{\Delta_G(T)} + 2 \sum_{n=1}^{\infty} (-)^{n+1} \frac{n}{kT} K_1 \left(\frac{n \Delta_G(T)}{kT} \right) \right\}$$

$$\ldots \qquad 7.39$$

where $K_o'(z) = - K_1(z)$, is the derivative of the Bessel function $K_o(z)$ with respect to z.

The difference in the Hemholtz free energy between the superconducting and normal states is obtained from eqs. (7.12) and (7.38) to be

$$F_S - F_N = - N(0) f \left\{ \frac{\Delta_G^2(T)}{2} - 2 \sum_{n=1}^{\infty} (-)^{n+1} \left(\frac{kT}{n}\right)^2 \right.$$

$$\left. x \int_0^{n\Delta_G/kT} K_1(x)\, x^2\, dx \right\} \quad \ldots \quad 7.40$$

where $x = n\Delta_G(T)/kT$ ... 7.41

At low temperatures, $\Delta_G(T)/kT >> 1$, and the integral appearing on the right of eq. (7.40) is replaced by (G.2):

$$\int_0^{n\Delta_G(T)/kT} K_1(x)\, x^2\, dx = 2 - \int_{n\Delta_G/kT}^{\infty} K_1(x)\, x^2\, dx \quad 7.42$$

Using the asymptotic expansion of $K_1(x)$ and retaining only the term $n = 1$ (which gives the largest contribution) leads to the following result

$$F_S - F_N = - \frac{N(0)}{3} (\pi kT)^2 - N(0) f \left\{ \frac{\Delta_{GO}^2}{2} + \sqrt{2\pi \Delta_{GO}^3 kT}\ x \right.$$

$$\left. x \left(1 + \frac{15}{8} \frac{kT}{\Delta_{GO}}\right) e^{-\Delta_{GO}/kT} \right\} \quad 7.43$$

The first term on the right of eq. (7.43) is the

contribution from the normal phase, and gives the linear relation for the electronic specific heat in the normal state, viz. :

$$C_N(T) = \frac{2}{3}\pi^2 k^2 N(0)\, T \qquad \ldots \quad 7.48$$

The terms in the curly brackets, on the other hand, give contributions to the Helmoholtz free energy in the superconducting phase, consequently, the contribution to the specific heat of the alloy in the superconducting phase is

$$C_S(T) = 2N(0) f \sqrt{\frac{2\pi}{(kT)^3}}\, \Delta_{GO}^{5}\, e^{-\Delta_{GO}/kT} \qquad \ldots \quad 7.49$$

Thus an exponential variation at temperatures much below T_c is obtained. The behaviour of the specific heat is illustrated in Fig. (25).

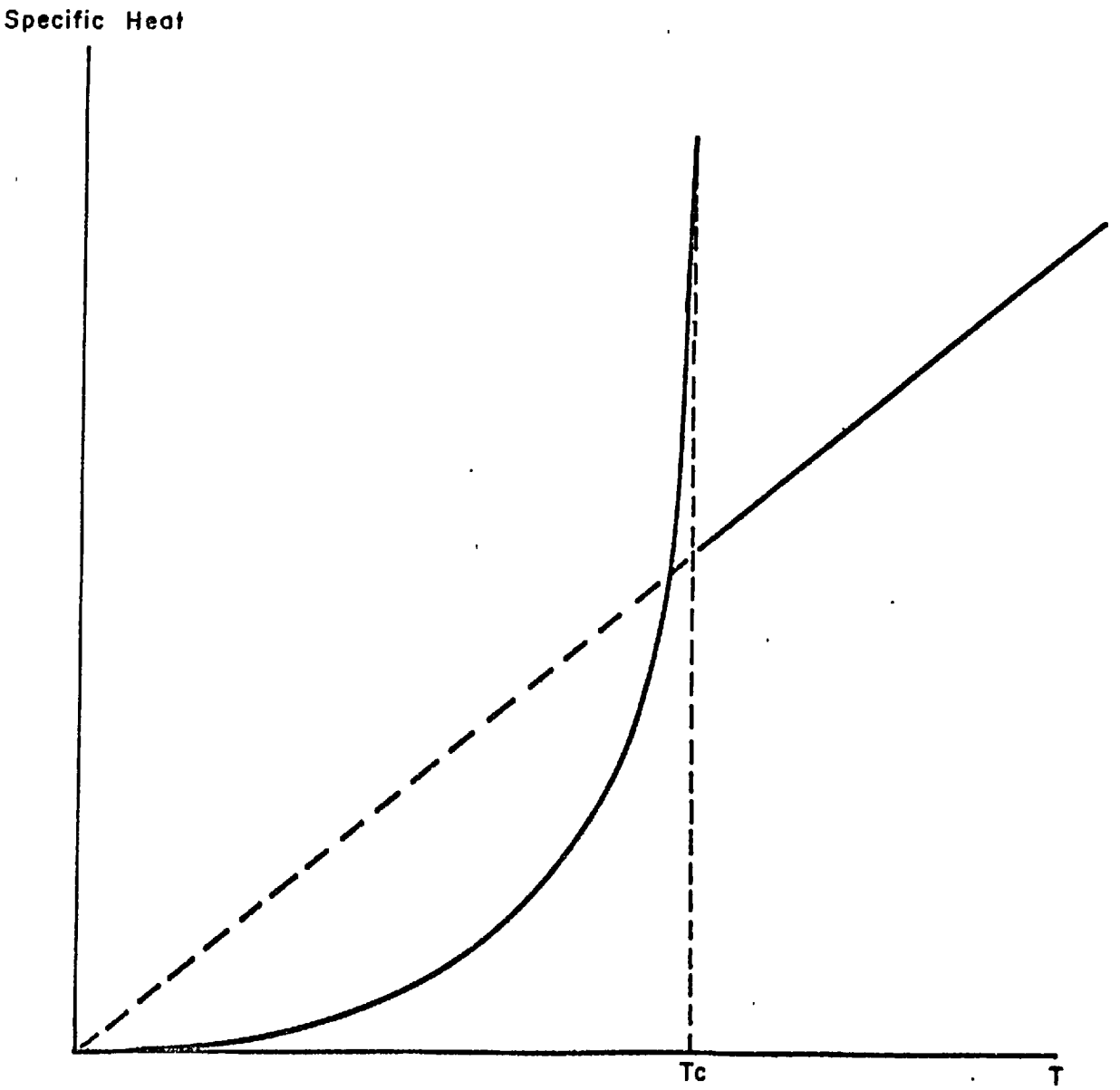


Fig. 25

CHAPTER EIGHT

8.1 DISCUSSION OF RESULTS

On the basis of the Anderson model for transition metal impurities in simple metal hosts, a number of results has been derived for both the normal and superconducting states of the alloy.

It is found that the Hamiltonian H_{sd} which describes the admixture of s- and d-states is modified to take account of the recoil of the impurity. Thus the new Hamiltonian H'_{sd} includes phonon creation and annihilation processes at the impurity site, and leads to an inelastic, incoherent scattering. In x-ray spectra, this corresponds to inelastic diffuse reflections as opposed to Bragg reflections which are recoil-less or elastic. Also in the Mossbauer effect, the sharp γ-ray line corresponds to recoil-less emission of the γ-ray, while the broad background results from the recoil of the atom. A significant result is that the recoil of the impurity does not produce any shift in the resonance level, and the energy of the conduction electron is also unchanged. However the width of

resonance shows a T^2 - dependence at low temperature ($T < \Theta_D$). At very low temperatures, ($T << \Theta_D/30$) $\Gamma(T)$ does not differ from Γ, as Fig. 15 indicates. The T^2-dependence is reflected in the impurity contribution to the resistivity. (i.e. residual resistivity). An enhancement of the conduction and localized electron masses due to the recoil is obtained. For Al-Mn this is found to be 1.017- about 2% over the band mass. In Al-Cr, the enhancement is not much noticeable ~ 1.003. The mass enhancement shows up in the density of states which is related to the specific heat. The relation between the mass enhancement and specific heat coefficient γ is given by

$$\frac{\gamma}{\gamma_o} = \frac{m^*}{m_o} \quad \ldots \quad 8.1$$

where

$$\gamma_o = \frac{2\pi^2}{3} N(0) = \frac{m_o k_F}{3} \quad \ldots \quad 8.2$$

is the specific heat coefficient for the bare electron. From the total impurity contribution to the specific heat coefficient $\Delta\gamma$ (including the recoil) the phonon-enhanced d-electron density of states at the ferm level $\tilde{N}_d(0)$ is found to be 9.26 for Al-Mn and

6.74 for Al-Cr. The bare values are 9.11 and 6.72, respectively.

In the superconducting state, a new mechanism which gives rise to attractive interaction between conduction and localized electrons was proposed in Chapter 6. The anslysis reveals that non-magnetic superconducting alloys of iron-group impurities dissolved in simple metal hosts behave just like BCS superconductors [16]. For these dilute alloys, it is shown that the coupling constant λ_s of the BCS theory must be replaced by $f\lambda_s$. An important consequence of this fact is that all calculations for physical quantities such as the energy gap, critical magnetic field and the specific heat which have been performed for the BCS superconductor, can be carried over to our model.

The parameter f is related to an effective coupling constant g_{eff} by

$$N(0)\,|g_{eff}| = f\lambda_s \qquad \ldots \qquad 8.3$$

and consists of two parts. One part produces a weakening of the Cooper pairs as a result of d-electron participation in superconductivity through the admixture term.

This has been discussed by several authors [1-12, 15-18]. The second part arises from the recoil and has the effect of enhancing superconductivity. This is reflected in the increase in the energy gap as shown in Fig. 21.

Superconductivity is destroyed at the critical impurity concentration of about 1 at.% for Al-Mn, and 1.7 at.% for Al-Cr.

Another feature of the present work is that gaplessness is not a property of these alloys. That is, unlike superconductors doped with para-magnetic impurities, there is no region of concentration in which the material is superconducting while the energy gap is zero at temperatures below T_c.

The superconducting density of states strongly depends on impurity concentration n_i and shows a sharp peak at the gap edge. The peak is shifted to the lower frequencies as n_i is increased.

The superconducting transition temperature T_c is also enhanced by the impurity recoil. In order to compare the theoretical prediction for the depression of transition temperature ΔT_c with experimental values, the contribution to ΔT_c from anisotropy must be substracted from the experimental result. It has been

shown by Zuckermann and Singh [11] and Nagashima and Soda [12] that the decrease in the transition temperature can be written as

$$\Delta T_c = (\Delta T_c)_{val} + (\Delta T_c)_{anis} \qquad 8.4$$

The first term is the valence effect, which in our case corresponds to the resonance scattering plus recoil contributions. The second term arises from the anisotropy of the energy gap. The two contributions have been shown to be independent of each other and $(\Delta T_c)_{anis}$ is the same as that given by the theory of Markowitz and Kadanoff [23] for non-transition metal impurities in superconducting hosts. The decrease in T_c due to d-resonance plus recoil is linear in n_i and this is shown in Fig. 22.

The d-density of states at the Fermi level calculated from the initial decrease of T_c was found to be 9.87 and 6.52 states/eV-atom for Al-Mn and Al-Cr, respectively. These values agree well with the values 9.11 and 6.72 states/eV-atom obtained from the normal state.

Localized spin fluctuations at the impurity site also give substantial contribution to ΔT_c [18,21], especially for Al-Mn.

The calculation performed for the ratio of the "specific heat jump" of the alloy to that of the pure metal S gives good agreement with that obtained by Martin. Using Martin's data [52], the present calculation yields the same result of $s = 0.73$ as he obtained for Al-Mn at 0.045 at.%. Previous calculation by Kiwi and Zuckermann gave $S = 0.72$.

8.2 CONCLUSION

In this thesis it has been demonstrated that virtual recoil of the impurity cannot be ignored in the resonant scattering problem. Some effect is obtained both in the normal state and superconducting state properties.

The analysis on the superconducting alloy has been made easy as a result of the simple form which was assumed for the s-d attractive interaction. A more elaborate theory on the lines of strong coupling theory of superconductivity [53] could be derived. However, it is reckoned that it will only lead to a fairly tedious computor programming, and may not yield results which, qualitatively, will be more superior to what has been obtained here.

The theory is also limited to low impurity concentration, thereby ignoring impurity-impurity

correlations. Recent work by Rizzuto et al [54] suggests that the impurity content of the alloys could be pushed to high values - as much as 5 at.%. Consequently, the Anderson Hamiltonian should be modified to take account of impurity-impurity interactions.

Only non-magnetic alloys have been considered in this thesis. It is hoped that the effect of recoil will also be felt in dilute magnetic alloys in both the normal and superconducting states, and is left for future investigations.

APPENDIX A

k-SUMMATION OF THE FULL GREEN'S FUNCTION $G_k(\omega)$

For a system of interacting electrons, the full Green's function $G_k(\omega)$ is given by

$$G_k(\omega) = \frac{1}{\left[G_k^o(\omega)\right]^{-1} - \Sigma(k,\omega)} \qquad \text{A.1}$$

where $G_k^o(\omega)$ is the non-interacting single particle Green's function, and $\Sigma(k,\omega)$ is the irreducible self-energy. $G_k^o(\omega)$ is given by

$$G_k^o(\omega) = (\omega - \epsilon_k + \delta_k)^{-1} \qquad \ldots \qquad \text{A.2}$$

with

$$\delta_k = \begin{cases} -\,0 & \text{for} \quad k > 0 \\ +\,0 & \text{for} \quad k < 0 \end{cases} \qquad \ldots \qquad \text{A.3}$$

In general, $\Sigma(k,\omega)$ has a weak k variation and a good approximation is to replace it by its value at $k = k_F$, where k_F is the Fermi momentum ($\hbar = 1$). Hence writing

$$\Sigma(k_F,\omega) = \Sigma(\omega) = \mathrm{Re}\ \Sigma(\omega) + i\ \mathrm{Im}\ \Sigma(\omega) \qquad \text{A.4}$$

yields

$$G_k(\omega) = \left[\omega - \tilde{\epsilon}_k - i \, \mathrm{Im} \, \Sigma(\omega) \right]^{-1} \qquad \text{A.5}$$

where

$$\tilde{\epsilon}_k = \epsilon_k + \mathrm{Re} \, \Sigma(\omega) \qquad \text{A.6}$$

gives the shift in the single-particle energy.

Thus

$$\sum_k G_k(\omega) = N(0) \int_{-E_B}^{E_B} \frac{d \tilde{\epsilon}}{\omega - \tilde{\epsilon} - i \, \mathrm{Im} \, \Sigma(\omega)} \qquad \text{A.7}$$

where the sum over k has been converted into an integral over the energy $\tilde{\epsilon}$, $N(0)$ is the density of states at Fermi level for one spin direction, and E_B is the bandwidth, of order E_F.

A.7 yields

$$\sum_k G_k(\omega) = N(0) \left\{ \frac{1}{2} \ln \left| \frac{(\omega - E_B)^2 + C^2}{(\omega + E_B)^2 + C^2} \right| \right\} + i \left\{ \tan^{-1} \left(\frac{\omega + E_B}{C} \right) - \tan^{-1} \left(\frac{\omega - E_B}{C} \right) \right\} \qquad \text{A.8}$$

where $C = \text{Im}\ \Sigma(\omega)$. For ω, $|\text{Im}\ \Sigma(\omega)| << E_B$, the inverse tangents can be replaced by

$$\tan^{-1}\left(\frac{-E_B}{C}\right) - \tan^{-1}\left(\frac{E_B}{C}\right) \approx -\pi\ \text{sgn}\ \omega \qquad \text{A.9}$$

where the general relation

$$\text{Im}\ \Sigma(\omega) = \begin{cases} +0 & \text{for } \omega < 0 \\ -0 & \text{for } \omega > 0 \end{cases}$$

has been used in deriving A.9.

In the flat band approximation, $E_B \to \infty$, we obtain

$$\sum_k G_k(\omega) = -\pi\ \text{sgn}\ \omega = -\pi \left|\frac{\omega}{\omega}\right| \ldots \qquad \text{A.10}$$

APPENDIX B

FREQUENCY SUMMATIONS USED IN TEXT

In order to evaluate the frequency summations, such as

$$k T \sum_{\substack{n \\ |\omega_n| < \omega_D}} \frac{1}{(\eta_n^2 \omega_n^2 + K)\ \eta_n^2 \omega_n^3}$$

the approximation $\Gamma >> \omega_D$ will be used. This corresponds to the physical case in which the resonance width is much larger than the Debye cutt-off energy.

Then

$$\eta_n^2 \omega_n^2 \approx \Gamma^2 \qquad \ldots \qquad B.1$$

where $$\eta_n = 1 + \left|\frac{\Gamma}{\omega_n}\right| \qquad \ldots \qquad B.2$$

So the sum becomes

$$k T \sum_{\substack{n \\ |\omega_n| < \omega_D}} \frac{1}{(\Gamma^2 + K)\ \Gamma^2 |\omega_n|} = \frac{1}{\Gamma^2(\Gamma^2 + K)} k T \sum_{\substack{n \\ |\omega_n| < \omega_D}} \left|\frac{1}{\omega_n}\right|$$

$$= \frac{\alpha}{\pi \Gamma^2 (\Gamma^2 + K)} \qquad B.3$$

where $\alpha = \ln\left(\frac{1.14\omega_D}{kT}\right)$.

Similarly

$$kT \sum_{\substack{n \\ |\omega_n| < \omega_D}} \frac{1}{(\eta_n^2\omega_n^2 + K)\,|\omega_n|} = \frac{1}{(\Gamma^2 + K)}\, kT \sum_{\substack{n \\ |\omega_n| < \omega_D}} \left|\frac{1}{\omega_n}\right|$$

$$= \frac{\alpha}{\pi(\Gamma^2 + K)} \qquad \text{B.4}$$

Also $$kT \sum_{\substack{n \\ |\omega_n| < \omega_D}} \frac{1}{\eta_n^2\omega_n^2} = \frac{1}{\Gamma^2}\, kT \sum_{\substack{n \\ |\omega_n| < \omega_D}} \left|\frac{1}{\omega_n}\right|$$

$$= \frac{\alpha}{\pi\Gamma^2} \quad \ldots \qquad \text{B.5}$$

and $$kT \sum_n \frac{1}{\eta_n^2\omega_n^2} = \frac{1}{2\pi^2 kT}\, \zeta(2, \lambda) \qquad \text{B.6}$$

where we have used

$$\sum_{n=0}^{\infty} \frac{1}{(|\omega_n| + \Gamma)^s} = \frac{1}{(2\pi kT)^s} \sum_{n=0}^{\infty} \frac{1}{(n + \lambda)^s}$$

$$= \frac{1}{(2\pi kT)^s}\, \zeta(S, \lambda) \qquad \text{B.7}$$

$$\lambda = \frac{1}{2} + \frac{\Gamma}{2\pi kT} \quad \ldots \qquad \text{B.8}$$

The asymptotic form of the generalized Riemann zeta function for large arguments is given by (G.11).

$$\zeta(S,\lambda) = \frac{1}{\lambda^{S-1}} \frac{\Gamma(S-1)}{\Gamma(S)} + \frac{1}{2\lambda^{S}} + O(\lambda^{-S-3}) \qquad B.9$$

For

$$S = 2, \quad \lambda_c = \frac{1}{2} + \frac{\Gamma}{2\pi k T} \approx \frac{\Gamma}{2\pi k T} \ldots \qquad B.10$$

(for $\Gamma >> k T$, which is valid in the case of non-magnetic alloys).

Thus

$$\frac{\zeta(2,\lambda)}{2\pi^2 k T} \approx \frac{1}{\pi\Gamma} = \frac{1}{5} N_d(0) \ldots \qquad B.11$$

REFERENCES

1. G. BOATO, M. BUGO and C. RIZZUTO, Nuovo Cimento 45, 226 (1966); Phys. Rev. 148, 353 (1966).
2. E.W. COLLINGS, F.T. HEDGCOCK and Y. MUTO, Phys. Rev. 134, A 1521 (1964).
3. F.T. HEDGCOCK and W.B. MUIR, Phys. Rev. 129, 2045 (1963.
4. R. AOKI and T. OHTSUKA, Phys. Letters 19, 456 (1965); J. Phys. Soc. (Japan).
5. M.J. ZUCKERMANN, Phys. Rev. 140, A 899 (1965); Nuovo Cimento 49, 41 (1967).
6. M. KIWI and M.J. ZUCKERMANN, Phys. Rev. 164, 548 (1967).
7. C.F. RATTO and A. BLANDIN, Phys. Rev. 164, 818 (1967).
8. M. KIWI, Ph. D. Thesis (unpublished) University of Virginia, (1967).
9. K. TAKANAKA and F. TAKANO, Progr. Theor. Phys. 36, 1080 (1966).
10. K. TAKANAKA and T. NAGASHIMA, Progr. Theor. Phys. 38, 291 (1967).
11. A.D. SINGH and M.J. ZUCKERMANN, Canadian J. Phys. 45, 37 (1967).
12. T. NAGASHIMA and T. SODA, Progr. Theor. Phys. 36, (1966).

13. B.R. COLES, Phil. Mag. 8, 335 (1958).

14. D. MARKOWITZ and L.P. KADANOFF, Phys. Rev. 131, 563 (1963).

15. P.W. ANDERSON, Phys. Rev. 124, 41 (1961).

16. A.B. KAISER, J. Phys. C : Solid St. Phys. 3, 410 (1970).

17. M.J. ZUCKERMANN, Preprint - "Superconductivity and the concept of localized spin fluctuations in dilute 'non-magnetic' alloys" - Lecture delivered at the 6th Annual Winter School of Theoretical Physics, Karpacz, Poland; Feb. 1969.

18. C.F. RATTO and E.G. d'AGLIANO, Preprint.

19. S. DONIACH, M.A. JENSEN, D.J. SCALAPINO and P. LEDERER, Preprint.

20. K. BANNEMANN, Preprint.

21. M.J. ZUCKERMANN, J. Phys. C, Solid State Physics 3, 2130 (1970).

22. A.D. CAPLIN, Phys. Letters 26A, 46 (1967).

23. A.D. CAPLIN and C. RIZZUTO, Phys. Rev. Letters 21, 746 (1968).

24. N. RIVIER, M.J. ZUCKERMANN and M. SUNJIC, Phys. Letters 28A, 492 (1969).

25. P.E. NIELSEN and P.L. TAYLOR, Phys. Rev. Lett. 21, 893 (1968).

26. P.L. TAYLOR, Phys. Rev. 178, 918 (1969).

27. J. KONDO, Progr. Theor. Phys. 32, 37 (1964).

28. S. DONIACH, Phys. Rev. 144, 382 (1966).

29. A.A. ABRIKOSOV, Physica 2, 5 (1965).

30. Y. NAGAOKA, Phys. Rev. 138, 1112 (1965); Progr. Theor. Phys. 37, 13 (1967).

31. D.N. ZUBAREV, Soviet Physics Uspekhi 3, 320 (1960).

32. P.E. BLOOMFIELD and D.R. HAMANN, Phys. Rev. 164 86 (1967).

33. A.A. ABRIKOSOV and L.P. GORKOV, Soviet Physics JETP 12, 1243 (1961).

34. M.J. ZUCKERMANN, Phys. Rev. 168, 390 (1968).
M.J. ZUCKERMANN and V. CELLI, Nuovo Cimento 58 154 (1968).

35. S.H. LIU, Phys. Rev. 137, A1209 (1965).

36. K. MAKI, Phys. Rev. 153, 428 (1967).
P. FULDE and K. MAKI, Phys. Rev. 142, 275 (1966).

37. S. SKALSKI, O. BETBEDER-MATIBET and P.R. WEISS Phys. Rev. 136, A1500 (1964).

38. A. GRIFFIN, Phys. Rev. Lett. 15, 703 (1965).

39. K. BANNEMANN, Phys. Rev. Lett. 17, 438 (1966).

40. J. FRIEDEL, Can. J. Phys. 34, 1190 (1956); Nuovo Cimento Suppl. 7, 287 (1958).

41. R.P. FEYNMAN, Phys. Rev. 74, 1430 (1948).

42. F.J. DYSON, Phys. Rev. 75, 486 and 1736 (1949).

43. G.E. STEDMAN, Contemporary Phys. 9, 49 (1968).

44. T. MATSUBARA, Progr. Theor. Phys. 14, 351 (1955).

45. G. RICKAYZEN, International Spring School of Physics, Bergen (1961). W.A. Benjamin Inc., New York (1964).

46. B. KJOLLERSTROM, D.J. SCALAPINO and J.R. SCHRIEFFER, Phys. Rev. 148, 665 (1966).

47. DUK-JOO KIM, Phys. Rev. 146, 455 (1966).

48. S. NAKAJIMA and M. WATABE, Progr. Theor. Phys. 29, 341 (1963).

49. J. BARDEEN, L.N. COOPER and J.R. SCHRIEFFER, Phys. Rev. 108, 1175 (1957).

50. J. ZITTATZ and E. MUELLER-HARTMANN,

51. W.L. McMILLAN, Phys. Rev. 167, 331 (1968).

52. D.L. MARTIN, Proc. Phys. Soc. 78, 1489 (1961).

53. D.J. SCALAPINO, J.R. SCHRIEFFER and J.W. WILKINS, Phys. Rev. 148, 263 (1966).

54. E. BABIC, R. KVSNIK, B. LEONTIC, Z. VUCIC, Y, ZORIC and C. RIZZUTO (to be published).

55. B.E. PATON and M.J. ZUCKERMANN, Preprint.

GENERAL REFERENCES

G.1. A.A. ABRIKOSOV, L.P. BORKOV and I.E. DZYALONSHINSKI, "Methods of Quantum Field Theory in Statistical Physics". Pergamon Press, Inc.

G.2. J.R. SCHRIEFFER, "Theory of Superconductivity" W.A. Benjamin Inc., New York, 1964.

G.3. "Theory of Condensed Matter" Lectures, International Centre for Physics, Trieste (1968). J. ZIMAN, F. BASSANI and G. CAGLIOTI (Directors).

G.4. American Institute of Physics Handbook, McGraw Hill Book Co., Inc., New York. 2nd edition (19).

G.5. P.M. MORSE and H. FESHBAH, Methods of Theoretical Physics, McGraw Hill Book. Co. Inc., New York, (1953).

G.6. R. MILLS, "Propagators for Many-Particle Systems", Gordon & Breach Science Publ. London, (1969).

G.7. J.M. ZIMAN - Principles of the Theory of Solids Cambridge University Press (1965), p.124.

G.8. A.H. WILSON, "The Theory of Metals, 2nd ed. Cambridge University Press, (1965), p.144.

G.9. E.A. LYNTON - Superconductivity, Methuen's Monograph, London, 1961.

G.10. C. KITTEL, "Quantum Theory of Solids", John Wiley & Sons, Inc., New York, London (1963).

G.11. A. ERDELYI, Asymptotic Expansions, Dover Publications, Inc., New York.